Characterizing endocannabinoid system development in zebrafish

and

investigating cannabidiol-mediated downregulation of the Sonic Hedgehog Pathway

by

Hae-Won Son

A thesis submitted in partial fulfillment of the requirements for the degree of

Master of Science

in

Physiology, Cell, and Developmental Biology

Department of Biological Sciences
University of Alberta

Abstract:

Cannabis is the most frequently used recreational drug during pregnancy. Nearly 4% of American women self-reported use during their pregnancies in 2014, which represents a 62% increase from 2002. The compounds in cannabis are mediated through interactions with the endocannabinoid system (ECS), which is well-studied for its role in synaptic plasticity and regulation of neural function, however, recent evidence suggests that the ECS is also responsible for regulating aspects of early development. Additionally, phytocannabinoids, such as cannabidiol (CBD), have been proposed to modulate signaling pathways outside of the ECS, including the Sonic Hedgehog (SHH) Pathway. As phytocannabinoids have the ability to pass freely through the placenta, it is critical to investigate the role of the ECS during development, as well as mechanisms of phytocannabinoid mediated-teratogenicity. In this thesis, two objectives were chosen to address both areas of research: 1) to characterize the expression of the ECS throughout early zebrafish development, and 2) identifying and assessing phytocannabinoid mediated downregulation of the Sonic Hedgehog (SHH) pathway.

The ECS contains numerous receptors that bind cannabinoid ligands. Once bound, a response occurs in the cell that mediates a myriad of physiological responses, which may include developmental decisions. Despite these receptors playing a major role in controlling the activity of the ECS, little is known about spatial and temporal expression of these receptors during early development. Combining reverse-transcriptase PCR with in situ hybridizations, I compiled a developmental timeline of six key cannabinoid receptors; *cb1, cb2, trpv1, trpa1a, trpa1b*, and *gpr55* to demonstrate spatial, temporal, and semi-quantitative expression of each receptor from the first six hours to three days of zebrafish development, which is roughly equivalent to two to ten weeks in human embryonic development. This timeline aims to provides a foundation at which further investigation of each receptor can be undertaken.

Secondly, exposure of zebrafish embryos to cannabidiol (CBD) during the period of gastrulation has been shown to cause deformities to axial curvature, reduced body length, cardiac and yolk-sac edema, altered motor neuron development, and reduction in survival and hatching rates. Evidence suggests that cannabinoids are able to bind to, and decrease the activity of Smoothened (SMO), a receptor within the SHH pathway, which may be responsible for toxic and teratogenic effects that were observed following phytocannabinoid exposure. Co-exposing zebrafish embryos to both CBD and a known SMO agonist resulted in improvement of parameters including mortality and hatching rate, gross morphology, free-swimming locomotion, and expression levels of *ptch2,* a key regulatory receptor of the SHH pathway. Moreover, exposure cyclopamine, a known antagonist of SMO, resulted in similar morphological abnormalities compared to CBD, verifying that SMO downregulation is able to cause the teratogenic effects described previously.

Taken together, this work provides a comprehensive overview of ECS expression during development, and is the first evidence of CBD exerting detrimental developmental effects through the SHH pathway in zebrafish.

Preface:

This thesis is an original work by Hae-Won Son. Approval for this study was obtained from the Animal Care and Use Committee: Biosciences, under protocol AUP00000816**.**

Locomotion experiments outlined in Section 2.3.5 were assisted by Md Ruhul Amin.

Acknowledgements

First of all, my deepest thanks goes to Dr. Declan Ali. Thank you for your endless amounts of patience and kindness through all of the challenges in the past three years. I am so grateful that you gave me the opportunity to pursue such an exciting project despite having no background in physiology, and supporting me every step of the way.

Thanks to past and current lab members: Dr. Kazi Ahmed, Md Shah Sufian, Md Ruhul Amin, Lakhan Khara, Andrew Kim, Kaijun Ma, and Mitchell Chorney. It was an honour to work alongside you all, and I will carry forward very fond memories of deep talks and potlucks.

Thanks to my committee members, Dr. Ted Allison and Dr. Andrew Waskiewicz for their very kind direction and encouragement throughout my degree. I appreciated all of the tips on everything in situ, and reining me in when ambitions got in the way of a cohesive project! Special thanks to James MacLagan, who taught me lab skills in the latter half of my undergraduate degree and then continued helping me through all of the obstacles in the first year of my graduate degree.

I am incredibly grateful for my support system during the last few years. To my entire family, who encouraged me and cheered me on even when they didn't quite understand my research – I couldn't do it without you. Thanks to my best friend Diana Tan, who always lent an ear when I needed to vent. To my friends in the Biological Sciences and beyond – our weekly beers night at Sherlock's, which migrated to nightly hangouts on Discord after March 2020 was one of the only things that made the grad school, and the pandemic, bearable. Special thanks to Kacey Mackowetzky, who was on the other side of a muted voice call every minute that I spent writing my thesis. Your support, encouragement, and optimism as we both slogged towards the end of our degrees was monumental. Thank you to Logan Brand, Niall Pollock, Spencer Goyette, Kacie Norton, Lindsay Canham, Lee Campbell, Pat Wang, Tejal Aslesh, Dr. Francesca Jean, Dr. Sonya Widen, all of my friends from the Ambassador program, and residence, and everyone else who I may have missed – I'm so thankful to have made such wonderful friends and been part of such incredible communities at the University of Alberta over the past seven years, and I can't wait to reconnect with you all in person at the end of this pesky pandemic!

Table of Contents

List of Tables:

List of Figures:

List of Abbreviations:

2-AG: 2-Arachidonoylglycerol

AC: adenylyl cyclase

AEA: anandamide

AP: alkaline phosphatase

BCIP: 5-bromo-4-chloro-3-indolyl phosphate

BSA: bovine serum albumin

CBD: cannabidiol

CNS: central nervous system

Cb1: cannabinoid receptor 1

Cb2: cannabinoid receptor 2

Cyc: cyclopamine

DIG: digoxygenin

DMSO: dimethyl sulfoxide

ECS: endocannabinoid system

EM: embryo media

FAB: antigen-binding fragment

FGF: fibroblast growth factor

LTD: long-term depression

GPCR: G-protein coupled receptor

Gpr55: G-protein coupled receptor 55

HM: hybridization media

IVT: in vitro transcription

MeOH: methanol

mg: milligram

$MgCl_2$: magnesium chloride

NaCl: sodium chloride

NBT: p-nitroblue tetrazolium chloride

PBST: phosphate buffered saline with tween

PCR: polymerase chain reaction

PFA: paraformaldehyde

PKA: protein kinase A

PM: purmorphamine

PTU: 1-phenyl 2-thiourea

Ptch: Patched

RNA: ribonucleic acid

RT: reverse-transcriptase

SHH: sonic hedgehog

Smo: Smoothened

SSC: saline-sodium citrate

THC: tetrahydrocannabinol

TL: Tupfel long-fin

Tris-HCl: tris hydrochloride

TRP: Transient receptor potential

Trpa1a: transient receptor potential cation channel, subfamily A, member 1a

Trpa1b: transient receptor potential cation channel, subfamily A, member 1b

Trpv1: transient receptor potential cation channel, subfamily V, member 1

dpf: days post fertilization

hpf: hours post fertilization

mRNA: messenger ribonucleic acid

WT: wild type

µL: microlitre

µM: micromolar

µg: microgram

1. Introduction

1.1 Cannabis in Pregnancy

1.1.1 Trends in Cannabis Use

Cannabis has been used by humans for centuries for both its psychoactive and medicinal effects [1], which are mainly attributed to delta-9-tetrahydrocannabinol (THC) [2] and cannabidiol (CBD) [3], respectively. Although cannabis is primarily regarded as a recreational drug, both components show promising anti-nociceptive properties. CBD in particular is a favourable candidate to use in pain relief medication [4–7], and to reduce symptoms of addiction [8] and anxiety [9–12]. Therapeutic use of this phytocannabinoid is continued to be investigated for treatment of movement disorders such as Parkinson's [13–15] and Huntington's Disease [15–17], as well as to reduce the number and severity of seizures in patients with epilepsy [18–20]. In Canada, CBD products are widely available in many different forms, including oils, capsules, topicals and edibles [21].

In 2019, 16.8% of Canadians aged 16 or older reported cannabis use within a three month period following cannabis legalization, an increase from 14.9% in 2018 [22]. Notably, 33% of respondents in the 18-24 year category reported cannabis consumption, exceeding all other age groups [22]. A study conducted across the United States and Canada surveying users of both legal and illegal sources of cannabis found that consumers generally had low knowledge of THC and CBD content in their products [23], indicating that users are likely unaware of the quantities of phytocannabinoids they are consuming. As legalization of cannabis carries a sense of perceived safety [24], which may be associated with increased trends in use and risky behaviour, questions are raised about potential health risks associated with cannabis consumption.

1.1.2 Effects of Prenatal Cannabis Exposure

In 2011, approximately 45% of pregnancies that occurred in the United States were considered unintended [25], which designates a large portion of pregnancies in which protective measures may not be taken. As pregnancies are often detected two or more weeks following fertilization [26], this opens up a window in which the embryo may be exposed to teratogens from a mother unaware of her pregnancy. Moreover, this period may potentially overlap with the process of gastrulation, a critical step in embryonic development highly susceptible to teratogens [27, 28]. As cannabinoids have been shown to pass freely through the placenta [29, 30] a structure that facilitates gas and nutrient exchange between mother to embryo, circulation of phytocannabinoids from the mother to the embryo and fetus may interfere with the process of development.

In 2014, nearly 4% of pregnant women in America reported using cannabis during their pregnancies [31]. The normalization of cannabis use following legalization carries a sense of perceived safety, despite little evidence that cannabis is safe to consume during pregnancies. This is especially important as CBD use is often discussed as a therapeutic agent during pregnancy on social media outlets [32], despite warnings from the National Institute of Health and the Food and Drug Administration to avoid cannabis products during pregnancy [33]. Women experiencing nausea and vomiting during their pregnancies have a higher prevalence of cannabis use [31], indicating that cannabis use may be a method of self-medication to treat pregnancy symptoms.

Unlike prenatal exposure to alcohol, which often results in clearly defined, diagnosable clinical characteristics [34], prenatal exposure to cannabis does not seem to have associated morphological or cognitive effects and current evidence remains conflicted about adverse

pregnancy outcomes. A systematic review of 24 studies found associations between cannabis exposure, low birth weight, and increased admissions to the neonatal ICU, but no correlation with other fetal growth parameters such as body length or head circumference [35]. However, the authors indicate that inconsistencies of the range of parameters reported between the studies warrant further investigation.

In 2019, a systematic review conducted within Colorado found a correlation between increased rates of congenital birth defects, and an increased trend of cannabis use [36]. Colorado is one of the first states to legalize cannabis, with medicinal use legalized in 2000 and recreational use legalized in 2012. The authors note that cannabis is the only drug that increased in use from 2000 to 2014, while the use of pain relievers, cocaine, alcohol, and tobacco remained stable or decreased. This trend correlated with birth defects such as spina bifida, microcephalus, Down's syndrome, and central nervous system defects, which outpaced the birth rate by 5 to 37 times. While correlative relationships should be taken cautiously, this observation suggests that congenital defects may be linked to cannabis teratology, which requires further investigation to establish causation.

Studies aimed at discerning less obvious symptoms of prenatal cannabis exposure are currently being undertaken. Such studies include longitudinal studies, which aim to determine cognitive or motor effects of children of mothers that report cannabis use during pregnancy, to investigate whether prenatal exposure results in long-term effects into childhood and young adulthood. To date, three longitudinal studies have been conducted [37]. The results of these studies suggest that adverse effects of aspects of cognition including memory [38–40], attention [38–40], and depressive symptoms [38, 41] may correlate with prenatal cannabis exposure. However, such studies should be taken with a grain of salt due to the difficulty in controlling for

external factors such socioeconomic status, enrichment during childhood, etc., in addition to imprecise estimates of the quantity of cannabis consumed during pregnancy.

The uncertainty of the teratogenic effects of cannabis, coupled with an increasing trend of cannabis use over time, poses a potential health risk that requires further investigation. This thesis aims to utilize zebrafish as a model organism to investigate the role of the endocannabinoid system (ECS) in development, which will pave the way to understanding disruptions to development caused by exogenous cannabinoids in humans. Although direct health implications cannot be drawn between zebrafish and humans, these conclusions may lay a framework in understanding how the ECS functions in human development, and possible outcomes of prenatal cannabinoid exposure.

1.2 The Endocannabinoid System

1.2.1 Endocannabinoid System Signaling

The effects of cannabinoid compounds are mediated through interactions with the endocannabinoid system (ECS). The ECS consists of ligands (cannabinoids), receptors, and enzymes that modulate activity by synthesizing and degrading the cannabinoids. Due to the neuromodulatory nature of endocannabinoid signaling, the ECS has been long considered to be critical for synaptic plasticity, which is responsible for processes such as learning and memory [42, 43]. Although past research on the ECS has been centered on its role in regulating synaptic activity, recent interest has shifted towards investigating a role in development as a result of concerns of cannabis use during pregnancy.

Historically, the endocannabinoid system consisted of just two receptors: cannabinoid receptor 1 (CB1) and cannabinoid receptor 2 (CB2). These receptors were first identified in the

1980s and cloned successfully in the 1990s [44]. More recent studies have identified receptors outside of the classical cannabinoid receptor family that are modulated by endocannabinoids, as discussed below. In 2001, endocannabinoid signaling was first reported to occur in a retrograde fashion to regulate synaptic activity [45, 46]. Unlike classical neurotransmitters, endocannabinoids – primarily 2-AG – are rapidly synthesized during periods of high synaptic activity from precursors present in the lipid membrane [47, 48]. Triggering of endocannabinoid synthesis has been proposed to occur through detection of high internal calcium concentrations [49] or through a G-protein activation mechanism [45]. The cannabinoids are then released to the synaptic cleft where they primarily bind to CB1 receptors on the pre-synaptic membrane, resulting in the G-protein mediated inhibition of voltage gated calcium channels [50], and activation of inwardly rectifying potassium channels, [51] ultimately reducing the likelihood for an action potential to occur. Moreover, CB1 and CB2 have been well documented to inhibit adenylyl cyclase activity upon activation, leading to the reduction of cyclic AMP (cAMP) levels [52–54]. Lower cAMP corresponds to decreased activity of Protein Kinase A (PKA), which results in a myriad of physiological processes, including inhibition of the release of the neurotransmitter GABA [55].

1.2.2 Endogenous Cannabinoids

Several endogenous cannabinoids have been characterized, but the main ligands are 2-Arachidonoylglycerol (2-AG) and anandamide (AEA). Although discovered after AEA, 2-AG is often considered to be the main endocannabinoid with concentrations 170 times greater than AEA [56]. 2-AG acts as a full agonist at both CB1 and CB2 [57–60] and has also been found to activate TRPV1 [61]. In contrast, AEA has reduced binding affinity compared to 2-AG and acts

as a partial agonist at both receptors [51, 62]. Both lipid-based cannabinoids are present as precursors in the plasma membranes and are synthesized rapidly in two distinct biosynthetic pathways upon stimulation [63, 64].

Although AEA acts as a partial agonist at CB1, it acts as a full agonist at transient potential vanilloid receptor TRPV1, in a non-retrograde method of endocannabinoid signaling [65]. Studies show that AEA activates TRPV1 in vagal efferent nerves and likely functions in a modulatory role in calcium dependent processes, rather than directly stimulating glutamate release [66]. Additionally, postsynaptic activation of TRPV1 by AEA in a CB1-independent manner stimulates long-term depression (LTD) of cells in the dentate gyrus [67] and nucleus accumbens [68], suggesting that AEA also targets non-cannabinoid receptors to modulate synaptic activity.

1.2.3 Phytocannabinoids

Cannabis Sativa, commonly referred to as cannabis, contains over 400 compounds which include cannabinoids, terpenes, nitrogenous compounds, hydrocarbons, sugars, and many more [69]. Two of the most prominent cannabinoids include delta-9-tetrahydrocannabinol (THC) and cannabidiol (CBD), which constitute the psychoactive and non-psychoactive components, respectively [2, 3]. The compounds are isomers of each other, characterized by a resorcinyl core with *para*-oriented terpenyl and pentyl groups [70]. Despite sharing nearly identical structures, the phytocannabinoids have very distinct biological activity, as discussed in the following sections.

1.2.4 Cannabinoid Receptors

As mentioned, two prominent receptors associated with the ECS are G-protein coupled receptors (GPCRs) CB1 and CB2 [44]. CB1 is regarded to be the most abundant GPCR in the central nervous system [71], with abundant expression found in the hippocampus and cerebellum [72], and specifically in projection neurons and within select interneurons of the striatum [73]. CB1 is primarily found in the presynaptic nerve terminal [74], but fluorescent imaging shows that CB1 is also present in periodic hotspots across the axons of inhibitory interneurons and associates with the cytoskeleton [75]. CB2, on the other hand, can be found primarily in peripheral tissues, especially in leukocytes [76], and other components of the immune system [77–80]. Although early northern blotting, RT-PCR and in situ hybridization experiments were not able to detect *cb2* expression in the central nervous system [81], emerging evidence suggests that *cb2* transcripts are present in distinct regions of the brain including the cerebral cortex [82, 83], hippocampus [82, 84–86], and brainstem [87], although at much lower levels than *cb1*.

THC has been described to be a partial or full agonist to CB1 and CB2 [88–90], which has been hypothesized to mediate the psychoactive effects. CBD is often described as an antagonist to CB1 and CB2 [90, 91], but Thomas et. al were the first to describe this action as inverse-agonism, due to the unexpectedly high efficacy at which CBD was able to antagonize synthetic agonists given its low affinity for either receptor [92]. As the ECS has been documented to have a basal level of tonic activity [93], CBD exerts the opposite effect than that of an agonist, thereby reducing baseline activity of the ECS [92]. In comparison, an antagonist would impart a neutral effect, which would only prevent further stimulation of the ECS, rather than affecting tonic activity. Therefore, the inverse agonism of CBD magnifies its inhibitory effect on the ECS, despite having low affinity for both CB receptors.

1.2.5 Transient Receptor Potential Channels

In addition to both classical cannabinoid receptors, endocannabinoids have been found to interact with receptors outside of the ECS. Notably, cannabinoids are able to modulate receptors part of the transient receptor potential (TRP) family of receptors, including ankyrin-rich TRPA1 [94–97] and vanilloid TRPV1 [94, 96–99], which has prompted some researchers to consider TRP channels as ionotropic cannabinoid receptors [95]. TRP receptors are primarily responsible for detecting sensory stimuli including thermosensation [100] and nociceptive stimuli [101], and as such are typically found in sensory neurons [102–104]. It has been theorized that most of the physiological effects of CBD activity are mediated through interactions with TRP channels [105]. In particular, activation of TRPV1 and TRPA1 channels results in desensitization to the stimuli, ultimately reducing nociception and likely accounting for the analgesic properties of CBD [106, 107].

Zebrafish express two paralogs of *trpa1* receptors – *trpa1a* and *trpa1b*. *Trpa1a* appears to be responsible for sensing chemical stimuli, whereas *trpa1b* may be responsible for thermosensation, however there is still disagreement surrounding *trpa1* receptors and their ability to sense temperature [102, 108]. Expression of *trpa1a* is localized to the posterior vagal sensory ganglion, while *trpa1b* is expressed in cranial sensory neurons, as well as Rohon-Beard neurons [109].

1.2.6 G-Protein Coupled Receptors

Similar to CB1 and CB2, several other G-protein coupled receptors have been identified and proposed to be modulated by endocannabinoids. One of the most promising candidates includes GPR55, a cannabinoid receptor identified in 1999 in rat and human brain tissue [110], and first

reported to be a potential cannabinoid receptor in 2006 [111]. Further studies reported expression found throughout the central nervous system – particularly in the dorsal root ganglia [112], as well as adrenal glands, and the gastrointestinal tract in adult mouse models [113]. THC is proposed to bind to, and activate GPR55 to increase intracellular calcium levels [112, 113]. In contrast, CBD does not act as an agonist at GPR55 [112, 113], and is instead capable of antagonizing the effects of synthetic cannabinoids [113], similar to its actions at other cannabinoid receptors.

Despite making waves as a novel cannabinoid receptor, very little is known about GPR55, such as its physiological function or role in the central nervous system [114]. This is true especially for zebrafish, which currently lack any form of expression data. There exists a large gap in our knowledge of this novel cannabinoid receptor, which must be characterized to determine its role within the ECS and early development.

1.3 Sonic Hedgehog Signaling Pathway

The sonic hedgehog (SHH) signaling pathway is critical during early embryonic development and has been implicated in a vast number of developmental functions including dorso-ventral [115] and neural tube [116, 117] patterning, bone formation [118, 119], cell proliferation [120–122], and organogenesis [123–125]. Canonical SHH signalling is initiated from the presence of sonic hedgehog (SHH), the ligand, binding to the Patched (PTCH) receptor, which relieves the PTCH-mediated suppression of Smoothened (SMO) by promoting internalization and degradation of PTCH (Figure 1) [126]. SMO is then trafficked to the primary cilia [127] where it initiates the downstream signaling cascade, ultimately resulting in the translocation of Gli family proteins to the nucleus and transcription of target genes [126]. Non-

canonical SHH signalling occurs without direct activation of SMO, and includes mechanisms that activates Gli transcription factors in the absence of SHH [128].

While this description represents a simplified mechanism of SHH signaling, the reality is much more complex. The SHH pathway exhibits cross-talk between numerous signaling pathways, including the fibroblast growth factor (FGF) [129, 130], Wnt [131], and Notch [132] signaling pathways, which introduces numerous avenues for modulation that exist outside of a simple hedgehog ligand-receptor interaction. One possible method of SHH modulation involves overlap with the endocannabinoid system, first documented by Khaliullina et. al [133]. They reported an in vivo inhibition of the SHH pathway by endocannabinoids in a *Drosophila* model organism, demonstrating that both endo- and phytocannabinoids are capable of binding to, and inhibiting the activation of SMO even in the presence of the SHH ligand, thus downregulating SHH signaling (Figure 1) [133].

This conclusion was supported by the Parnell research group, who furthermore documented an interaction between CB1 and SMO, suggesting that receptor dimerization allows both pathways to be modulated by both cannabinoids and SHH [134]. However, CB1 expression is nearly undetectable until 24 hpf [135], which is many hours following the time period investigated in this study. Therefore, simultaneous activation of CB1 and SMO receptors was not pursued, but, this discovery was nonetheless highly substantial as further evidence of crosstalk between the endocannabinoid system and the SHH pathway.

1.4 Zebrafish Development

Zebrafish are a prime model organism to study early development for a number of reasons. Females are capable of laying hundreds of eggs per clutch, and the large brood sizes are

extremely beneficial for high-throughput studies. Embryos develop rapidly, with morphogenesis of most organs complete by 2 to 3 dpf [136] and sexual maturity is reached at approximately two months post fertilization [137]. Embryos and chorions are largely transparent which allows development to be observed with ease compared to mammalian models such as mice or rats, in which dams must undergo surgery to extract embryos if early observation is necessary. Additionally, external embryonic development allows for tight control of external factors, decreasing the potential for confounding factors to affect experimental outcomes. In comparison, although murine models provide greater similarity to humans due to internal prenatal development, altered behaviour of the dam in response to cannabinoid exposures may unintentionally modify experimental outcomes in the pups. For example, changes in maternal feeding patterns following cannabinoid exposure may affect parameters such as body weight in the pups, raising questions of whether changes to these metrics can truly be attributed to prenatal cannabinoid exposure [138]. Nonetheless, a clear drawback to the zebrafish model is the lack of a maternal/embryo interaction, which more closely resembles the mechanism of prenatal cannabinoid exposure in humans.

Embryonic development in zebrafish can be divided into seven stages: zygote, cleavage, blastula, gastrula, segmentation, pharyngula, and hatching periods [136]. Following hatching, the fish are referred to as larvae. This study focuses on the time period of gastrulation, a critical timepoint in early development that results in the rearrangement of cells to form the three embryonic germ layers [139]. In zebrafish, the period of gastrulation occurs between 5.25 hours post fertilization (hpf) and 10.75 hpf, and includes the initiation of nervous system development at the induction of the neural plate [136]. Notably, the zygotic genome begins transcription at the midblastula transition directly preceding gastrulation [136]. Environmental pressures may now

have the opportunity to alter transcription rates of zygotic genes, which may be responsible for aberrant development linked to improper gastrulation.

Despite having simpler brain organization than humans, zebrafish share functionally similar structures and have highly conserved neurochemistry, including all primary neurotransmitter systems [140, 141]. Although direct implications regarding human health cannot be drawn from comparisons with zebrafish, this model organism serves as an excellent basis for teasing the mechanism underlying conserved physiological and developmental functions.

1.5 Zebrafish as models for ECS perturbation on Early Development

In the past several years, increased interest of the endocannabinoid system in development has resulted in numerous studies spanning different model organisms, particularly in zebrafish and murine models. The zebrafish in particular makes for a robust vertebrate model not only for the reasons stated above, but also due to a functioning endocannabinoid system that shares high similarity with mammals. Zebrafish *cb1* shares 69% sequence identity, and 73.6% amino acid identity with human *CB1* [135]. In contrast, *cb2* shares 39% of amino acid identity with human *CB2* [142].

Knock down of *cb1* using antisense morpholinos resulted in defects in the axonal growth of reticulospinal neurons, with disorganized fasciculi and an increased number of axons crossing the midline [143]. Additionally, the ECS has been proposed to couple with the FGF pathway to control axonal growth and guidance [144]. Taken together, there exists strong evidence that the CB1 receptor is involved in neurogenesis. Zebrafish with loss-of-function mutations of *cb2* showed no obvious changes in morphology, fertility, or mortality, but larvae at 6 dpf showed

altered swimming patterns, including both hyper- and hypo- activity in dark and light environments, respectively [145]. Despite having low expression levels in the brain, this receptor is currently being investigated for its role in neurogenesis, with conflicting evidence suggesting that *cb2* does, or does not contribute to neurodevelopment [146, 147].

Furthermore, this model organism is very well suited for screening toxicity of medicinal plants due to the ease of high-throughput studies and as such, has been used widely to screen dozens of plant-derived compounds [150]. Several studies have been recently published which examine both cognitive/behavioural and morphological effects of phytocannabinoids exposure in zebrafish development.

Carty et. al reported that developmental exposure to THC and CBD during the first 96 hpf results in dose-dependent morphological and behavioural toxicities, with the LC50 of CBD reported as nearly seven times lower than THC [149]. Morphological defects observed include parameters such as axial curvature, yolk sac and pericardial edema, and mortality, while behavioural assessments demonstrated hyperactivity at low concentrations and hypolocomotion at high concentrations. CBD and THC have both been linked to lowered longevity and health following developmental exposure [150, 151]. Studies showed THC to have a biphasic effect, suggesting that effects are seen at low and high concentrations, rather than following a simple dose-dependent response [150]. This biphasic response of THC has also been characterized on behavioural and physiological functions in rat models [152, 153].

Previous work in the Ali lab has demonstrated similar alterations in mortality, morphology, and locomotion as a result of developmental THC and CBD exposure [154, 155]. We have also demonstrated that exposures to both cannabinoids result in altered development in both primary

and secondary motor neuron branches, which appears to correspond with CB1's role in neurogenesis [154, 155].

As of yet, most research has been purely observational, but little has been done to uncover the molecular mechanism that directly cause the observed developmental effects – whether these are mediated through interactions within receptors part of the ECS, or other signaling pathways that share crosstalk with the ECS. As we learn more about the ECS in development, it is necessary to shift our focus towards elucidating mechanisms of the described developmental effects.

1.6 Research Objectives

Recent insight has shown that the ECS plays a role in early development, however the mechanism responsible for causing detrimental effects following perturbation of the ECS has yet to be characterized. Therefore, to address this gap in the literature, the overall purpose of this study is to develop a greater understanding of the ECS throughout development, including crosstalk with the SHH signaling pathway, which will provide a framework for elucidating the effects of perturbing the ECS by exposure to phytocannabinoids.

Two research objectives were designed to address this overarching purpose:

1. To visualize the expression pattern of key cannabinoid and cannabinoid-interacting receptors throughout early development

   Rationale: In recent years, receptors belonging to the ECS have been identified and characterized, however, little is known about spatial or temporal expression of these receptors throughout early development. Wholemount in situ hybridizations are a

technique in which probes bind to their mRNA target and produce a stain in the tissue present, allowing observation of gene expression temporally and spatially. By visualizing the expression pattern of key cannabinoid receptors, combined with RT-PCR to confirm the presence or absence of expression at a given timepoint, adverse developmental effects at specific timepoints, or affecting specific tissues, can be narrowed down to receptors present temporally or spatially. Timepoints spanning 6 hpf through 3 dpf were chosen to encompass early development, including processes of gastrulation, nervous system development, and organogenesis. A literature search produced six receptors that are the most likely to be modulated by interactions with endo- and phytocannabinoids. I hypothesized that each receptor would be expressed within this period of early development, and likely present within the central and peripheral nervous systems. This study will serve as a comprehensive resource outlining the expression of cannabinoid receptors throughout early development as a foundation for further investigations.

2. To determine if adverse effects of CBD exposure are mediated through downregulation of the SHH signaling pathway

   Rationale: Recent evidence suggests that endocannabinoids and phytocannabinoids are potent inhibitors of the SHH signalling pathway by binding to and inhibiting the activity of SMO, even in the presence of SHH [133]. Additionally, past research shows that developmental exposure of cannabinoids results in detrimental morphological and behavioural effects to zebrafish embryos. As the SHH signaling pathway is known to organize many developmental events, downregulation of this pathway may be responsible for the toxic and teratogenic effects of phytocannabinoids during early

development. Therefore, I hypothesized that CBD is exerting its teratogenic effects by downregulating activity of the SHH pathway at the SMO receptor. By increasing SMO activity in the presence of CBD, deleterious effects of phytocannabinoid exposure such as decreased survival/hatching rates, reduced body length, decreased behaviour, and aberrant gene expression of SHH pathway components should be ameliorated. Furthermore, downregulating the SHH pathway using a known antagonist against SMO should result in similar morphological and behavioural outcomes compared to CBD exposures. Such results would support the hypothesis that the teratogenic effects of phytocannabinoids are mediated through downregulation of the SHH signalling pathway.

By addressing both objectives, this study increases our understanding of the endocannabinoid system, while also providing insight into the mechanism by which phytocannabinoids may interact with signaling pathways adjacent to the ECS to exert its teratogenic effects.

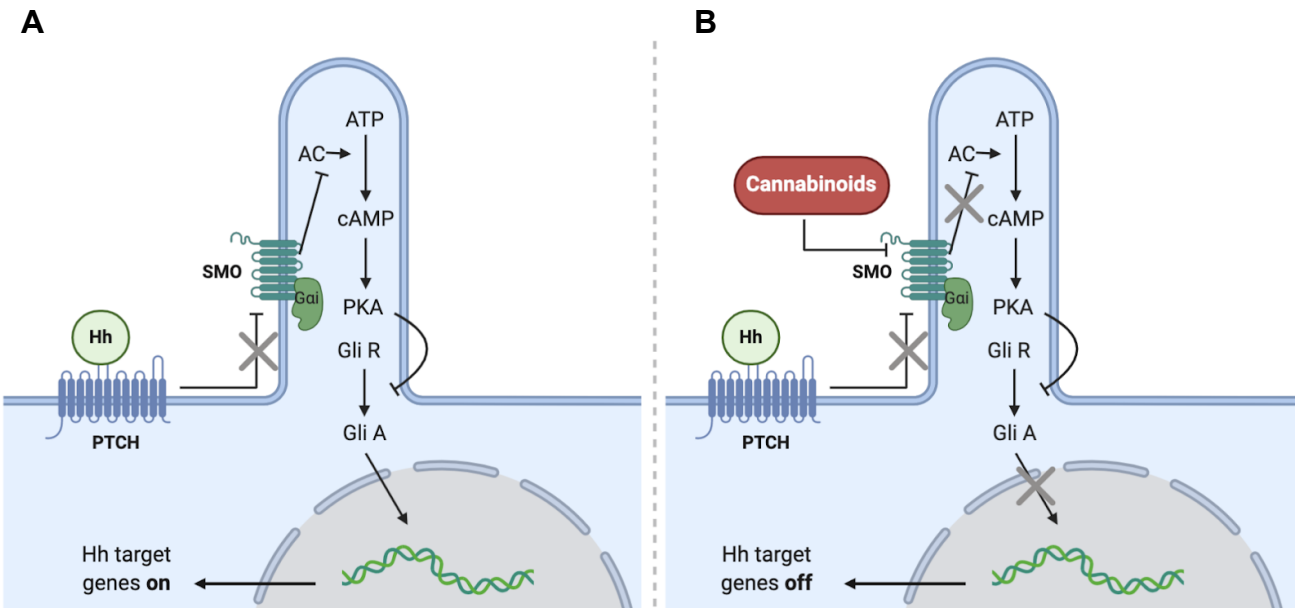
A
ATP
AC
cAMP
SMO
Gαi
PKA
Hh
Gli R
PTCH
Gli A
Hh target
genes on
B
Cannabinoids
ATP
AC
cAMP
SMO
Gαi
PKA
Hh
Gli R
PTCH
Gli A
Hh target
genes off

Figure 1. Mechanism of canonical signaling of the Sonic Hedgehog (SHH) Pathway and proposed mechanism of cannabinoid-mediated downregulation. **A)** The SHH pathway is stimulated by the presence of the hedgehog (HH) ligand, which binds to the Patched (PTCH) receptor. PTCH is internalized, relieving the suppression of Smoothened (SMO) and SMO translocates to the primary cilium to activate the signalling cascade by inhibiting adenylyl cyclase (AC). AC no longer converts ATP to cyclic AMP (cAMP), which reduces activation of Protein Kinase A (PKA). In the absence of PKA, the activated form of Gli transcription factors (Gli A) is predominant, and translocates to the nucleus to activate transcription of SHH target genes. **B)** In the presence of cannabinoids, the lipid compounds directly bind and inhibit SMO, preventing activity even in the presence of the HH ligand. PKA ultimately catalyzes proteolysis of Gli A into the repressor form Gli R and hedgehog target genes remain off. Figure adapted from Fish et. al 2019 [134] and created using BioRender.

2. Materials and Methods

2.1 Animal Care

Wild type (WT) zebrafish (*Danio rerio*) of the Tupfel long-fin (TL) strain were housed in the University of Alberta Aquatic Facility and used in accordance with the University of Alberta Animal Care and Use Committee guidelines, under protocol AUP00000816. Approximately 15 adult fish were kept in each tank and maintained at a standard 14L:10D cycle at 28°C. During breeding, either 2 females and 1 male, or 3 females and 2 males were placed into breeding tanks the evening prior to egg collection. The following morning, fertilized eggs were collected, placed in embryo media (EM; 60 mg/L Instant Ocean) and transferred to an incubator at 28.5°C. For in situ hybridization experiments, embryos post gastrulation were incubated in a 0.0045% 1-Phenyl-2-Thiourea (PTU) solution in EM to prevent melanization [156].

2.2 Receptor Expression Developmental Outline

2.2.1 RT-PCR

Reverse-Transcriptase (RT) PCR was conducted to detect the presence or absence of mRNA transcripts at each timepoint of interest. Primers were designed to span at least one exon-exon boundary for each of the six candidate genes and produced an amplicon between 600-900 bp in length. EF1α was chosen as a control gene due to relatively stable expression throughout zebrafish development [157]. Primer sequences can be found in Table 1.

Total RNA was extracted using TRIzol from WT zebrafish embryos at 6 hpf, 12 hpf, 1 dpf, 2 dpf, and 3 dpf. RNA was pooled between approximately 50 embryos for 6 hpf, to 30 embryos at 3 dpf to ensure adequate concentrations. Following RNA extraction, samples were quantified using a Nanodrop and adjusted to a final concentration of 500 ng/mL. A total of 1µg was used

for cDNA synthesis, which was completed using Maxima H Minus First Strand cDNA Synthesis Kit (ThermoFisher). cDNA was diluted from an original volume of 20 µL to 50 µL with nuclease free water.

Following cDNA synthesis, PCR was conducted using the DreamTaq DNA Polymerase (ThermoFisher) at 30 cycles. 10 µL of PCR product (5 µL of EF1α) of was loaded on a 1% agarose gel, run for 30 minutes (100V) and imaged at an exposure of 400 m/s. Relative expression of each gene was determined by visual assessment of band intensity in comparison between the timepoints tested.

2.2.2 Probe Design and Synthesis

Primers were designed to span at least one exon-exon boundary on the cDNA template, with the reverse primer containing a T3 or T7 RNA Polymerase promoter at the 5' end. Primer sequences can be found in Table 2. Primers sequences for *ptch2* were taken from Thisse and Thisse (2008) [158], and sequences targeting *cb2* were taken from Colon-Cruz et al (2020) [159]. PCR at 35 cycles was performed on zebrafish cDNA at timepoints showing high expression, as observed by the RT-PCR timeline. The resulting PCR product was verified by gel electrophoresis (100V for 30 min on a 1% agarose gel), cleaned using a Qiagen PCR Cleanup Kit and quantified using a Nanodrop. 1 µg of product, adjusted to a volume of 14 µL with nuclease free water, was used as a template for in vitro transcription (IVT) alongside RNA transcription buffer (New England Biolabs), Digoxygenin-labeled RNA (Sigma), T3 or T7 RNA polymerase (New England Biolabs), and RNasin® Ribonuclease Inhibitor (Promega). The IVT reaction was incubated at 37°C for four hours and then cleaned up to remove unincorporated nucleotides, template, and enzyme using the Monarch® RNA Cleanup Kit (New England

Biolabs). 1 µL of the resulting product of the resulting IVT reaction was run out on a 1% agarose gel for 30 min (100V) and imaged to confirm integrity and yield of the transcript.

Once confirmed, 5 µL of the probe mixture was added to 995 µL of hybridization media (HM) (50% formamide, 5X SSC buffer [20X stock: 3M NaCl, 300mM trisodium citrate, pH 7.0], 50µg/mL heparin [Sigma], 500µg/mL Type II-C Ribonucleic acid from torula yeast core [tRNA replacement; Sigma], 0.1% Tween-20 [Fisher Scientific], 0.092M Citric acid) for a ratio of 1:200. Probe to HM ratios were adjusted to 1:100 or 1:50 in cases of IVT reactions that resulted in a low yield of product, or genes that failed to show any staining patterns.

2.2.3 In Situ Hybridization

The in situ hybridization protocol was modified from Thisse and Thisse (2008) [156]. Zebrafish embryos were collected in 4% paraformaldehyde (PFA) at 6 hpf, 12 hpf, 1 dpf, 2 dpf and 3 dpf. At timepoints older than 1 dpf, embryos were treated with 0.0045% PTU after gastrulation to prevent melanization and dechorionated before collection. Following overnight fixation at 4°C, embryos were washed 1 x 15 min in methanol and stored at -20°C.

Embryos were rehydrated in a series of ascending PBST:Methanol solutions and washed for 5 x 5 min in PBST. Embryos at 6 hpf and 12 hpf were dechorionated after two PBST washes. Embryos 1 dpf and older were then permeabilized in 10 µg/mL of Proteinase K (1 dpf), or 20 µg/mL (2 and 3 dpf) and fixed for 20 minutes in 4% PFA at room temperature to deactivate the enzyme. Following 5 x 5 min PBST washes, embryos were prehybridized in HM at 65°C for 1-3 hours, then hybridized with 500 µL of probe in HM overnight. A negative control was conducted in which embryos were incubated in HM in the absence of probe to sense background stain caused by NBT/BCIP in the colouration reaction.

The following morning, probe was removed and stored at -20°C. Samples were washed in a series of ascending 2X SSC:HM solutions at 65°C to remove unbound probe, before being exhibited to higher stringency washes at 0.2X SSC + tween and 0.1X SSC + tween to ensure that non-specific binding is removed. After the high-stringency washes, embryos were washed in ascending PBST:0.2X SSC solutions at room temperature and gently rocked in blocking solution (PBST, Bovine Serum Albumin (BSA) (Sigma-Aldrich), Sheep Serum (Sigma-Aldrich)) for 1-3 hours. After blocking, embryos were rocked in a solution of 1:5000 Anti-Digoxygenin-AP Fab fragments (Millipore Sigma) in block solution at 4°C overnight.

After blocking, embryos were gently washed for 7 x 15 min in PBST at room temperature to remove unbound antibody. Then, samples were rinsed for 4 x 5 min in colouration buffer (Tris-HCl, $MgCl_2$, NaCl, and tween) and incubated in coloration buffer plus NBT/BCIP for 2-4+ hours at room temperature. For weaker expression patterns that require longer staining, embryos were stored at 4°C overnight and continued to colour at room temperature the next day. Samples were observed under a dissecting microscope periodically until staining was observed. When adequate staining was reached, samples were rinsed quickly 2-4x in methanol, then washed for 2 x 10 min in methanol and stored at 4°C. Prior to imaging, embryos were rehydrated in ascending PBST:Methanol washes, then incubated in 30%, 50%, and 70% glycerol/PBST for 15 min each. Finally, embryos were mounted in 100% glycerol and imaged under a dissecting microscope.

2.3 SHH Pathway Upregulation

A comprehensive overview of experiments directed towards determining CBD mediated downregulation of the SHH pathway can be found in Figure 2.

2.3.1 Purmorphamine and Cannabidiol Exposure Paradigm

Zebrafish mates were set up as described in section 2.1. After collection, embryos were separated into groups of 25 and placed in 3.5 mm x 10 mm petri dishes with 4 mL of embryo media. At 4.75 hpf, embryos were incubation in either 0.2% DMSO, or 20 µM, 10 µM, 5 µM or 1µM of purmorphamine (PM) (Sigma, SML0868). After 30 minutes of preincubation, 0.3% methanol or 3 mg/L of CBD (Sigma, C-045) was added to the appropriate dish. An untreated control group was run simultaneously with the absence of all compounds. The embryos were returned to the incubator at 28.5°C for the duration of gastrulation (5.25 hpf to 10.75 hpf). At 10.75 hpf, each plate was rinsed three times in embryo media then returned to the incubator to continue development. Embryo survival and hatching rates were recorded each morning from 1 dpf to 5 dpf.

Embryos saved for in situ hybridization analysis were collected at either 10.75 hpf or 1 dpf, fixed overnight in 4% PFA, and then probed for *ptch2* following protocols described in Sections 2.2.2 and 2.2.3.

2.3.2 Swim Bladder Quantification

Following the PM exposure paradigm described in Section 2.3.1, larvae were grown until 5 dpf, then anaesthetized in 0.02% tricaine and imaged under a 5X objective lens using a Lumenera Infinity2-1R colour microscope camera mounted on a Leica DM 2500 microscope to capture swim bladder (SB) inflation. Following imaging, larvae were scored on the basis of full SB inflation (Figure 13A), or partial/no SB inflation (Figure 13B, C). The results were compiled in GraphPad Prism 9.

2.3.3 Cyclopamine Exposure Paradigm

Zebrafish mates were set up, and embryos were collected and prepared as described in sections 2.1 and 2.3.1. Embryos were exposed to 3 mg/L CBD (Sigma), 1% DMSO, 25 μM, 50 μM, or 100 μM of cyclopamine (Sigma-Aldrich) throughout the duration of gastrulation (5.25 hpf to 10.75 hpf). At 10.75 hpf, embryos were rinsed thoroughly three times and returned to the 28.5°C incubator to continue development until 5 dpf. Embryo survival and hatching rates were recorded each morning from 1 dpf to 5 dpf. Larvae were preserved in 4% PFA at 5 dpf and imaged under a dissecting microscope at 3X magnification.

2.3.4 Morphology and Length Measurements

Larvae at all drug treatments and concentrations were collected at 5 dpf, placed under a dissecting microscope, and imaged at 3X magnification using AOS Imaging Study V3 software. The length of each larvae was measured in millimetres with ProAnalyst and measurements were compiled in GraphPad Prism 9. Following length measurements, larvae were anaesthetized in 0.02% tricaine and captured under a 2.5X objective lens using a Lumenera Infinity2-1R colour microscope camera mounted on a Leica DM 2500 microscope to visualize overall morphology.

2.3.5 Locomotion

To track locomotor activity of CBD and PM treated larvae, individual larvae following the PM exposure paradigm outlined in Section 2.3.1 were placed in single wells of a 96-well plate at 5 dpf. Larvae were positioned in the centre of wells containing 150 μL embryo media and plates were placed atop of an infrared backlight source. Plates were left on the light source for 60 minutes prior to video recording to allow larvae to become acclimated. Half of the wells per 96-

well plate (Costar #3599) were observed per run. A Basler GenlCaM (Basler acA 1300-60) scanning camera with a 75 mm f2.8 C-mount lens, provided by Noldus (Wageningen, Netherlands) was used to track movement of each individual larvae for periods of one hour.

EthoVision ® XT-11.5 software (Noldus) was used to quantify the average percentage of activity over the period of 1 hour, average speed (cm/s), the frequency of swim bouts, and the total distance travelled (mm). To exclude background noise, ≥ 0.2 mm was defined as active movement. Activity was defined as % pixel change within a corresponding well between samples as reported previously [160]. Results were compiled in GraphPad Prism 9.

2.3.6 Statistics

All statistics were performed on GraphPad Prism 9. Survival, hatching, length measurements, and locomotion assays were analyzed using One-Way Anova and significance was further explored with a Tukey post-hoc multiple comparisons test to assess significance between specific treatment groups. Swim bladder inflation was assessed using Fisher's Exact Tests to compare the proportion of inflated and non-inflated swim bladders between treatment groups. All values are reported as means +/- Standard Error of Means (SEM).

Table 1. Reverse-Transcriptase PCR Primers

Gene	zFIN ID	Forward Primer (5' – 3')	Reverse Primer (5' – 3')
cb1	ZDB-GENE-040312-3	GATCTCCTCGGCAGTGTTATATTC	TCCGACTCCAGGCTGTTAT
cb2	ZDB-GENE-040702-7	GGGCAGTATGAGGAAGATGTG	GAAGCCTGGTAGATGCAAAGA
trpv1	ZDB-GENE-030912-8	GCGATTGAAAGGAGGAGTATGA	CCTTCCCTTCTTCGTGGTAAA
trpa1a	ZDB-GENE-050105-6	ATCCACTGCTCTCCACTTTG	GACCTGACCAACCTCTGTAATC
trpa1b	ZDB-GENE-050106-1	CCTCACATACCTCATCCTCAATC	TCTCCTACAGCCAAACCAATC
gpr55a	ZDB-GENE-051113-260	CCTGCTCTACGTCAACATCTAC	GTATCGCCATTCTCCTCTCT T T
ef1α	ZDB-GENE-990415-52	GGACTTTCCGGAGTCGACGTGGCC	CCTTACAGCCAGGCTCGTTTTGA

Table 2. In Situ Hybridization PCR Primers

Gene	zFIN ID	Forward Primer (5' – 3')	Reverse Primer (5' – 3')	Probe Length (bp)
cb1	ZDB-GENE-040312-3	GATCTCCTCGGCAGTGTTATATTC	ATTAACCCTCACTAAAGGGTCCGACTCCAGGCTGTTAT	809
cb2	ZDB-GENE-040702-7	GATCAAGAAGCTACGACTGTGC [161]	ATTAACCCTCACTAAAGGGACTACCACTCACTGCCGGAT [159]	1080
trpv1	ZDB-GENE-030912-8	GTCTTGCCTTGAGCTGGATAA	ATTAACCCTCACTAAAGGGCTCTGAACGTTAGCTGGAGAAG	811
trpa1a	ZDB-GENE-050105-6	CAAAGCACACCTGCTCAATATG	ATTAACCCTCACTAAAGGGCCAAAGTCAAATCAGGGAAAG	660
trpa1b	ZDB-GENE-050106-1	CCTCACATACCTCATCCTCAATC	ATTAACCCTCACTAAAGGGAGAAGAATGGGCATGAGAAGA	655
gpr55a	ZDB-GENE-051113-260	CAGCATGTAGCGGAAACTTAAAC	ATTAACCCTCACTAAAGGGGAGAACTGCTGGAAACAGTAA	667
ptch2	ZDB-GENE-980526-44	TCCTGTGCTGTTTCTACAGG [158]	ATTAACCCTCACTAAAGGGAATGCGCAGAACAAGTTATAGG [158]	740

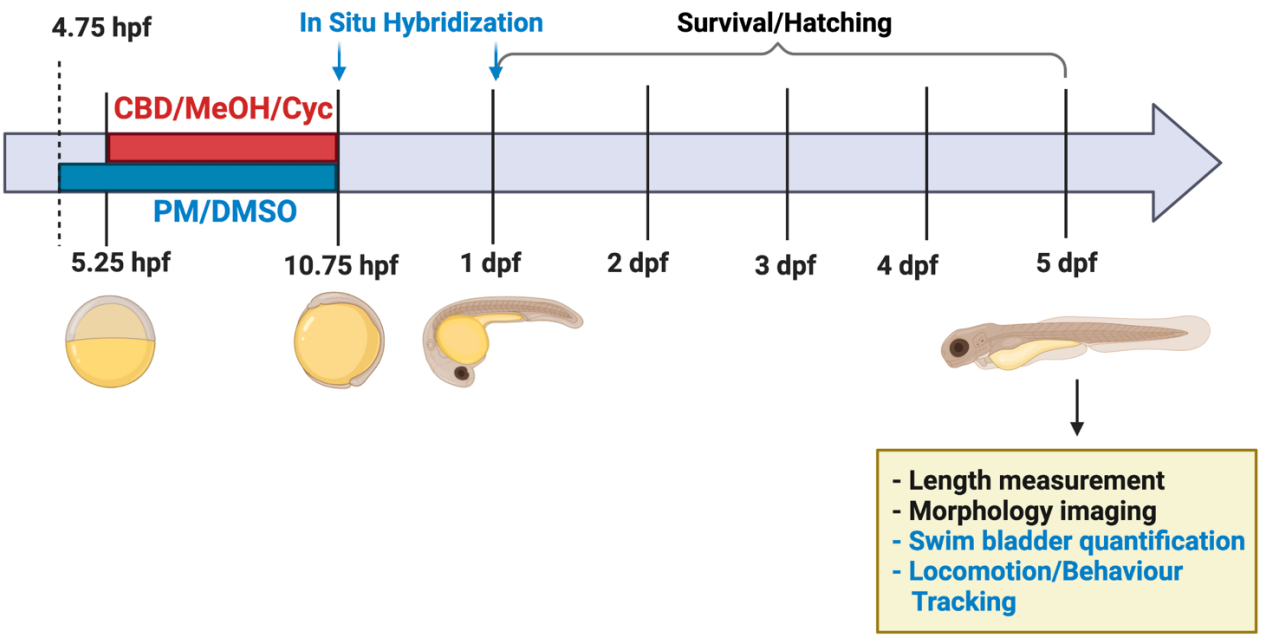
4.75 hpf
In Situ Hybridization
Survival/Hatching
CBD/MeOH/Cyc
PM/DMSO
5.25 hpf
10.75 hpf
1 dpf
2 dpf
3 dpf
4 dpf
5 dpf
- Length measurement
- Morphology imaging
- Swim bladder quantification
- Locomotion/Behaviour Tracking

Figure 2. Outline of experiments investigating the role of the Sonic Hedgehog Pathway (SHH) on mediating detrimental effects from cannabidiol (CBD) exposure during gastrulation. Embryos were exposed to purmorphamine (PM) or dimethyl sulfoxide (DMSO) at 4.75 hpf, 30 minutes prior to gastrulation. During gastrulation, embryos were co-exposed to CBD or methanol (MeOH). Cyclopamine (Cyc) or DMSO was administered throughout gastrulation without the presence of PM to compare to CBD treatment alone. Embryos were incubated at 28.5 °C and rinsed thoroughly at 10.75 hpf to remove compounds from the media. CBD and PM treated embryos were preserved at 10.75 hpf and 1 dpf to analyze *ptch2* expression pattern by in situ hybridization. All treatment groups were monitored daily from 1 to 5 dpf to assess hatching/survival rates, and then imaged at 5 dpf to record body lengths and overall morphology. At 5 dpf, CBD and PM treated embryos were also assessed for swim bladder inflation levels and free-swimming behaviour.

3. Results

3.1 Endocannabinoid System Developmental Timeline

3.1.1 Cannabinoid Receptors

RT-PCR of *cb1* mRNA reveals that expression begins with relatively low levels at 12 hpf, and increases throughout development (Figure 3A). This is observed by no stain at 6 hpf (Figure 3B), and despite the presence of a faint band signaling the presence of transcript at 12 hpf, expression was likely too low to be detected by in situ hybridization (Figure 3C). Staining is first observed in 1 dpf embryos, with expression spatially restricted to the preoptic area (PA) and the lens (Figure 3D-E). Expression is limited to specific structures in the brain at 2 and 3 dpf, including the telencephalon, tegmentum, and the hypothalamus, consistent with previously published in situ hybridization data (Figure 3F-I) [135]. Additionally, staining can be seen in the lens at 2 dpf (Figures 3F, G), and to the liver/gut region at 3 dpf, which corresponds to its role in liver development and metabolism (Figure 3H, I) [162].

Cb2 has proven to be a difficult gene to characterize via in situ hybridization. The receptor is commonly associated with immune function [77, 78], but emerging evidence suggests that expression is present in the brain, although at levels that may be too low to detected by in situ hybridization [81]. Limited published in situ hybridization data shows *cb2* expression in the liver [162] and in hair cells within neuromast structures [159] in zebrafish embryos.

RT-PCR data shows that *cb2* expression is present at 6 hpf, ceases by 12 hpf, and is expressed at relatively low levels from 1 to 3 dpf (Figure 4A). Similarly, in situ hybridization data shows a stain at 6 hpf, verified by the lack of a stain shown in the no-probe control, and no stain present in 12 hpf embryos (Figure 4B-D). Although the RT-PCR data showed expression from 1 to 3 dpf, no expression was seen at ages older than 6 hpf (Figure 4E-G).

3.1.2 Transient Receptor Potential Channels

Trpv1 begins expression at 1 dpf, and expression levels are fairly consistently from 1-3 dpf (Figure 5A). RT-PCR data is supported by the lack of a stain at 6 and 12 hpf (Figure 5 B-C). At 1 dpf, expression is localized to the trigeminal sensory neurons, posterior and anterior lateral line neurons and the Rohon-Beard neurons, which are transient sensory neurons that exist along the length of the body (Figure 5D-E). This expression pattern is consistent with published in situ hybridization data [163]. At 2 and 3 dpf, expression is limited to the trigeminal sensory neurons and the posterior/anterior lateral line neurons (Figure 5F-I).

Trpa1a expression begins much later in development, and is only perceptible beginning at 3 dpf (Figure 6A). As such, in situ hybridization data showed no staining from 6 hpf to 2 dpf (Figure 6B-E). At 3 dpf, expression is highly localized to a small cluster of cells identified as the vagal sensory ganglion, as consistent with previously published data (Figure 6F-G) [109].

Trpa1b begins expressing at relatively low levels at 1 and 2 dpf, with increased expression at 3 dpf (Figure 7A). Probes targeting fish at 3 dpf show expression in the trigeminal sensory neurons as well as anterior and posterior lateral line neurons (Figure 7F-G), which is consistent with previous in situ hybridization data [102]. However, I have not been able to detect a stain at 1 or 2 dpf (Figure 7D-E), likely because my current protocol does not have the required level of sensitivity. It is possible that transcript abundance per cell is too low to stimulate visible staining in comparison to *trpa1a* expression, which also showed very low expression (Figure 6A), but localization of transcripts to a small region of cells allowed the signal to be detected.

3.1.3 G-Protein Coupled Receptor 55

Gpr55 shows relatively low expression from 12 hpf to 3 dpf (Figure 8A). While adult mouse models have demonstrated expression in brain tissue and the gastrointestinal tract [113], embryonic expression is unknown. Additionally, expression data is not available in zebrafish models at any timepoint. In situ hybridizations were not able to detect a stain at 12 hpf or 1 dpf (Figure 8B-E). A faint hindbrain stain can be seen in 2 dpf embryos (Figure 8F), in addition to diffuse staining throughout the head and brain region was at 2 and 3 dpf. This non-specific stain was verified by no staining present in the no-probe control (Figure 8F-J).

3.2 Investigating Cannabidiol mediated downregulation of the SHH pathway

3.2.1 Counteracting downregulation of SHH activity with Purmorphamine

Co-incubation of PM at each concentration improved the overall morphology of the larvae at 5 dpf compared to CBD treatment alone ($p < 0.0001$, N = 5 experiments, n = 42-80 total fish per treatment) (Figure 9A-F). All four concentrations of PM at 1 μM, 5 μm, 10 μM and 20 μM were sufficient at stimulating increased body lengths in the presence of CBD (Figure 9G). CBD treated fish had an average body length of 2.7 ± 0.09 mm, compared to body lengths of 3.15 ± 0.05 mm, 3.40 ± 0.03 mm, 3.49 ± 0.02 mm, and 3.44 ± 0.02 mm for co-exposures of 1 μM, 5 μM, 10 μM, and 20 μM, respectively. Fish exposed to 5-20 μM PM and CBD resulted in a 29% increase in body length compared to fish treated with CBD alone. There was no difference between fish treated with 5, 10, and 20 μM of PM, but all three concentrations demonstrated a significant increase compared to fish treated with 1 μM ($p < 0.0001$). Notably, PM was not able to rescue larvae to lengths exhibited by the untreated control or vehicle control, which had an average of 3.75 ± 0.02 mm and 3.73 ± 0.02 mm, respectively ($p < 0.0001$). 10 μM and 20 μM of PM, on its own, were capable of reducing body length ($p < 0.01$, Figure 10). Both concentrations

resulted in an average body length of 3.59 ± 0.19 mm. CBD and CBD co-treated with DMSO, the vehicle for PM, did not exhibit significant differences in body length (Figure 10). This data shows that activation of the SHH pathway by PM prevents CBD-mediated effects on body lengths.

Increased survival rates were apparent for embryos treated with CBD and 5, 10, and 20 μM of PM beginning at 1 dpf, compared to treatments with CBD alone (N=5 experiments, n=125 total fish per treatment) (Figure 11A). Embryos co-treated with PM range from an average of 60.8% to 78.4% survival, to just 38.4% survival for CBD alone. By 5 dpf, the survival rate of CBD treated embryos falls to just 25.6%, while the range for CBD and PM treatments are at 60.8% to 75.2% survival, with each concentration showing a significant increase in survival ($p<0.05$). This parameter follows a dose-dependent trend, with survival rates averaging at 60.8%, 66.4%, 72%, and 75.2% corresponding to CBD + 1, 5, 10, and 20 μM respectively. By 5 dpf, there is no significant difference between any of the PM treated embryos compared to the vehicle control, which had an average survival rate of 73.6% ($p>0.05$). There was no significance in survival rates between any PM treatment on its own, the vehicle control, or untreated control ($p>0.05$) (Figure 11B).

Hatching rates were improved for all concentrations except 1 μM PM (N = 5, n = 125 total fish per treatment) (Figure 12A). Improved hatching rates were apparent beginning at 3 dpf, and both 10 μM and 20 μM of PM were able to stimulate 100% hatching rates at 4 dpf, compared to just 15.8% for CBD treated fish ($p<0.0001$). There was no difference between the hatching rate of all PM treatments on their own, vehicle control, or the untreated control ($p>0.05$) (Figure 12B).

3.2.2 Assessing Swim Bladder Morphology

Larvae treated with CBD were demonstrated to have improper swim bladder (SB) inflation by 5 dpf (Figure 13). SB morphology ranges from fully inflated (Figure 13A), partially inflated (Figure 13B), and non-inflated (Figure 13C). Partially and non-inflated SB morphologies were grouped together due to the difficulty in scoring for the presence or absence of a SB from light microscopy.

Notably, high concentrations of PM are able to induce improper SB inflation in a dose-dependent pattern. Embryos treated with 1 μM and 5 μM of PM resulted in 91.7% and 90.4% of larvae having fully inflated embryos by 5 dpf, which was not significantly different from the vehicle control at 90.4% ($p>0.05$, N = 4 experiments, n = 36-73 total fish per treatment) (Figure 13D). Treatment groups of 10 and 20 μM PM resulted in just 64.8% and 46.3% of larvae with fully inflated SBs, which demonstrated significance compared to the vehicle control ($p<0.001$, N = 4 experiments, n = 67-91 total fish per treatment). However, both concentrations still exhibited greater percentages of properly inflated SBs compared to CBD, which only resulted in 10% of fish with full inflation ($p<0.001$, N = 4 experiments, n = 58-91 total fish per treatment).

Surprisingly, only co-treatments of 1 μM and 20 μM PM with CBD were able to increase the level of fully-inflated SBs, with 40.5% and 31.0% larvae demonstrating full inflation, respectively (Figure 13D) ($p<0.05$, N = 4 experiments, n = 37-58 total fish per treatment). Although a degree of rescue was observed, the SB inflation rates were statistically significant compared to the vehicle control ($p<0.0001$, N = 4 experiments, n = 37-73 total fish per treatment), indicating that the rescue did not achieve levels of full SB inflation of fish unexposed to CBD. Co-treatment of 5 μM and 10 μM of PM with CBD only resulted in 17.1% and 15.1%

full inflation, which were not significant compared to CBD ($p>0.05$, N = 4 experiments, n = 41-58 total fish per treatment).

3.2.3 Locomotion/behaviour Following Upregulation of the SHH pathway

Previously, we have shown that zebrafish embryos exposed to THC during gastrulation demonstrate reduced free-swimming activity [155]. To determine if CBD has the same effect on locomotion, and whether PM is able to mediate those effects, free-swimming behaviour of CBD and CBD plus PM treated embryos as described previously were assessed at 5 dpf (Figure 14). Control treatments of the two highest concentrations of PM, 10 and 20 μM, were assessed on their own to determine if PM itself affects swimming behaviour.

CBD demonstrated significantly reduced activity at all four metrics including total distance travelled (mm), average speed (cm/s), frequency of movement per hour, and percent activity per hour (N = 4 experiments, n = 46-61 total fish per treatment group). At each metric, I observed trends in increased activity for embryos treated with CBD and PM, however, the only statistically significant increase in activity occurred in two metrics: the total distance travelled, and the frequency of movement for larvae treated with CBD and 10 μM PM. For total distance, CBD treated fish travelled an average of 44.0 ± 8 x 10 mm, whereas larvae treated with CBD + 10 μM covered 232 ± 28 x 10 mm ($p<0.05$, N = 4 experiments, n = 22 –59 total fish per treatment group) (Figure 14A). Larvae treated with 1, 5, and 20 μM PM travelled a total of 210 ± 46 x 10 mm, 189 ± 28 x 10 mm, and 183 ± 65 x 10 mm respectively, which although appear to have a large increase in activity, are not considered to be statistically significant due to the large amount of variation within each treatment group.

The second parameter, which was frequency of movement, also saw a significant increase in the number of movements per hour of fish treated with CBD and 10 μM PM compared to the CBD control (N=4 experiments, n=24-64 total fish per treatment group) (Figure 14C). CBD treated fish had an average of 79.0 ± 15 movements per hour, whereas co-treatment with 10 μM PM increased the frequency to 404 ± 76. However, this metric was also statistically significant compared to the vehicle control, which measured an average of 687 ± 122 movements per hour, suggesting that although 10 μM of PM was able to increase activity, it could not stimulate activity to the level of the vehicle control ($p<0.05$). It was also seen that embryos treated with 10 and 20 μM PM alone, as well as embryos treated with CBD and 1 μM PM, also demonstrated a significantly reduced level of activity compared to the vehicle, of 187 ± 62, 281 ± 63, and 425 ± 115 movements per hour, respectively. Co-exposures of 5 μM and 20 μM of PM demonstrated frequencies of 314 ± 45 and 236 ± 65, which showed a trend in increased activity compared to the CBD control, but were not considered to be statistically significant.

There were no significant differences between CBD and PM treated fish in the average speed of movement, or the percentage of time spent actively moving, despite both parameters showing a trend of increased activity for PM treated fish (N=4, n = 22-63 total fish per treatment) (Figure 14B, D).

3.2.4 Investigating Regulation of *ptch2* Expression

To determine whether CBD and PM exposure is capable of altering the expression of SHH pathway components, in situ hybridization was performed using a probe targeting *ptch2*, a key receptor in the SHH pathway that regulates activity of SMO, following the procedures outlined in Section 2.2.2, 2.2.3, and 2.3.1. Embryos were preserved either directly following CBD and

PM exposure at 10.75 hpf, or at 1 dpf, to give an overview of gene expression during, and following exposure to the compounds of interest. 10.75 hpf embryos were assessed three times, and 24 hpf embryos were performed twice, with 10-20 embryos probed per treatment for each experiment.

These results revealed that expression of *ptch2* appears to decrease following CBD exposure, which is maintained for co-exposures of 1 and 5 μM of PM (Figure 15A-C). Interestingly – expression of *ptch2* within the adaxial cells, which are precursors to slow muscle, appears to be disorganized. While expression of *ptch2* normally resembles two parallel tracts running along the neural plate [164], as demonstrated by the vehicle control and 20 μM exposures (Figure 13E-F), the pattern deviates and results in large gaps between the tracts, which appears to be corrected with the co-exposure of 20 μM PM (Figure 15D). Expression increases for embryos treated with CBD + 20 μM PM, 20 μM itself, and the vehicle control (Figure 15D-F).

Ptch2 expression appears to be mostly restored by 1 dpf. CBD treated fish may have slight reduction of *ptch2* expression in the diencephalon compared to the vehicle control and 20 μM alone (Figure 16A, E-F), but is restored in embryos treated with 1, 5, and 20 μM PM (Figure 16B-D). However, due to the semi-quantitative nature of in situ hybridizations, measures such as quantitative PCR must be undertaken before conclusions can be made about gene expression levels.

3.2.5 Downregulating SHH Activity with Cyclopamine

To confirm that teratogenic effects of CBD are mediated through downregulation at SMO, embryos were treated with cyclopamine, a known SMO agonist throughout gastrulation at

concentrations of 25, 50, or 100 μM, monitored through the first five days of development, and then imaged at 5 dpf.

Embryos treated with cyclopamine demonstrated shortened lengths, axial curvature, and pericardial edema by 5 dpf, all of which are common morphologies of embryos treated with CBD (Figure 16A-F). Decreased body lengths were observed in a dose-dependent trend, with average length measurements of 2.89 ± 0.10 mm, 2.176 ± 0.04 mm, and 1.524 ± 0.02 mm for 25 μM, 50 μM, and 100 μM of cyclopamine exposures, respectively (Figure 16G) (N=3 experiments, n=42-50 total fish per treatment). This was compared to an average of 3.8 ± 0.02 mm for DMSO-treated fish, and 3.33 ± 0.06 mm for CBD treated fish. However, it is important to note that previous experiments resulted in an average of 2.7 ± 0.09 mm for CBD treated fish (Figure 9G) (N=5 experiments, n=42 total fish), and the greater length is likely attributable to a less-effective batch of CBD, which was used throughout the duration of this experiment.

Surprisingly, cyclopamine exposures did not have a toxic effect at the concentrations tested (Figure 17A). Although only 53% of larvae treated with 100 μM survived until 5 dpf, this metric was not significant compared to a 69% survival rate in the vehicle control (N=3 experiments, n = 75 total fish per treatment, $p>0.05$). Larvae treated with 25 μM and 50 μM of cyclopamine resulted in survival rates of 69% and 71%, respectively. CBD treated fish demonstrated a survival rate of 57%, which was also non-significant compared to the vehicle control. However, past experiments have demonstrated a survival rate of just 25.6% survival following CBD treatment, which indicates that this discrepancy may also be attributed to a less-effective drug.

Despite showing no significant difference in survival, cyclopamine exposures had a dramatic effect on hatching rate. Zero embryos treated with 100 μM cyclopamine hatched out of

their chorions by 5 dpf (Figure 17B). Similar results were seen in the 50 μM treatment, where only four embryos in a single replicate hatched by 5 dpf, out of a total of 53 surviving embryos. The 25 μM treatment group demonstrated a delay in hatching rate compared to the vehicle control, where only 2% of larvae were hatched at 2 dpf, 35% were hatched at 3 dpf, 53% were hatched at 4 dpf, and 81% of larvae were hatched by 5 dpf. In comparison, the vehicle control demonstrated a 4% hatching rate at 2 dpf, and achieved 100% hatching rate by 3 dpf. The hatching rate of 25 μM treated embryos was similar to CBD, which demonstrated no hatching at 2 or 3 dpf, but saw 37% of larvae hatching at 4 dpf and 92% of embryos fully hatched by 5 dpf. These rates are greater than hatching rates seen in previous experiments (Figure 12A), which again, alludes to a less-potent batch of CBD.

These results suggest that cyclopamine is able to mediate morphology, length, and hatching rates similar to those seen in CBD treated embryos, but seems to have no, or limited, effect in terms of mortality at the concentrations tested.

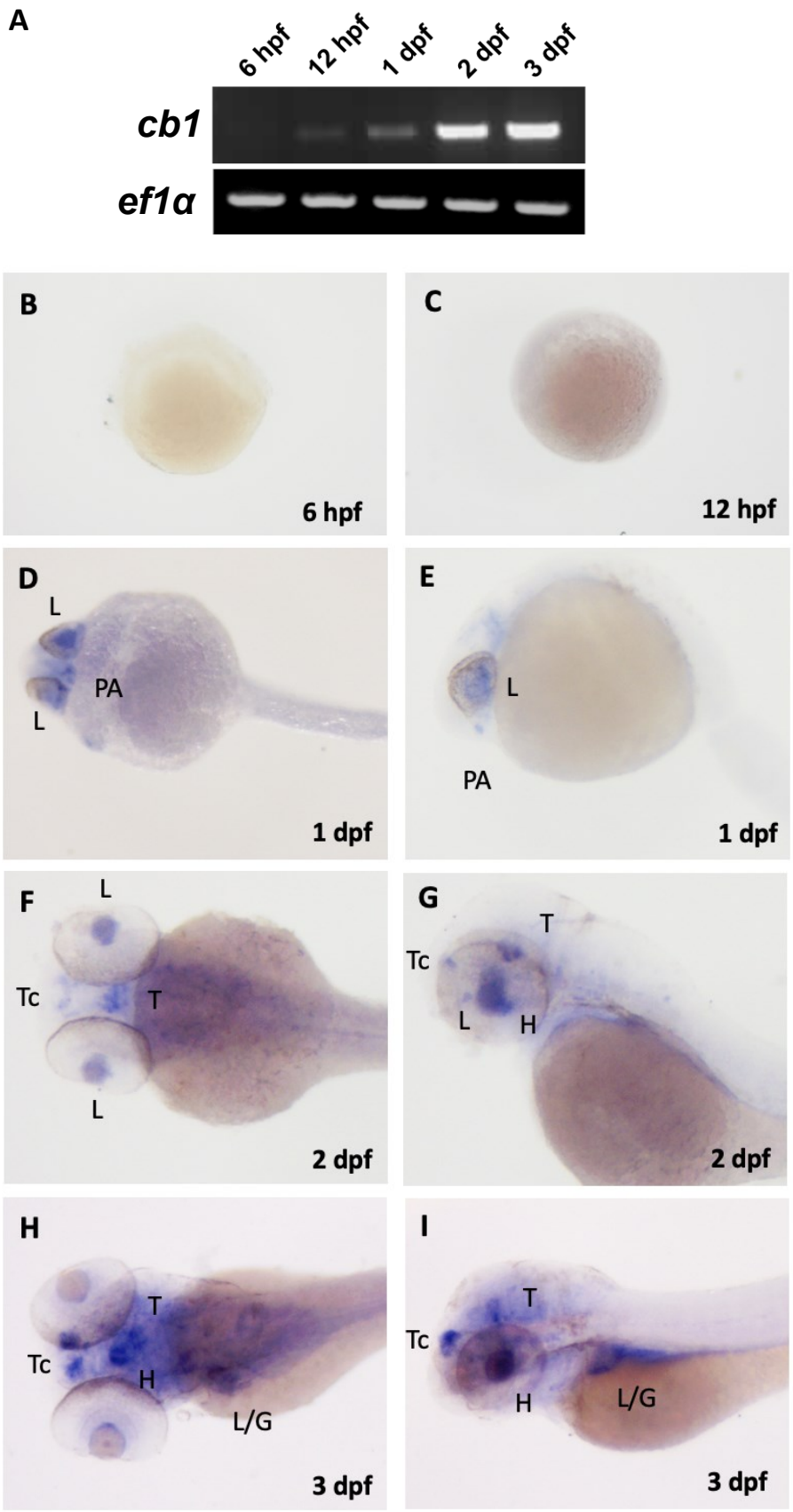
A
6 hpf
12 hpf
1 dpf
2 dpf
3 dpf
cb1
ef1α
B
6 hpf
C
12 hpf
D
L
PA
L
1 dpf
E
L
PA
1 dpf
F
L
Tc
T
L
2 dpf
G
T
Tc
L
H
2 dpf
H
T
Tc
H
L/G
3 dpf
I
T
Tc
H
L/G
3 dpf

Figure 3. Reverse transcriptase (RT) PCR and in situ hybridization of *cb1*. **A)** RT-PCR of *cb1* and *ef1*α at 6 hours post fertilization (hpf), 12 hpf, 1 day post fertilization (dpf), 2 dpf, and 3 dpf. Expression is undetectable at **B)** 6 hpf and **C)** 12 hpf. **D, E)** At 1 dpf, expression is present in the preoptic area (PA) and the lens (L). **F, G)** At 2 dpf, expression is found in the telencephalon (Tc), tegmentum (T), lens (L), and the hypothalamus (H) **H, I)** At 3 dpf, expression is observed in the telencephalon, tegmentum, hypothalamus, and liver/gut region.

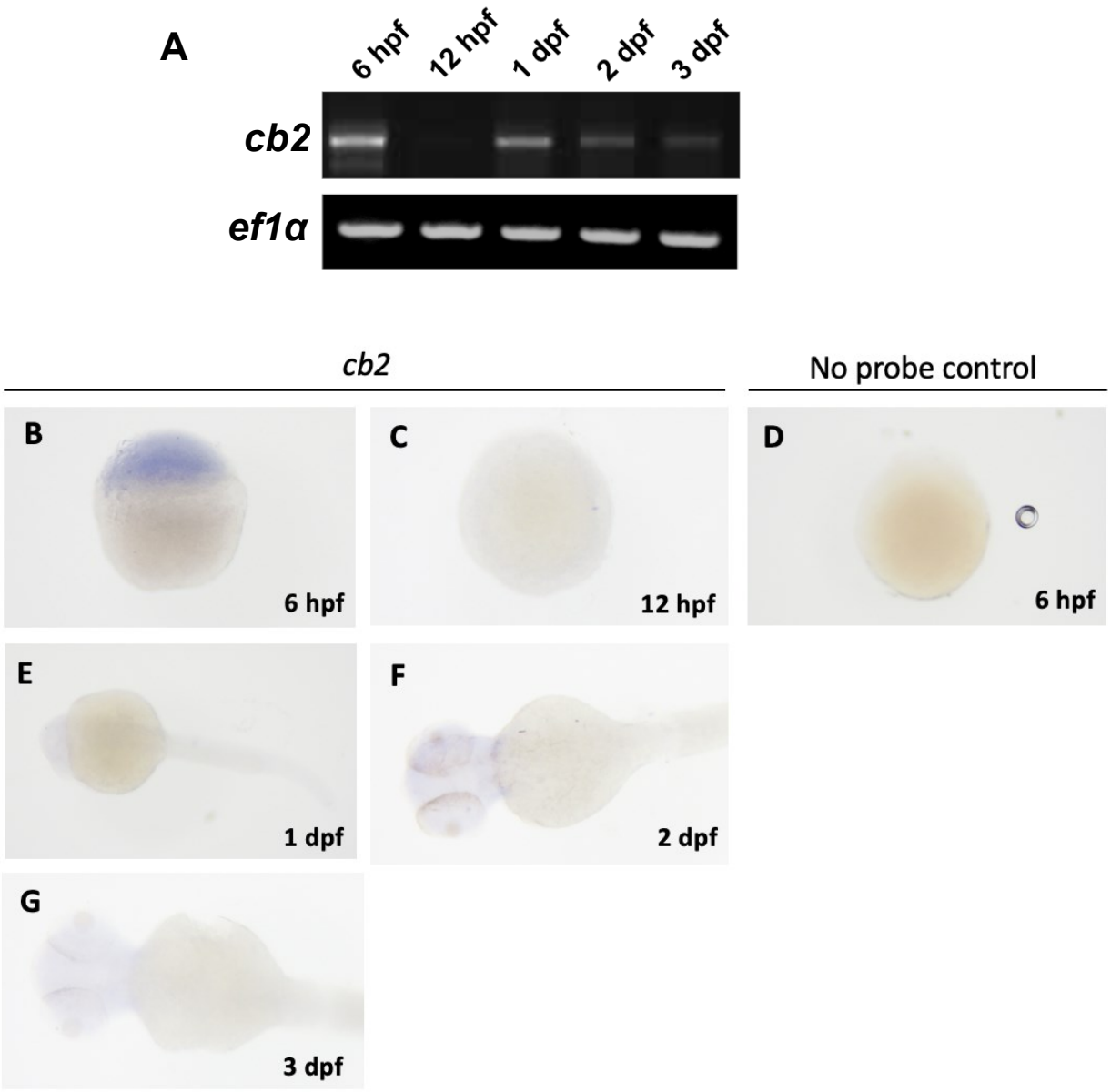
A
6 hpf
12 hpf
1 dpf
2 dpf
3 dpf
cb2
ef1α
cb2
No probe control
B
6 hpf
C
12 hpf
D
6 hpf
E
1 dpf
F
2 dpf
G
3 dpf

Figure 4. Reverse-Transcriptase (RT) – PCR and in situ hybridization of *cb2*. **A)** RT-PCR of *cb2* and *ef1*α at 6 hours post fertilization (hpf), 12 hpf, 1 day post fertilization (dpf), 2 dpf, and 3 dpf. **B)** Expression is present at 6 hpf, but not at **C)** 12 hpf. **D)** A no-probe control at 6 hpf shows no stain. **E-G)** At 1, 2, and 3 dpf, no expression can be detected.

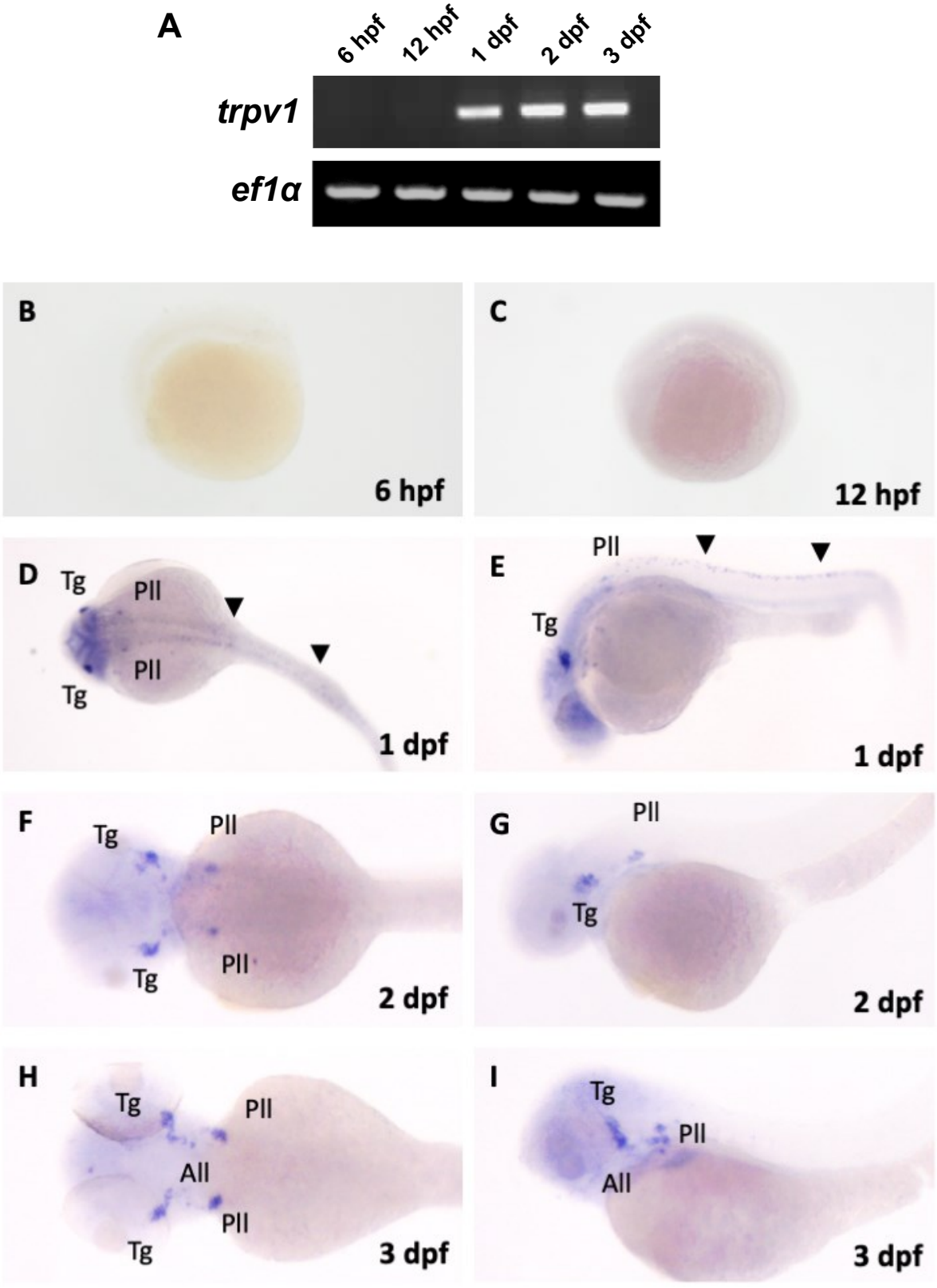
A
6 hpf
12 hpf
1 dpf
2 dpf
3 dpf
trpv1
ef1α
B
6 hpf
C
12 hpf
D
Tg
PII
PII
Tg
1 dpf
E
PII
Tg
1 dpf
F
Tg
PII
Tg
PII
2 dpf
G
PII
Tg
2 dpf
H
Tg
PII
AII
PII
Tg
3 dpf
I
Tg
PII
AII
3 dpf

Figure 5. Reverse-transcriptase (RT) PCR and in situ hybridization of *trpv1*. **A**) RT-PCR of *trpv1* and *ef1α* at 6 hours post fertilization (hpf), 12 hpf, 1 day post fertilization (dpf), 2 dpf, and 3 dpf. No expression is present in **B)** 6 hpf and **C)** 12 hpf embryos. **D, E)** At 1 dpf, expression is found in the trigeminal sensory neurons (Tg), posterior lateral line neurons (Pll), and the Rohon-Beard neurons (arrowheads). **F, G)**At 2 dpf, expression is restricted to the trigeminal sensory neurons, anterior lateral line neurons (All) and posterior lateral line neurons (Pll). **H, I)** At 3 dpf, expression pattern remains consistent with 2 dpf.

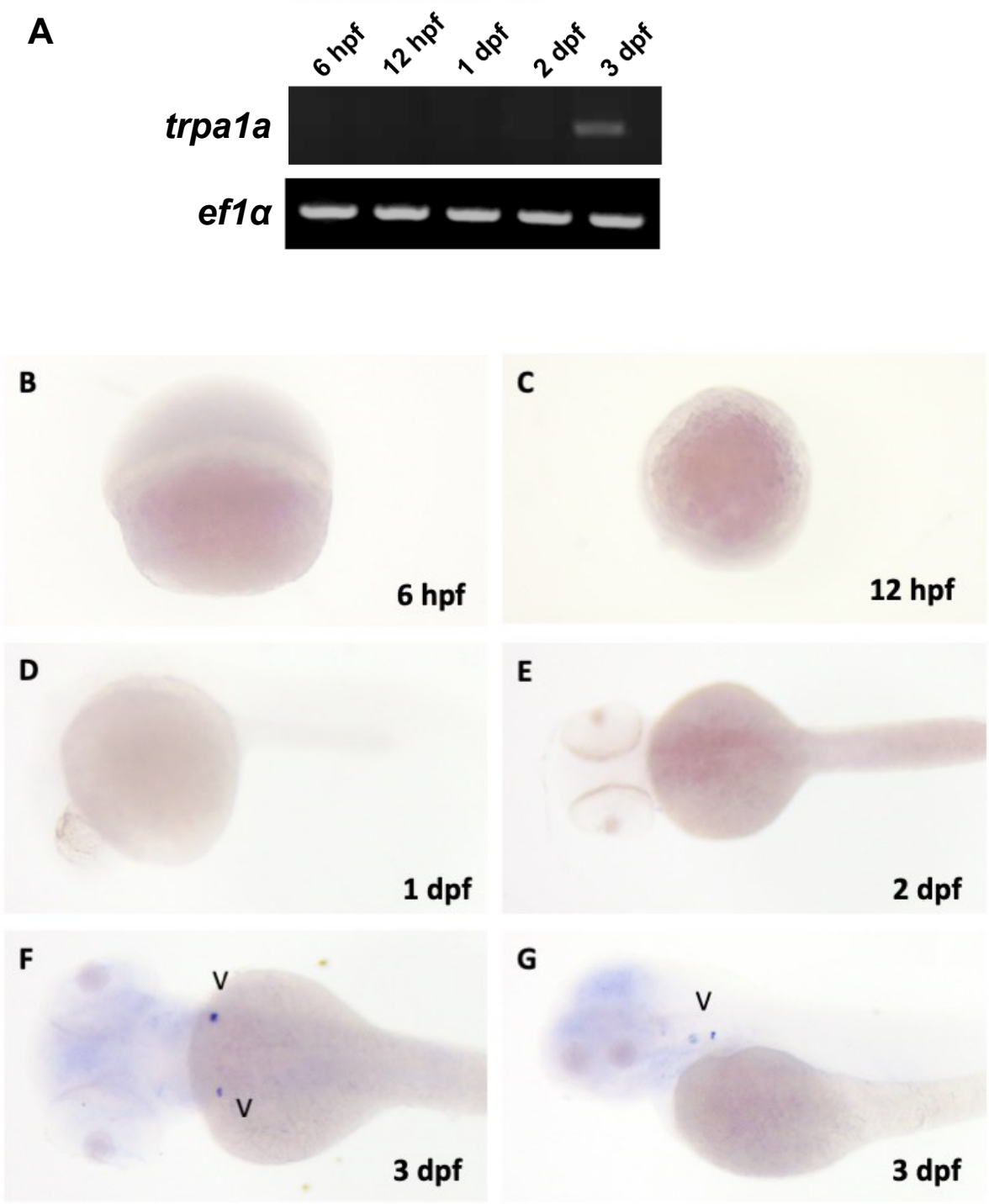
A
6 hpf
12 hpf
1 dpf
2 dpf
3 dpf
trpa1a
ef1α
B
6 hpf
C
12 hpf
D
1 dpf
E
2 dpf
F
V
V
3 dpf
G
V
3 dpf

Figure 6. Reverse-Transcriptase (RT) PCR and in situ hybridization of *trpa1a*. **A)** RT-PCR of *trpa1a* and *ef1α* at 6 hours post fertilization (hpf), 12 hpf, 1 day post fertilization (dpf), 2 dpf, and 3 dpf. No expression is found in **B)** 6 hpf, **C)** 12 hpf, **D)** 1 dpf, or **E)** 2 dpf embryos. **F, G)** At 3 dpf, *trpa1a* expression is restricted to the vagal sensory neuron (V).

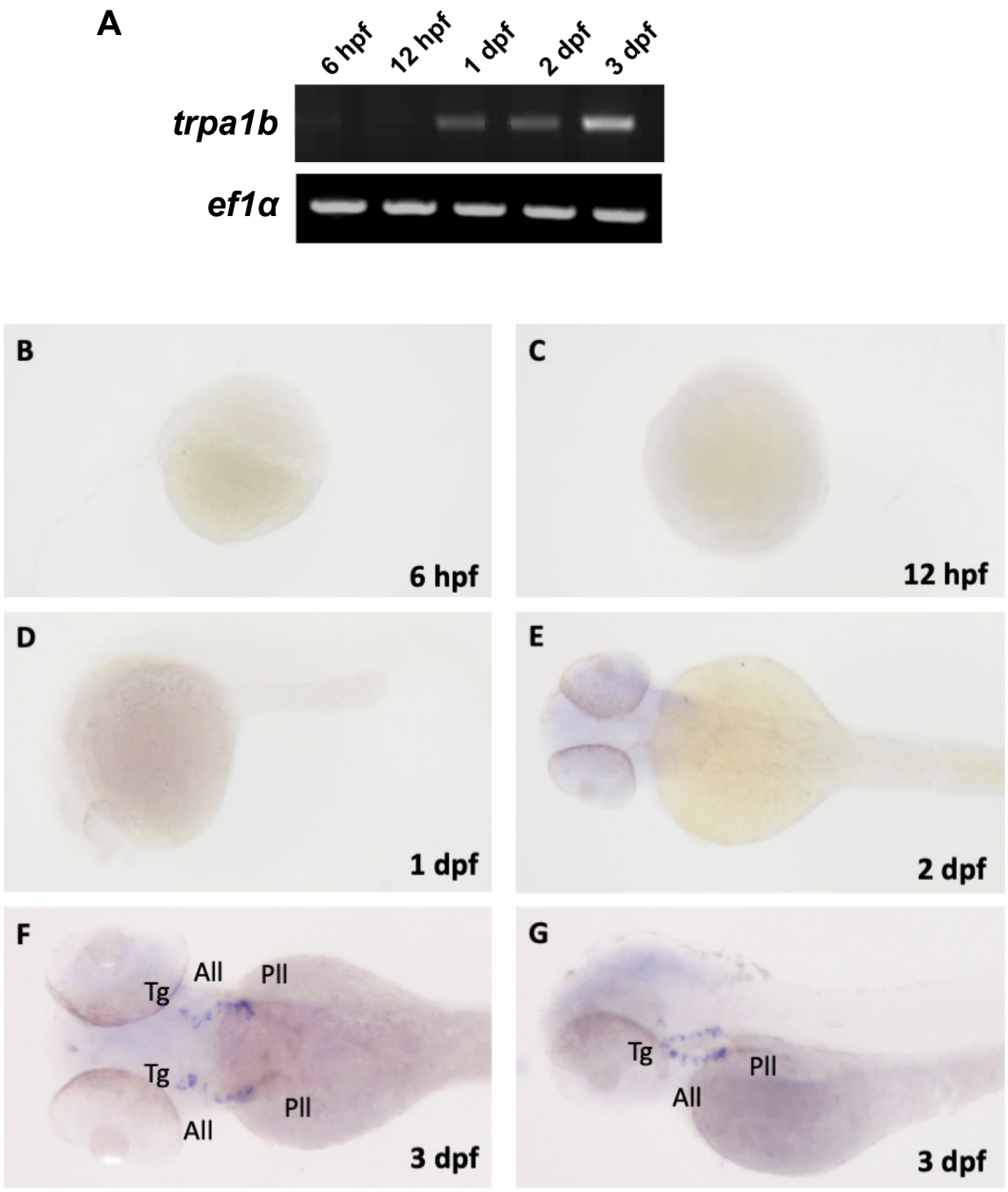
A
6 hpf
12 hpf
1 dpf
2 dpf
3 dpf
trpa1b
ef1α
B
6 hpf
C
12 hpf
D
1 dpf
E
2 dpf
F
Tg
AII
PII
Tg
PII
AII
3 dpf
G
Tg
PII
AII
3 dpf

Figure 7. Reverse-Transcriptase (RT) PCR and in situ hybridization of *trpa1b.* **A)** RT-PCR of *cb2* and *ef1*α at 6 hours post fertilization (hpf), 12 hpf, 1 day post fertilization (dpf), 2 dpf, and 3 dpf. *Trpa1b* expression is undetectable at **B)** 6 hpf, **C)** 12 hpf, **D)** 1 dpf, and **E)** 2 dpf. **F, G)** At 3 dpf, expression can observed in the trigeminal sensory neurons and the anterior (All) and posterior (Pll) lateral line neurons.

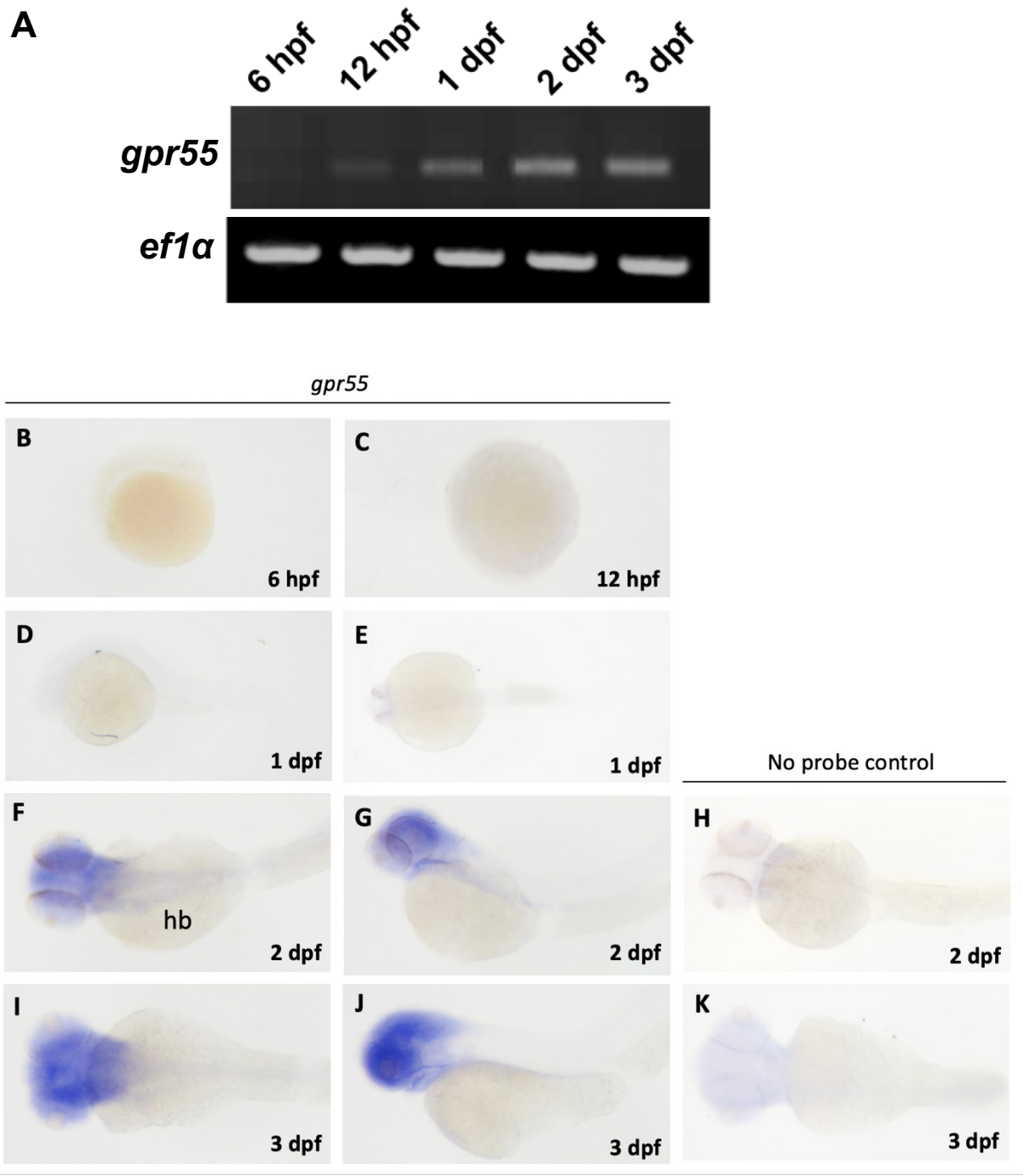
A
6 hpf
12 hpf
1 dpf
2 dpf
3 dpf
gpr55
ef1α
gpr55
B
6 hpf
C
12 hpf
D
1 dpf
E
1 dpf
No probe control
F
hb
2 dpf
G
2 dpf
H
2 dpf
I
3 dpf
J
3 dpf
K
3 dpf

Figure 8. Reverse-Transcriptase (RT) PCR and in situ hybridization of *gpr55*. **A)** RT-PCR of *cb2* and *ef1*α at 6 hours post fertilization (hpf), 12 hpf, 1 day post fertilization (dpf), 2 dpf, and 3 dpf. Expression is undetectable at **B)** 6 hpf, **C)** 12 hpf, and **D, E)** 1 dpf. **F, G)** At 2 dpf, diffuse expression throughout the head is observed. **H)** No staining is observed in no-probe control at 2 dpf. **I, J)** At 3 dpf, expression is maintained throughout the head. **K)** No staining is observed in the no-probe control at 3 dpf.

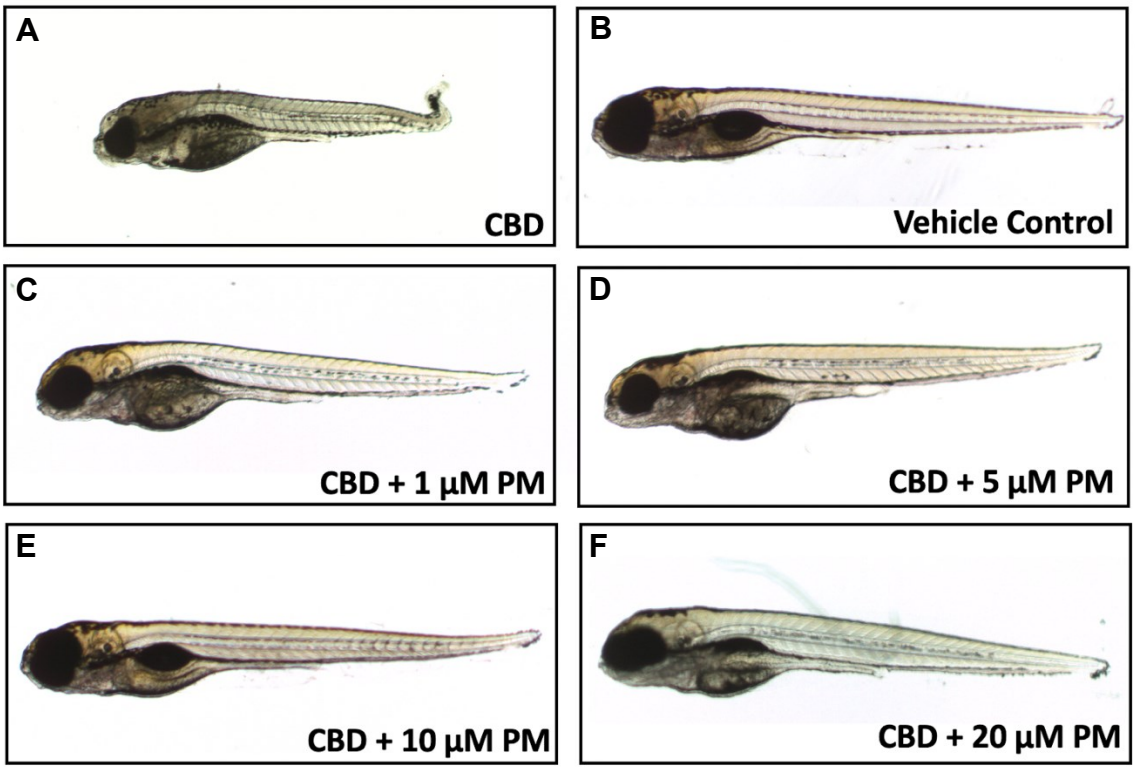
A
CBD
B
Vehicle Control
C
CBD + 1 µM PM
D
CBD + 5 µM PM
E
CBD + 10 µM PM
F
CBD + 20 µM PM

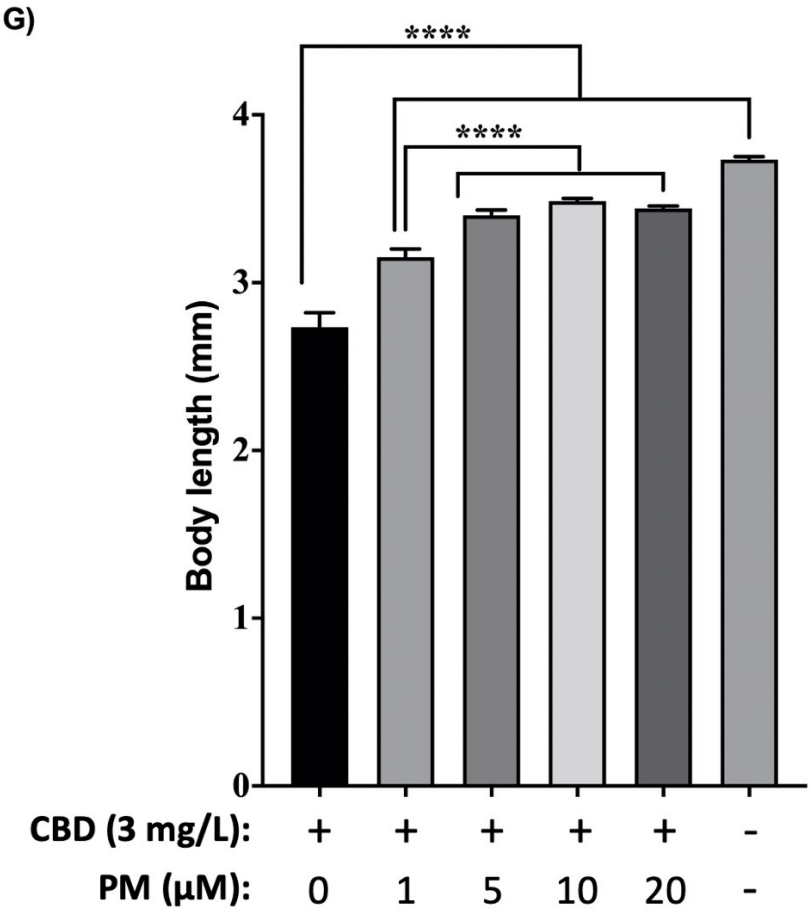
G)
****
****
Body length (mm)
0
1
2
3
4
CBD (3 mg/L): + + + + + -
PM (µM): 0 1 5 10 20 -

Figure 9. Upregulating the Sonic Hedgehog pathway by co-exposing zebrafish larvae to Purmorphamine (PM) and cannabidiol during gastrulation improves body lengths at 5 dpf. Embryos were exposed to **A)** 3 mg/L CBD, **B)** Vehicle (0.3% Methanol and 0.2% DMSO), **C)** 3 mg/L CBD + 1 μM PM, **D)** 3 mg/L CBD + 5 μM PM, **E)** 3 mg/L CBD + 10 μM PM, and **F)** 3 mg/L CBD + 20 μM PM during the period of gastrulation (5.25 hours post fertilization (hpf) to 10.75 hpf) and then allowed to develop in embryo media (EM) at 28.5° C. All PM and DMSO treatments were preincubated for 30 min prior to gastrulation. Representative images were taken at 5 dpf under a 2.5X objective lens. **E)** Body lengths of larvae at 5 dpf in CBD treated control (N = 5 experiments, n = 41 total fish), co-exposures of CBD and PM treatments (N = 5 experiments, n = 60, 50, 71, and 79 total fish for CBD + 1, 5, 10, and 20 μM PM treated fish respectively), vehicle control (N = 5 experiments, n = 59 total fish) and untreated control (N = 5 experiments, n = 52 total fish). Length measurements were determined using ProAnalyst and compiled in GraphPad Prism 9. One-way ANOVA and post hoc Tukey's test were performed to assess significance. **** = $p < 0.0001$, error bars represent SEM

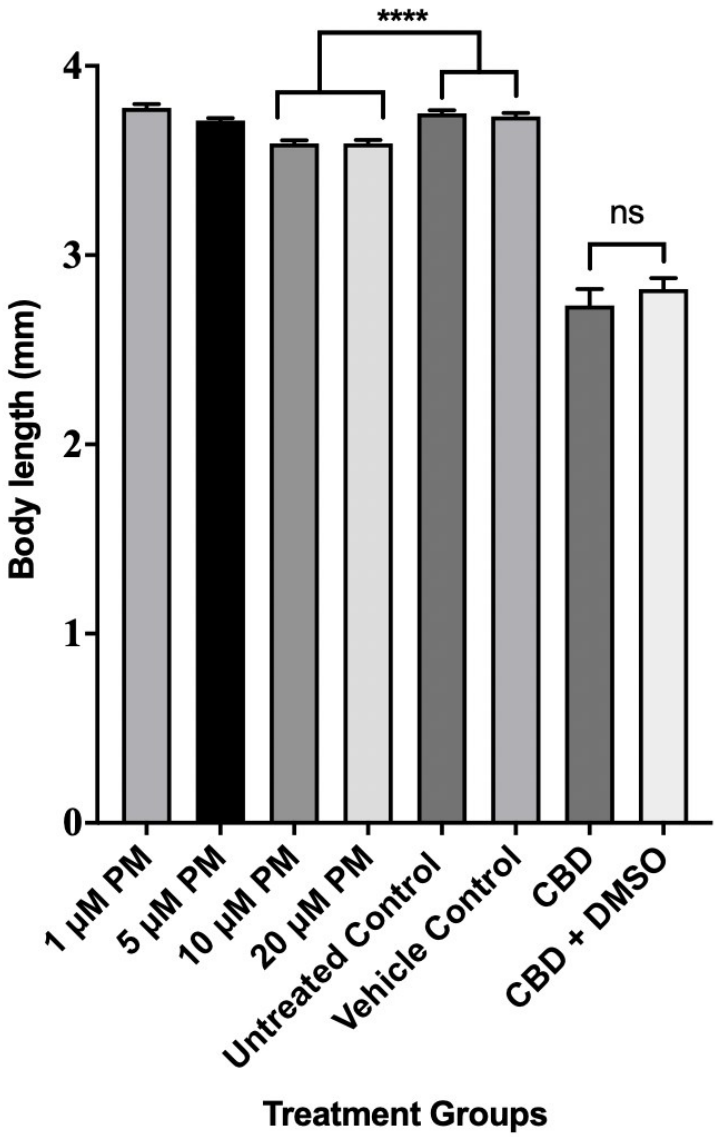
****
ns
4
3
2
1
0
Body length (mm)
1 µM PM
5 µM PM
10 µM PM
20 µM PM
Untreated Control
Vehicle Control
CBD
CBD + DMSO
Treatment Groups

Figure 10. Body lengths of zebrafish at 5 days post fertilization (dpf) following exposure to purmorphamine (PM), vehicles, and cannabidiol (CBD), during gastrulation. Embryos were exposed to 1, 5, 10, or 20 μM purmorphamine (n = 51, 55, 71, and 85 fish respectively), only embryo media (EM) (n = 53 fish), vehicle consisting of 0.3% Methanol and 0.2% DMSO (n = 60 fish), 3 mg/L of CBD (n = 42 fish) or 3 mg/L CBD + 0.2% DMSO (n = 36 fish) from 5.25 hours post fertilization (hpf) to 10.75 hpf and then allowed to develop in EM at 28.5° C. All PM and dimethyl sulfoxide (DMSO) treatments were preincubated for 30 min prior to gastrulation. Length measurements were determined using ProAnalyst and compiled in GraphPad Prism 9. One-way ANOVA and post hoc Tukey's test were performed to assess significance. **** = $p<0.0001$, error bars represent SEM.

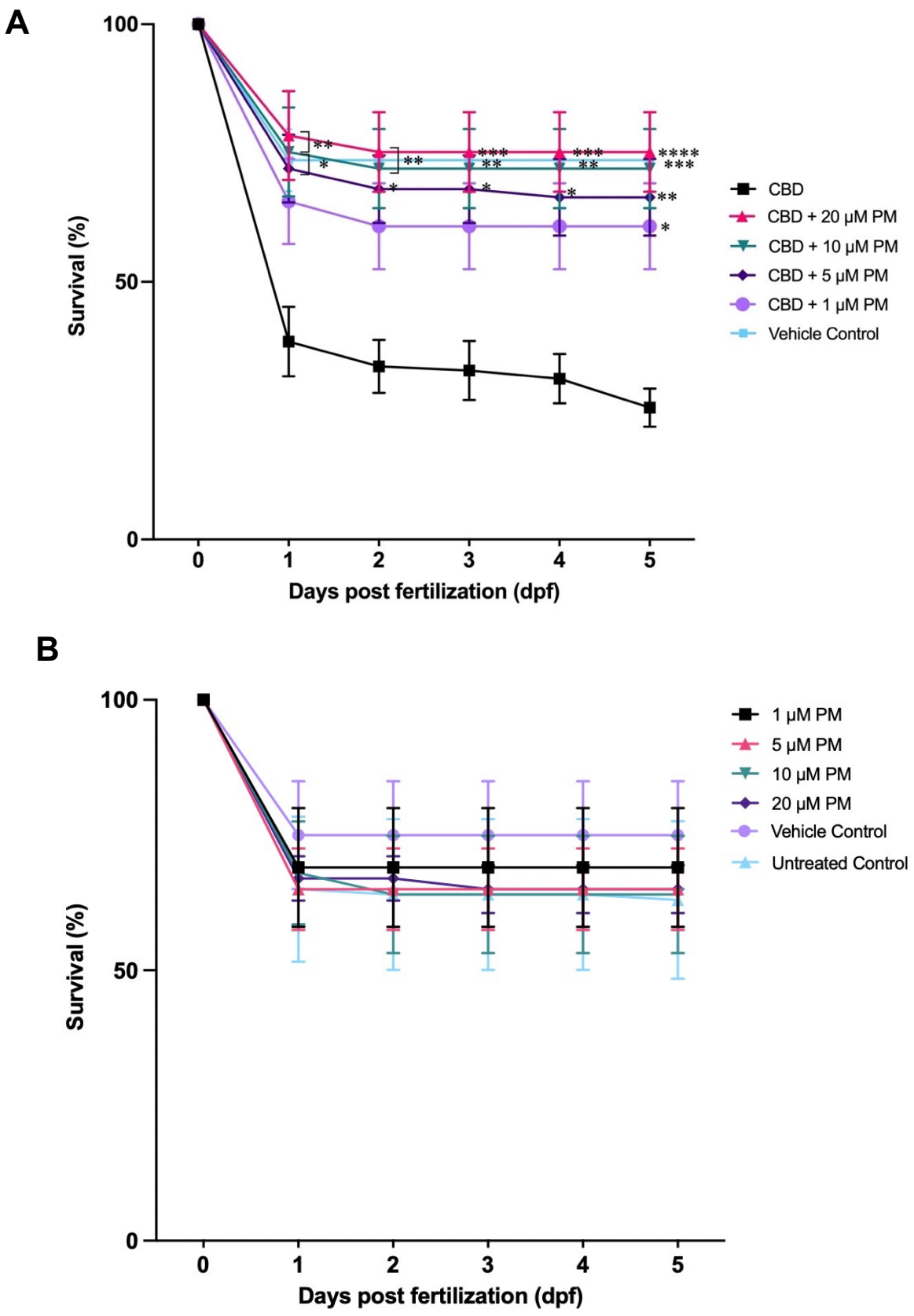
A
100
50
0
Survival (%)
0
1
2
3
4
5
Days post fertilization (dpf)
CBD
CBD + 20 µM PM
CBD + 10 µM PM
CBD + 5 µM PM
CBD + 1 µM PM
Vehicle Control
B
100
50
0
Survival (%)
0
1
2
3
4
5
Days post fertilization (dpf)
1 µM PM
5 µM PM
10 µM PM
20 µM PM
Vehicle Control
Untreated Control

Figure 11. Survival rates of embryos treated with cannabidiol (CBD) and purmorphamine (PM). Embryos were exposed to A) CBD at 3 mg/L, PM at concentrations of 1 μM, 5 μM, 10 μM, and 20 μM, and vehicles (0.3% Methanol and 0.2% DMSO) and B) control treatments consisting of individual PM exposures of 1 μM, 5 μM, 10 μM, and 20 μM, vehicles, or no treatment (untreated control). Zebrafish embryos were pre-incubated to dimethyl sulfide (DMSO) or PM from 4.75 to 5.25 hours post fertilization (hpf). CBD (3 mg/L) or methanol (0.3%) were added at 5.25 hpf and embryos were incubated until 10.75 hpf at 28.5°C. Numbers of live embryos were recorded each day from 1 day post fertilization (dpf) to 5 dpf. N = 5 experiments, n = 125 total fish per treatment. Error bars represent SEM. One-way ANOVA and post hoc Tukey's test were performed to assess significance. Significance described in relation to CBD treatment group. * = $p<0.05$, ** = $p<0.01$, *** = $p<0.001$, **** = $p<0.0001$. There was no significance between vehicle and untreated controls and independent concentrations of PM.

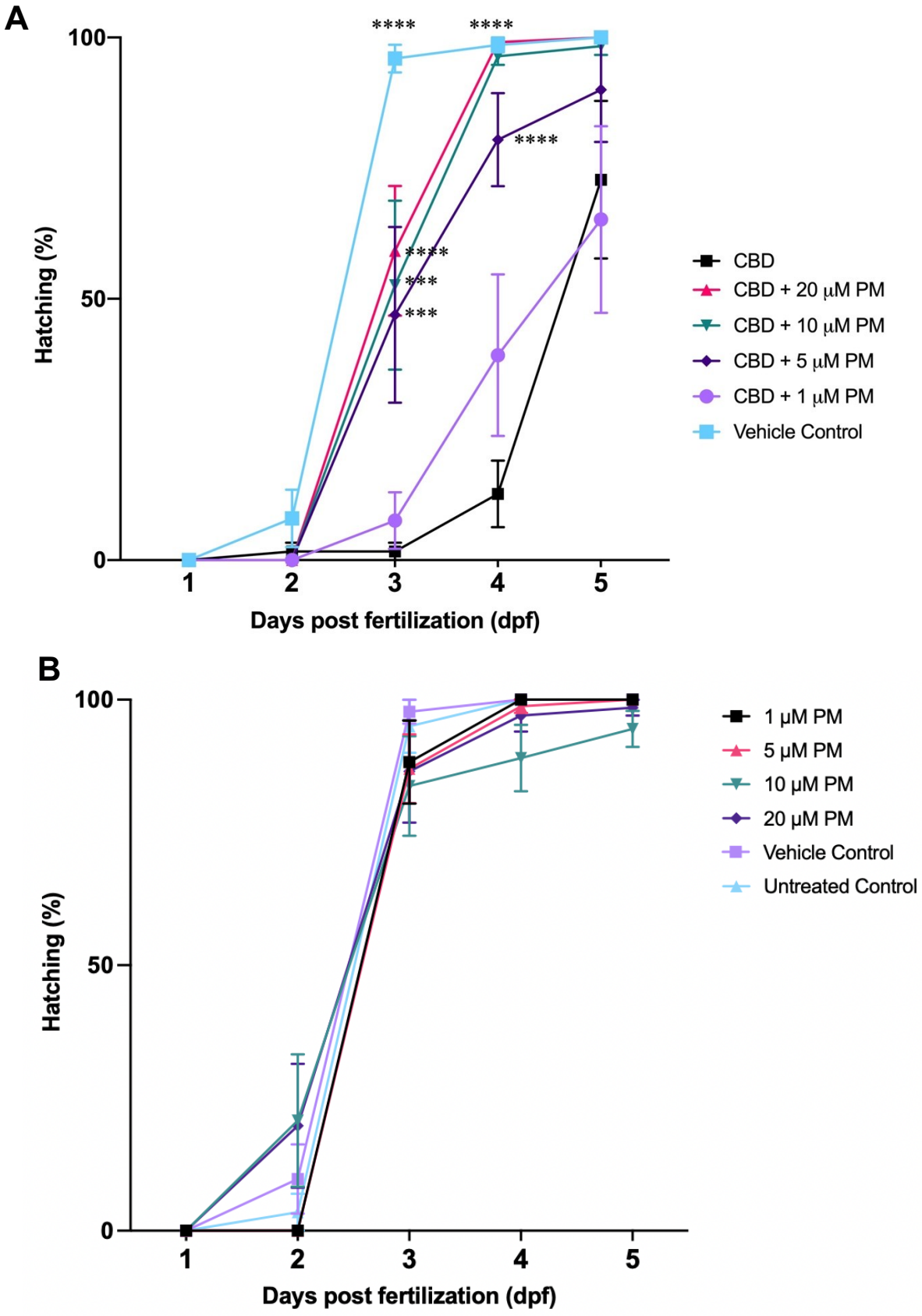
A
100
50
0
Hatching (%)
1
2
3
4
5
Days post fertilization (dpf)
****
****
****
***
***
CBD
CBD + 20 μM PM
CBD + 10 μM PM
CBD + 5 μM PM
CBD + 1 μM PM
Vehicle Control
B
100
50
0
Hatching (%)
1
2
3
4
5
Days post fertilization (dpf)
1 μM PM
5 μM PM
10 μM PM
20 μM PM
Vehicle Control
Untreated Control

Figure 12. Hatching rates of embryos treated with cannabidiol (CBD) and purmorphamine (PM). Embryos were treated with **A)** CBD at 3 mg/L, PM at concentrations of 1 μM, 5 μM, 10 μM, and 20 μM, and vehicles (0.3% Methanol and 0.2% DMSO), and **B)** control treatments consisting of individual PM exposures of 1 μM, 5 μM, 10 μM, and 20 μM, vehicles (0.3% Methanol and 0.2% DMSO), and non-treatment (untreated embryos). Embryos were pre-incubated to dimethyl sulfide (DMSO) or PM from 4.75 to 5.25 hours post fertilization (hpf). CBD or methanol (0.3%) were added at 5.25 hpf and embryos were incubated until 10.75 hpf at 28.5°C. Numbers of hatched embryos were recorded each day from 1 day post fertilization (dpf) to 5 dpf. N = 5 experiments, n = 125 total fish per treatment. Error bars represent SEM. One-way ANOVA and post hoc Tukey's test were performed to assess significance. Significance in relation to CBD treatment group. * = $p<0.05$, ** = $p<0.01$, *** = $p<0.001$, **** = $p<0.0001$. There was no significance between vehicle and untreated controls and independent concentrations of PM.

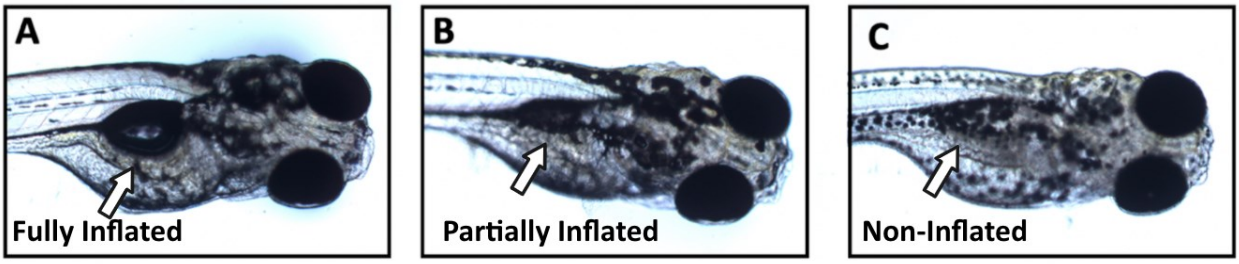
A
Fully Inflated
B
Partially Inflated
C
Non-Inflated

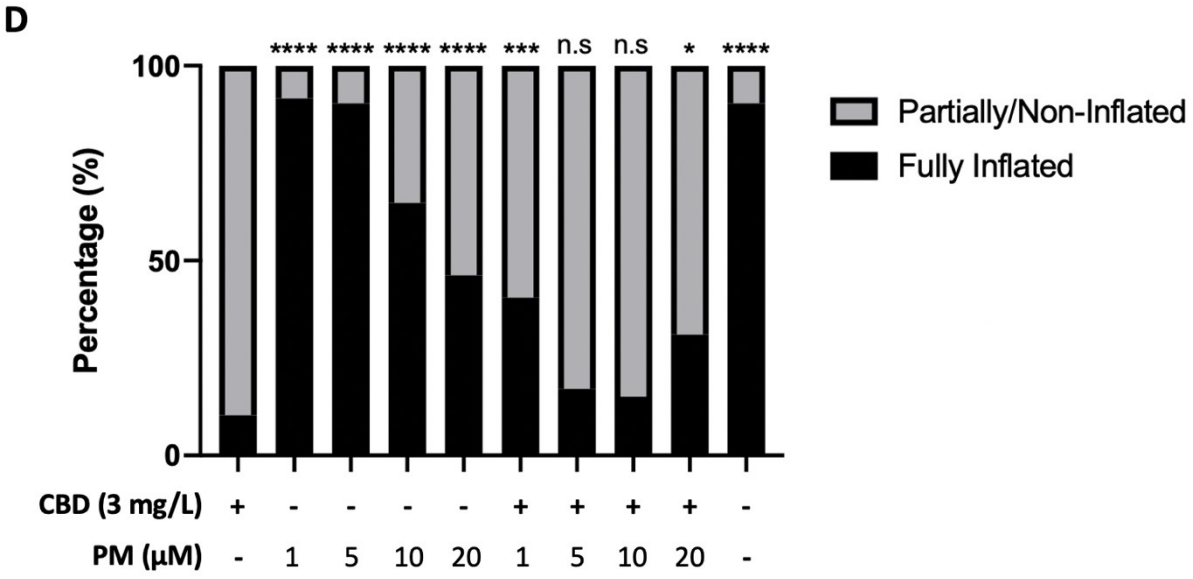
D
**** **** **** **** *** n.s n.s * ****
100
50
0
Percentage (%)
Partially/Non-Inflated
Fully Inflated
CBD (3 mg/L) + - - - - + + + + -
PM (µM) - 1 5 10 20 1 5 10 20 -

Figure 13. Purmorphamine (PM) and cannabidiol (CBD) exposure during gastrulation affects swim bladder (SB) development at 5 days post fertilization (dpf). Representative images of A) fully inflated SB (arrow), B) partially inflated SB (arrow), and C) non-inflated SB (arrow). Embryos were exposed to CBD at 3 mg/L, individual PM exposures at concentrations of 1 μM, 5 μM, 10 μM, and 20 μM, co-exposure to both CBD and each PM concentration, or vehicles (0.3% Methanol and 0.2% Dimethyl sulfoxide (DMSO)). Embryos were pre-incubated to DMSO or PM from 4.75 to 5.25 hours post fertilization (hpf). CBD or methanol were added at 5.25 hpf and embryos were incubated until 10.75 hpf at 28.5°C before being rinsed thoroughly and allowed to grow until 5 dpf. Larvae were captured under a 5X objective lens using a Lumenera Infinity2-1R colour microscope camera mounted on a Leica DM 2500 microscope and D) scored for the presence of a fully inflated SB, or a partial/non-inflated bladder. N = 4 experiments, n = 36-91 total fish per treatment. Fisher's Exact test was performed to assess significance. Significance denoted is in relation to CBD treatment group. * = $p<0.05$, *** = $p<0.001$, **** = $p<0.0001$

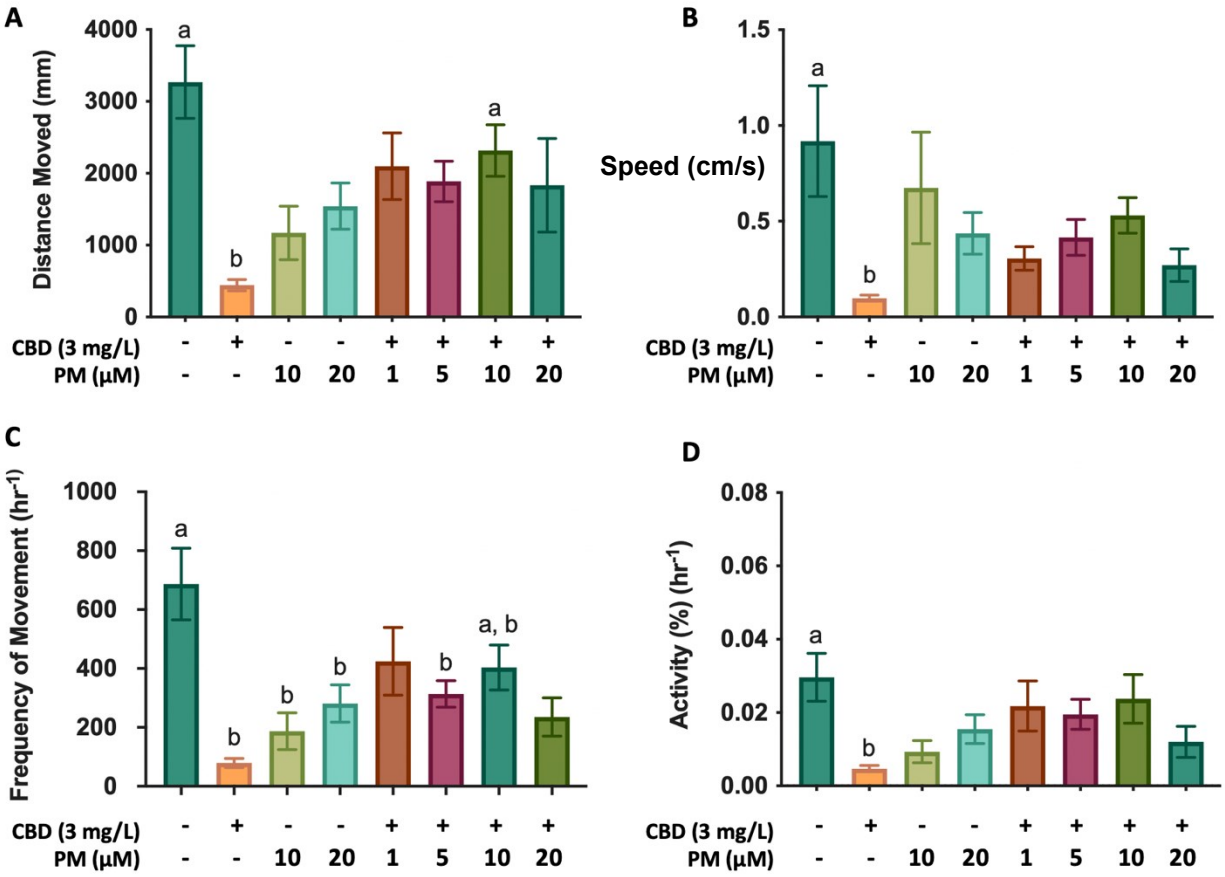
A
Distance Moved (mm)
4000
3000
2000
1000
0
a
b
a
B
Speed (cm/s)
1.5
1.0
0.5
0.0
a
b
C
Frequency of Movement (hr-1)
1000
800
600
400
200
0
a
b
b
b
b
a, b
D
Activity (%) (hr-1)
0.08
0.06
0.04
0.02
0.00
a
b
CBD (3 mg/L) - + - - + + + +
PM (µM) - - 10 20 1 5 10 20

Figure 14. Locomotive behaviour of free swimming zebrafish at 5 dpf following exposure to cannabidiol (CBD) and purmorphamine (PM) during gastrulation. Zebrafish embryos were exposed to 1, 5, 10, or 20 μM of PM or 0.2% dimethyl sulfoxide (DMSO) at 4.75 hour post fertilization (hpf). CBD or 0.3% methanol (MeOH) was added at 5.25 hpf and embryos were incubated until 10.75 hpf at 28.5°C. Embryos were thoroughly rinsed and allowed to continue developing at 28.5°C until 5 dpf. Larvae were separated in individual wells of a 96 well plate and tracked with Ethovision software for 1 hour to determine **A)** total distance travelled (mm), **B)** average speed (cm/s), **C)** Frequency of movements per hour, and **D)** Percentage of active movement per hour. N = 4 experiments, n = 22-64 total fish per treatment. Error bars represent SEM. a: significantly different from CBD treatment ($p<0.05$), b: significantly different from vehicle control ($p<0.05$).

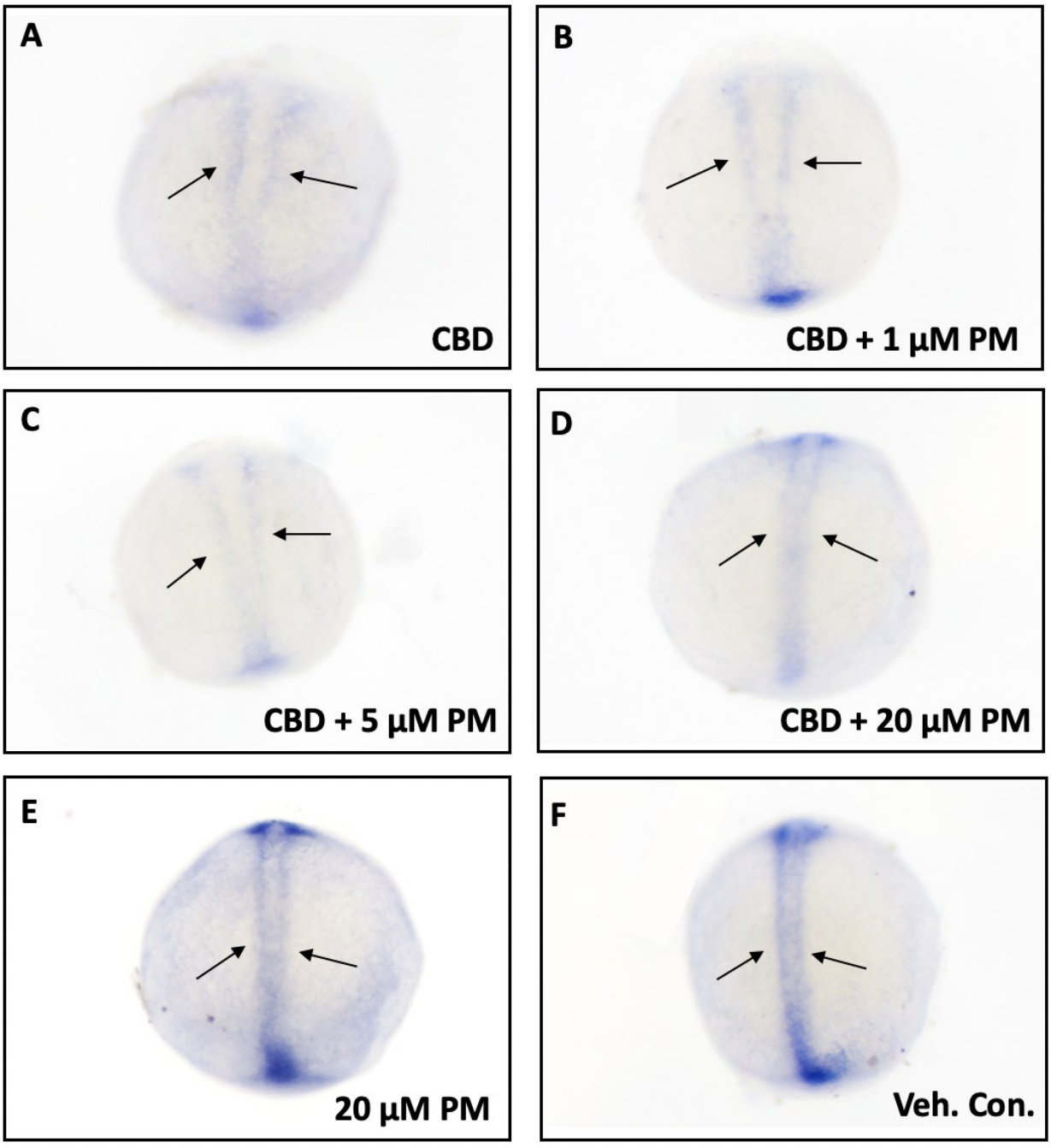
A
CBD
B
CBD + 1 µM PM
C
CBD + 5 µM PM
D
CBD + 20 µM PM
E
20 µM PM
F
Veh. Con.

Figure 15. Purmorphamine (PM) rescues reduced *ptch2* expression and midline abnormalities induced by cannabidiol (CBD) exposure during gastrulation at 10.75 hpf. Zebrafish embryos were co-exposed to 3 mg/L CBD and 1, 5, or 20 μM of PM, or 20 μM PM alone, or a vehicle control of 0.3% methanol and 0.2% dimethyl sulfoxide (DMSO) from 5.25 hpf to 10.75 hpf. PM and DMSO were administered 30 minutes prior to gastrulation. At the end of gastrulation, embryos were fixed in 4% PFA and in situ hybridization was performed to probe for *ptch2*. Embryos treated with **A)** CBD, **B)** CBD + 1 μM PM, and **C)** CBD + 5 μM PM demonstrate reduced expression and disorganized adaxial cells (arrows). Embryos treated with **D)** CBD + 20 μM PM, **E)** 20 μM PM and **F)** vehicles show normal *ptch2* expression. Experiment was replicated three times.

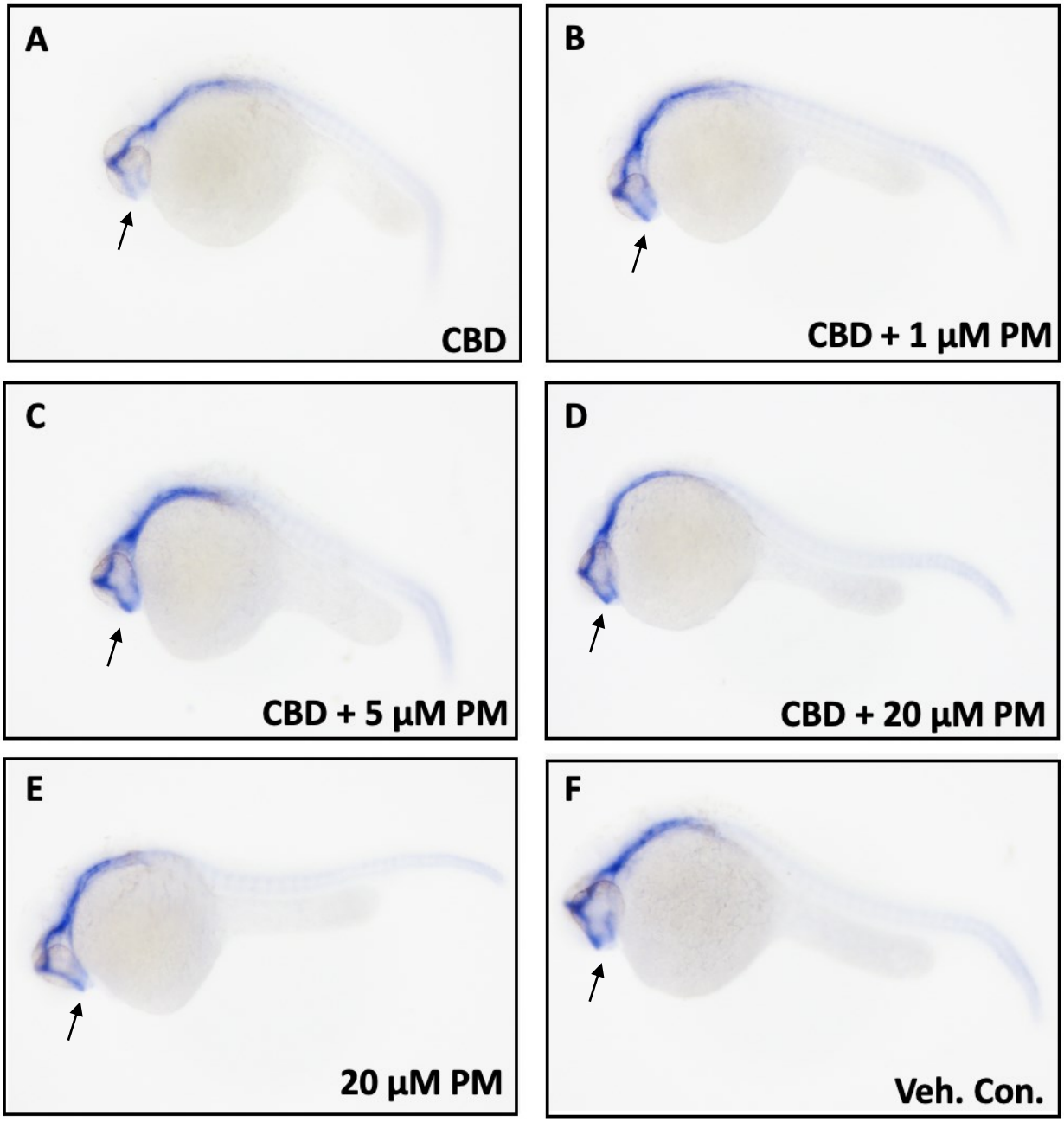
A
CBD
B
CBD + 1 µM PM
C
CBD + 5 µM PM
D
CBD + 20 µM PM
E
20 µM PM
F
Veh. Con.

Figure 16. Purmorphamine (PM) rescues reduced *ptch2* expression induced by cannabidiol (CBD) exposure during gastrulation at 24 hpf. Zebrafish embryos were co-exposed to 3 mg/L CBD and 1, 5, or 20 μM of PM, or 20 μM PM alone, or a vehicle control of 0.3% methanol and 0.2% dimethyl sulfoxide (DMSO) from 5.25 hpf to 10.75 hpf. PM and DMSO were administered 30 minutes prior to gastrulation. At the end of gastrulation, embryos were rinsed three times in embryo media and incubated at 28.5ºC overnight. At 1 dpf, embryos were fixed in 4% PFA and in situ hybridization was performed to probe for *ptch2*. Embryos treated with **A)** CBD demonstrate reduced *ptch2* expression particularly in the diencephalon (arrow). Embryos treated with **B)** CBD + 1 μM PM **C)** CBD + 5 μM PM, **D)** CBD + 20 μM PM, **E)** 20 μM PM and **F)** vehicles share similar levels of expression. Experiment was replicated two times.

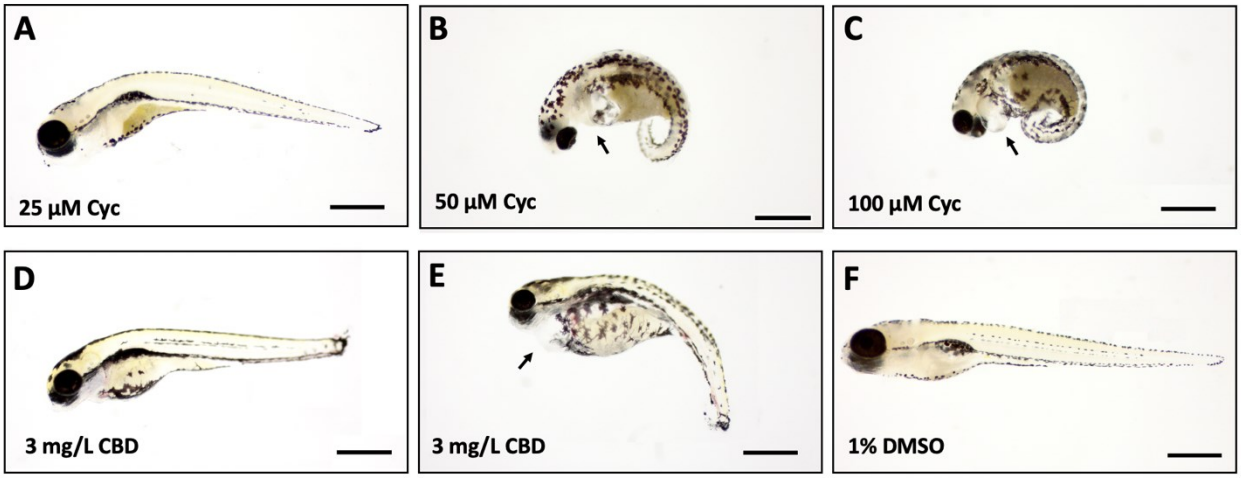
A
25 µM Cyc
B
50 µM Cyc
C
100 µM Cyc
D
3 mg/L CBD
E
3 mg/L CBD
F
1% DMSO

G

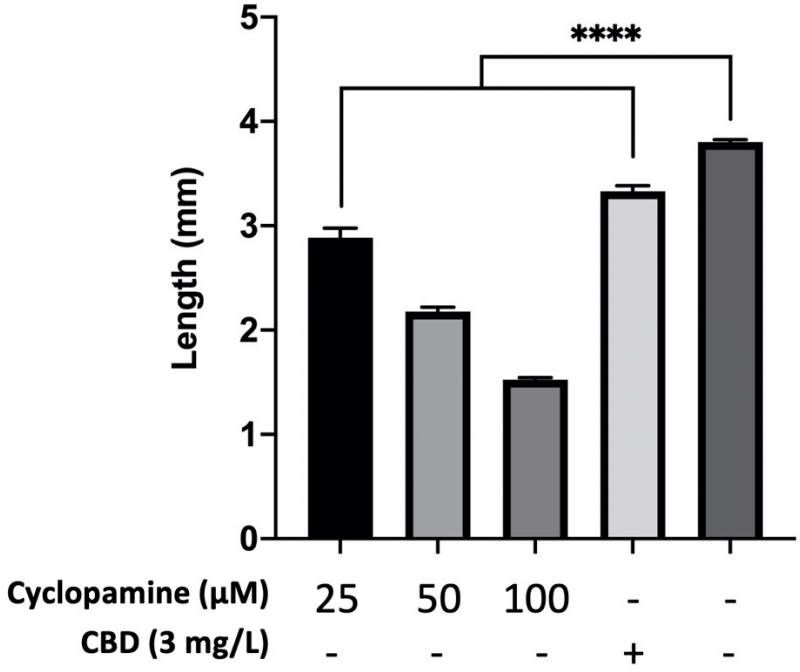
****
Length (mm)
0
1
2
3
4
5
Cyclopamine (µM) 25 50 100 - -
CBD (3 mg/L) - - - + -

Figure 17. Cyclopamine (Cyc) induces teratogenic effects including axial curvature, pericardial edema (arrows), and decreased body lengths by 5 days post fertilization (dpf). Embryos were treated with either **A)** 25 μM (n=42 fish), **B)** 50 μM (n=43 fish), or **C)** 100 μM cyclopamine (n=44 fish), or **D, E)** 3 mg/L cannabidiol (CBD) (n=50 fish), or **F)** 1% dimethyl sulfoxide (DMSO) (n=50 fish) from 5.25 hours post fertilization (hpf) to 10.75 hpf. At 10.75 hpf, embryos were thoroughly rinsed and incubated at 28.5°C until 5dpf, when larvae were imaged under a dissecting microscope at 3X magnification. Scale bar = 0.5 mm. **G)** Average lengths of embryos treated with cyclopamine or CBD throughout gastrulation. Length measurements were determined using ProAnalyst and compiled in GraphPad Prism 9. Error bars represent SEM. One-Way ANOVA and post hoc Tukey's Test were performed to assess significance between treatment groups. **** = $p<0.0001$.

A

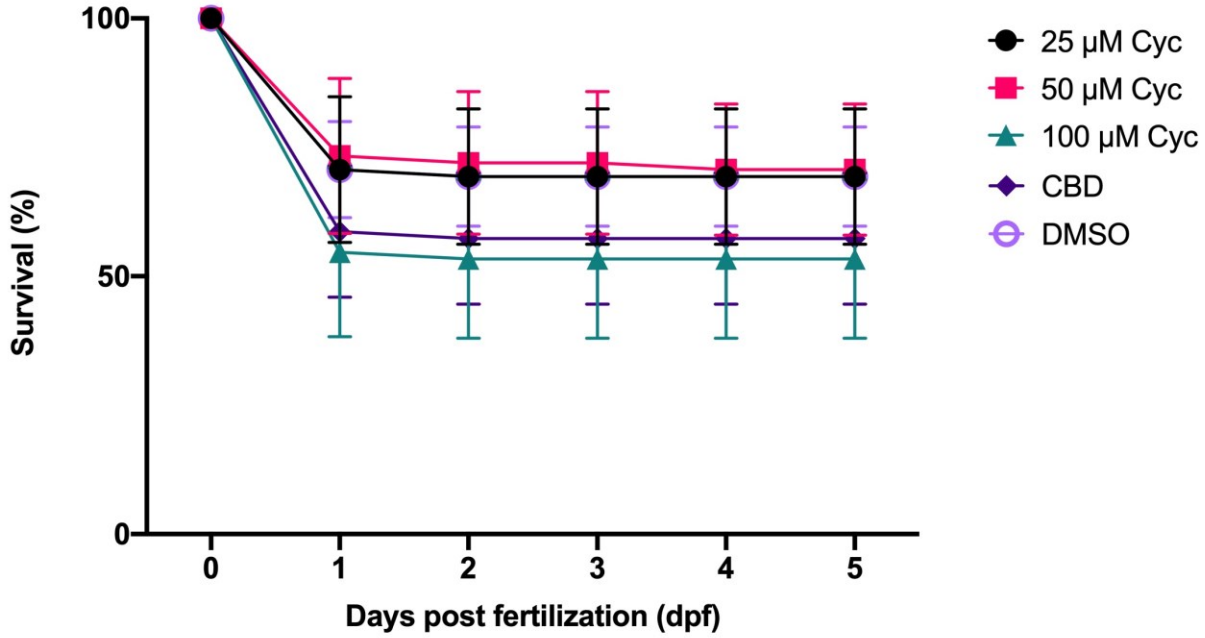
100
50
0
Survival (%)
0
1
2
3
4
5
Days post fertilization (dpf)
25 µM Cyc
50 µM Cyc
100 µM Cyc
CBD
DMSO

B

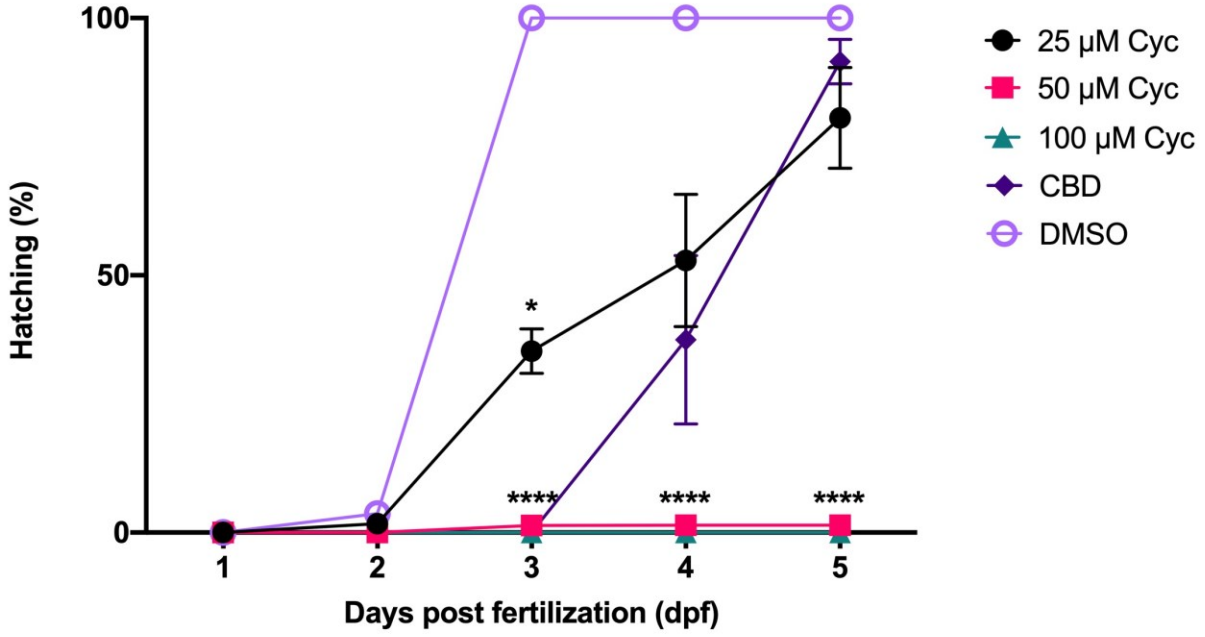
100
50
0
Hatching (%)
*
****
****
****
1
2
3
4
5
Days post fertilization (dpf)
25 µM Cyc
50 µM Cyc
100 µM Cyc
CBD
DMSO

Figure 18. Hatching rate, but not survival rate, is decreased in embryos treated with cyclopamine (Cyc) during gastrulation. Embryos were exposed to either 25, 50, or 100 μM cyclopamine, or 3 mg/L cannabidiol (CBD), or 1% DMSO from 5.25 hours post fertilization (hpf) to 10.75 hpf. At 10.75 hpf, embryos were thoroughly rinsed and incubated at 28.5°C. Numbers of **A)** live and **B)** hatched embryos were recorded each day from 1 day post fertilization (dpf) to 5 dpf. N = 3 experiments, n = 75 total fish per treatment. Error bars represent SEM. One-Way ANOVA and post hoc Tukey's Test were performed to assess significance between treatment groups. Significance described in relation to vehicle control. *= $p<0.05$, **** = $p<0.0001$. There was no significance in survival between all treatment groups.

4. Discussion

4.1 Endocannabinoid System in Development

4.1.1 Cannabinoid Receptors

As predicted, both *cb1* and *cb2* are expressed during early zebrafish development. *Cb1* expression has been shown to increase steadily throughout development after about 12 hpf (Figure 3A). Starting at 1 dpf, expression is localized within the preoptic area, which likely represents newly differentiated neurons (Figure 3B, C) [135]. Expression throughout the brain becomes far more widespread throughout development, in addition to the lens and the liver/gut region (Figure 3D-G). The abundance of CB1 receptors within the central nervous system makes it a prime candidate as a key regulator in the development of the nervous system, which is necessary to investigate due to the possibility of phytocannabinoids interfering with neurodevelopment by modulating CB1. As discussed previously, CB1 has been implicated for being involved in axonal growth and fasciculation [143], and blocking CB1 activity using synthetic antagonists during early development results in reduced locomotive activity [165, 166] and hatching rate [166], as well as aberrant motor neuron development and gross morphological defects [165]. Therefore, strong evidence suggests that CB1 activity is necessary in regulating proper embryonic development.

Cb2 is of particular interest due to relatively high transcript abundance at 6 hpf, followed by absence of expression at 12 hpf, and then presence again at 1 dpf and onward (Figure 4A). This regulation pattern suggests that *cb2* may play an important developmental role at the onset of gastrulation. Despite expression at 1, 2, and 3 dpf being revealed through RT-PCR data (Figure 4A), expression was not detected via in situ hybridization at those timepoints (Figure 4E-K). This is potentially due to diffuse expression spread out amongst different groups of tissues

and structures, which results in transcript abundance too low to be picked up by this technique. As such, *cb2* expression has been fairly controversial, with only two whole-mount in situ hybridizations being published as of yet, showing relatively questionable of *cb2* across the entire body at 18 hpf and 24 hpf [167] and in the liver at 2 dpf [162]. A promising preprint demonstrated the expression of *cb2* within hair cells at 3 dpf [159], however repeat in situs using the probe sequence provided were not able to replicate those results. As mentioned previously, there was much debate over the presence of *cb2* expression within cells of the central nervous system, which have yet to be shown via whole mount in situ hybridization, although the presence of transcripts in sections of adult zebrafish brain have been reported [142].

Rat models also support the presence of *cb1* and *cb2* expression in early embryonic development. Following implantation, both *cb1* and *cb2* mRNA was detected in the dam's uterine tissue, and *cb1* was detected in the placenta [168]. By embryonic day 11 (E11), *cb1* is present in early neural tissues including the telencephalon, and expression progresses to the spinal ganglia, and sympathetic ganglia by E13. Expression remains constant within areas such as the neocortex, olfactory bulb, thalamas, hypothalamus, and hippocampus until birth. Additionally, *cb1* expression is noted in the lens vesicle by E12, which corresponds to expression in the lens seen in zebrafish. In comparison, *cb2* mRNA is only found to be expressed in the liver in the mouse embryo, which begins at E13 and lasts throughout gestation [168].

Despite being investigated for their role in development, zebrafish knock-out models of both *cb1* and *cb2* have not been shown to cause any obvious morphological or behavioural abnormalities [145, 162]. But, known patterns of genetic compensation in knock-out models of zebrafish suggest that compensatory mechanisms may prevent full penetrance of the mutant phenotype [169, 170]. Therefore, knockdowns using morpholinos targeting *cb1* and *cb2* should

be conducted in addition to using knockout models to determine if CB receptors serve a developmental role.

4.1.2 TRP Receptors

The TRP family of receptors, which have been implicated as targets of endo- and phytocannabinoids, are all present within sensory neurons during early development (Figures 5-7). Although these receptors are well studied for their role in processing thermosensation, nociception, and sensing mechanical stimuli [100–104], little is known about whether signaling at these receptors is necessary for aspects of development.

Trpv1 and *trpa1b* are both expressed from 1 to 3 dpf (Figure 5A, 7A). *Trpv1* has relatively stable levels of expression, while *trpa1b* shows relatively low expression from 1 to 2 dpf, and increased expression at 3 dpf. As such, in situ hybridizations have only been able to detect expression at 3 dpf, likely because transcript abundance is too low to be detected at any earlier timepoint with the current protocol. The receptors share overlapping developmental profiles at 3 dpf, with both receptors present in lateral line ganglion and the trigeminal sensory neurons (Figures 5H, I, 7F, G). Lateral line ganglion are responsible for transmitting nerve impulses initiated by deflected stereocilia in response to water movement [171]. The trigeminal sensory neurons are a bundle of neurons innervating targets along the hindbrain and spinal cord, which relays mechanical, chemical, and temperature stimuli [172]. Although these neurons are well studied in their role for sensory perception, it is unknown whether signaling at these neurons is necessary for development.

Trpv1 is also expressed within Rohon-beard neurons at 1 dpf (Figure 5D, E). These are transient mechanosensory neurons present along the length of the body during early embryonic/larval stages, before undergoing apoptosis and replaced by the development of the dorsal root ganglion [173]. These neurons have not been linked to having a developmental function as of yet.

Trpv1 knockout models in mice are well-utilized to study the implications of the receptor on sensory perception. *Trpv1* was found to be expressed in the dorsal root ganglia by E13, and expanded expression to peripheral organs such as the developing lungs, cardiovascular tissue, the gastrointestinal tract, the urinary tract, and nerve fibers in the skin throughout gestation [174]. Homozygotes lacking TRPV1 channels are not associated with distinct morphological abnormalities or changes to survival, but do possess greater body masses, subtle changes in thermoregulation, and hypometabolism [175]. While *trv1* knockouts have not been performed in zebrafish, knockdown studies have shown that *trpv1* is essential for responding to heat sensation, however no observations were provided regarding survival rate, morphological, or behavioural abnormalities unrelated to heat stimuli [163]. Morpholinos targeting a *trpa1b* in zebrafish resulted in a significant decrease in the development and/or function of lateral line hair cells by approximately 3 dpf [176], but it is unclear whether knockdown of *trpa1b* resulted in any other abnormalities that may point to additional developmental roles.

Interestingly, TRPV1 mediated Ca^{2+} influx has been demonstrated to be required for axon degeneration in dorsal root ganglia in a mouse model [177]. Activation of TRPV1 by capsaicin stimulated an influx of Ca^{2+}, which in turn resulted in degeneration of sensory nerve fibres. This suggests that this receptor may be important in the process of pruning, which is an important event during neurodevelopment in which weaker synapses are removed to prevent excessive

synaptic connections [178]. However, it has not been determined if *trpv1* knockouts results in disorganized dorsal root ganglia. This discovery is exciting due to the prospect of TRPV1 activation playing a role in neurodevelopment, which may manifest in physiological outputs that have yet to be characterized.

Trpa1a expression in zebrafish is only present beginning at 3 dpf, at which expression is limited to the most posterior vagal sensory ganglion as consistent with literature [109], differentiating between the *trpa1b* paralog. The vagal sensory nerve innervates the pharyngeal jaws and teeth, but due to relatively late appearance of this nerve fiber during cytodifferentiation, it is unlikely for signaling to be responsible for stimulating tooth development [179]. There appears to be controversy of whether *trpa1a* is responsible for inner ear and lateral line hair cell function, with morpholinos and siRNA knockdown showing inhibited hair cell function [176], while loss-of-function mutants demonstrate no changes to hair cell function [109]. The lack of consensus on the role of *trpa1a* mediating proper function of hair cells warrants further investigation.

In mouse models, *Trpa1* is first detected within hair cells at E15-16 and expression is present throughout gestation [176]. Mouse models containing a loss-of-function mutation in *Trpa1* have shown reduced response to nociception and decreased generation of slowly adapting mechanically-activated currents in sensory neurons, but it is unknown whether TRPA1 mediates development [180].

Taken together, *trp* receptor expression is present throughout the developing zebrafish embryo, starting at 24 hours post fertilization. Receptors are enriched in sensory neurons including the vagal nerve, trigeminal sensory neurons, lateral line ganglion, and Rohon-beard neurons. While these neurons have been well studied in their role in sensing different types of

stimuli, they have yet to be investigated in a developmental role. Further research should be conducted on whether perturbations of TRP receptors result in abnormalities in development, especially in potential roles in regulating synaptic pruning.

4.1.3 G-Protein Coupled Receptor 55

GPR55 is an elusive target within the endocannabinoid system. Following identification and cloning of the potential cannabinoid receptor, little was done to investigate the function or role of this receptor [114]. This is especially true in zebrafish, which currently lacks any expression data.

RT-PCR of *gpr55* showed relatively low expression at 12 hpf, which increased slightly at 1 to 3 dpf (Figure 8A). In situ hybridizations did not detect expression at 12 hpf or 1 dpf (Figure 8C-E), but did pick up a stain specifically in the hindbrain at 2 dpf (Figure 8F), and diffusely throughout the brain at 2 dpf and 3 dpf (Figure 8F, G, I, J). Staining in the head was not present in the no-probe control (Figure 8I, K). Expression in the brain is supported by adult mouse models, which report enrichment of *gpr55* in the frontal cortex, striatum, hypothalamus, and brain stem [112] – which is a structure within the hindbrain and evolutionarily similar to the zebrafish hindbrain.

Recently, *gpr55* knockouts in mice have shown that the receptor may play an important role in the development of the nervous system by modulating axonal growth and innervation of target cells [181]. Stimulation of GPR55 using agonists resulted in chemoattraction of retinal ganglion cells, and stimulated growth of growth cones. In contrast, mice with $gpr55^{-/-}$ knockouts showed decreased branching in the dorsal terminal nucleus, as well as lower projections in retinal ganglia. Additionally, *lyso*-phosphatidyl-β-D-glucoside, a ligand that binds to GPR55

with high affinity, was shown to modulate the growth of spinal cord sensory neurons by repulsively guiding the growth of nociceptive axon projections in chick and mouse embryos [182].

These studies suggest that *gpr55* may play an important role in the development of the nervous system by modulating axonal growth and branching. As administrations of THC and CBD have been shown to alter branching of motor neurons [154], it is important to investigate whether this mechanism may be facilitated by aberrant GPR55 signaling. Knockout or knockdown studies on zebrafish embryos should be conducted to elucidate whether GPR55 is responsible for proper neurodevelopment.

4.1.4 General Conclusions

In summary, key receptors that are modulated by endo- and phytocannabinoids, including classical cannabinoid receptors, receptors part of the *trp* family of receptors, and miscellaneous G-protein receptors are expressed during early development in the zebrafish embryo. The presence of expression within the nervous system, coupled with strong evidence suggesting that several receptors, including CB1, TRPV1 and GPR55 may be involved in aspects of neurodevelopment, raises questions of whether perturbing signaling at these receptors, potentially by exposure to phytocannabinoids, may cause alterations in proper development. This comprehensive timeline mapping out temporal and spatial expression of these receptors throughout embryonic development provides a foundation at which each receptor can be further investigated.

4.2 Upregulating the SHH pathway to prevent Cannabidiol teratogenicity with Purmorphamine

4.2.1 General Parameters

To determine if toxic and teratogenic effects of CBD are mediated through downregulation of the SHH pathway, CBD was co-exposed to zebrafish embryos in the presence of purmorphamine (PM), a known agonist for Smoothened (SMO). Phytocannabinoids are proposed to modulate the SHH pathway at SMO by binding to, and reducing activity of the receptor [133, 134]. Typically, SMO activity is stimulated following activation of Patched (PTCH) by SHH, which stimulates internalization and degradation of the receptor, relieving the inhibition on SMO [126]. Once relieved, SMO initiates the downstream signaling cascade by inhibiting adenylyl cyclase (AC), which ultimately results in transcription of SHH target gene expression. In the presence of a SMO inhibitor, pathway activation is reduced, resulting in downregulation of SHH target genes, and potentially resulting in teratogenic effects which may be resolved by co-exposure to a SMO agonist. I hypothesized that co-exposure of PM would be able to rescue detrimental effects of CBD, including stimulating greater body length, reducing mortality rates, and increasing hatching rates, which would ultimately implicate reduced SHH signaling as a major factor in CBD mediated teratogenicity.

I chose to investigate concentrations of 1, 5, 10, and 20 μM of PM, in accordance with previous literature [183–185]. Furthermore, a concentration of 3 mg/L of CBD was chosen to be consistent with past work in the Ali lab [154]. This concentration consistently results in embryos with morphological abnormalities, as well as a mortality rate of approximately 60%, which leaves a sufficient number of embryos able to survive until 5 dpf that can undergo further testing.

Physiologically, this concentration does represent a very high dose of CBD. For context, Ohlsson et. al showed that smoking a single cigarette containing 19.2 mg of CBD resulted in a plasma concentration of 0.11 mg/L three minutes after administration, which decreased steadily over time [186]. However, oral supplements often contain higher CBD content [187], which may translate to individuals being exposed to much higher concentrations of CBD. As well, it is important to note that the presence of an intact chorion likely prevents zebrafish embryos from being exposed to the full extent of the drug exposure [188], and lower concentrations of the drug are likely to be absorbed by the embryo. We chose to keep the chorions intact rather than dechorionating the samples to prevent increased mortality of the embryos, as well as to measure hatching rate as an important parameter of development.

Embryos were pre-exposed to PM for 30 min prior to gastrulation to allow activation of the SHH pathway before administration of CBD. Then, embryos were exposed to both PM and CBD throughout the duration of gastrulation. The time period of gastrulation was chosen as it represents a major developmental event in early embryonic development, and proper specification of the three tissue layers and establishment of the embryonic axis is necessary for development of the whole organism. This timepoint has been shown to be particularly susceptible to teratogens, seen especially in ethanol teratogenicity [28, 189]. Additionally, gastrulation is the time period at which nervous system development is initiated, with induction of the neural plate [136]. As such, disrupting this process may have consequences in early neurodevelopment.

Co-exposure of PM with CBD resulted in a significant increase in body lengths at each concentration tested (1 μM to 20 μM PM ranging from 3.15 ± 0.05 to 3.49 ± 0.02 mm) compared to CBD itself (2.7 ± 0.09 mm) by 5 dpf (Figure 9). The body lengths of embryos treated with 5,

10, and 20 μM were not significantly different from each other, but all three exhibited greater lengths than embryos treated with CBD and 1 μM PM by approximately 0.3 mm (Figure 9G). These results suggest that the dose-dependent response is only present from 1 μM and 5 μM, and reaches its maximum efficacy from 5 μM to 20 μM. However, I observed a significant difference between all four PM experimental treatment groups and the vehicle control, with body lengths of PM treated fish ranging from 3.15 to 3.49 mm, compared to 3.73 ± 0.02 mm in the vehicle control. Of note, the addition of DMSO, which is the vehicle for PM, does not have an effect on the ability of CBD to decrease body lengths (Figure 10). Since there was no difference between the ranges of 5 μM to 20 μM PM, it is unlikely that increasingly higher concentrations would result in improved rescue conditions. There are at least three possibilities as to why PM was not able to stimulate growth to the level of the vehicle control:

1) Body lengths may only be partially mediated by the SHH pathway. SHH is well known to regulate cell proliferation and body patterning [122], which makes an attractive target to investigate in altered growth of treated larvae. However, as previously discussed, CBD has been implicated in interacting with a wide range of receptors, including CB, TRP, and other G-protein coupled receptors. Therefore, effects on numerous signaling pathway may have additive effects on body length, and targeting only one of these pathways may result in a marginal increase in body length.

2) CBD may be able to outcompete PM to inhibit SMO, so that even if embryos are exposed to high concentrations of PM, the presence of CBD is still able to downregulate the SHH pathway to a certain degree. CBD was shown to reduce the ability of Smoothened Agonist (SAG), a known SMO agonist similar to PM, to activate the SHH pathway [133]. Moreover, CBD was able to compete with cyclopamine, a known antagonist that binds directly to SMO, to

reduce binding efficacy, suggesting that CBD may either bind in the transmembrane pocket or act as an allosteric modulator of SMO. Based on this study, it is highly likely that PM is unable to promote SHH activity to baseline levels due to the inhibitory effect of CBD.

3) PM itself may cause teratogenic effects, which results in reduction of body length. High doses of PM at 10 and 20 μM had slight detrimental effects on body length, with both doses resulting in average body lengths of 3.59 ± 0.19 mm, compared to 3.73 ± 0.02 mm in the vehicle control (Figure 10). While this difference is only at the magnitude of 0.14 mm, the consistency of this trend suggests that high doses of PM may have teratogenic effects on their own, which manifests by reducing body lengths. Therefore, increasing the concentration of PM to combat the effects of CBD may be ineffective due to the possibility of PM exerting dose-dependent teratogenic effects at high concentrations.

Despite not achieving 100% rescue, the ability for PM to stimulate increased body lengths is highly significant, as it provides strong evidence that CBD exerts teratogenic effects at least partially through the SHH pathway.

The results of survival/hatching rates were able to support these conclusions. Significant increases in survival rate were observed by all four concentrations of PM treatments (60.8% to 75.2% survival) compared to CBD (25.6% survival) by 5 dpf (Figure 11A). Additionally, concentrations of 5, 10, and 20 μM of PM were able to stimulate increased hatching rates compared to CBD, especially at 3 and 4 dpf (Figure 12A). Survival and hatching rates were not affected by the presence of PM itself at all four concentrations in comparison to the vehicle control or untreated control (Figure 11B, 12B). The ability of PM to be able to decrease mortality indicates that CBD-mediated downregulation of the SHH pathway results in toxicity, which can be counteracted by stimulating activity of the pathway.

Hatching is a parameter that provides a rough estimate of the rate of zebrafish development. Typically, embryos hatch from their chorions at around 3 dpf, although there is often large variability between 2 and 4 dpf. The inability of embryos to hatch from their chorions may result from two possible factors: the degradation of the chorion, or locomotive ability of the zebrafish. The chorion, which is a thick membrane encasing the developing embryo, is broken down by the secretion of choriolysins into the perivitelline space [190]. Delays in development may also delay the timepoint at which these choriolytic enzymes are secreted, as demonstrated by embryos raised in low temperatures [191]. As the chorion is broken down, spontaneous movements of the embryo are required to lead to hatching. Embryos that have severe axial curvature or severely reduced lengths are often completely immobile, leading to those embryos never gaining the ability to hatch from their chorions. Therefore, reductions in hatching rate caused by CBD, and a subsequent rescue by PM, may be facilitated by an increase in the rate of development, leading to the production and secretion of choriolysins, and/or increased locomotive ability of the fish to be able to break free from the membrane.

In summary, the ability of PM to mediate the teratogenic effects of CBD by increasing body lengths, and improving survival and hatching rates of treated fish is extremely promising, as this is the first time that upregulating the SHH pathway has been shown to improve the teratogenic effects of phytocannabinoids in zebrafish. Together, these results provide strong evidence that the SHH pathway is modulated by cannabinoids, and provides a basis at which further investigations can occur.

4.2.2 Swim Bladder Morphology of Cannabidiol and Purmorphamine treated fish

During assessments of gross morphology following phytocannabinoid exposure, it was noted that many treated fish lacked fully inflated swim bladders (SB), which typically result in a spherical shape by 5 dpf. As SB development in zebrafish is hypothesized to be homologous to lung development in mammals [192], studying the impact of CBD exposure on this structure is imperative to determining developmental consequences of prenatal cannabinoid exposure. I hypothesized that SB development may be controlled by the SHH pathway, such that increasing activity with the addition of PM may be able to counteract the detrimental effects of CBD and result in greater proportions of fish with properly inflated SBs.

The SB is of particular interest because the SHH pathway is theorized to control development of this structure by directing cell specification and organization of the three tissue layers [125]. Therefore, impaired SHH signaling may result in improper SB development, and ultimately prevent proper inflation. However, an alternate explanation of deflation is that larvae are required to swim to the surface of the water to initially inflate their bladders [193] – therefore, impaired locomotion or delayed hatching rates could also result in deflated SBs. While most larvae do retain the basic escape response movement following mechanical stimuli, it is unknown whether larvae are able to demonstrate swim-up movement to reach the air/water interface. I hypothesized that CBD mediated downregulation of the SHH pathway was responsible for causing defective SB inflation, either by directly interfering with SB development, or indirectly by causing impaired locomotion, which may prevent fish from swimming to the surface of the water.

As predicted, CBD exposures resulted in only 10% of the fish exhibiting fully inflated SBs (Figure 13D). Surprisingly, high concentrations of PM were able to induce deflated SBs on their

own, with 10 μM and 20 μM resulting in 64.8% and 46.3% fully inflated SBs, respectively. Although this was unexpected, the results validate the role of the SHH pathway in SB formation because perturbing the pathway via overstimulation may also result in aberrant development, similar to the effects of reduced signaling.

Unexpectedly, the only significant levels of rescue following CBD and PM exposure occurred at the lowest and highest concentrations of PM. 1 and 20 μM stimulated full SB inflation in 40.5% and 31.0% of fish, respectively (Figure 13D). This is the first time that PM has displayed a biphasic pattern in efficacy, as most previous experiments have shown a dose-dependent trend. To determine whether this response can be extended beyond the extremes of the concentration gradient studied, and to identify an optimal concentration for SB inflation, embryos should be exposed to concentrations lower than 1 μM and greater than 20 μM. This pattern suggests that SB development is very complex, and may require very specific levels of SHH activity to stimulate proper inflation.

In conclusion, the results of SB quantification are somewhat inconclusive. Abnormal SB inflation at higher concentrations of PM suggest that perturbations of SHH pathway result in altered SB inflation – whether this effect is due to reduced ability to swim to the air/water interface or due to impaired organization of the tissue layers of the SB itself is unknown. Marginal rescues were seen at two extremes of the concentrations tested, with no significant rescue at the two middle concentrations of 5 and 10 μM, which deviated from trends seen in other parameters. Ultimately, the rescue seen at 1 and 20 μM does support the conclusion that SB development may be reliant on proper SHH signaling, and the detrimental effects of CBD may be rescued to a certain degree by upregulating the pathway.

As this experiment only looked at a snapshot at 5 dpf, further follow-up with embryos at 6

and 7 dpf would be able to discern whether fish are experiencing a complete lack of SB inflation, or merely a delay in bladder inflation. Additionally, fish should be observed for "swim-up" behaviour following hatching to observe whether impaired ability to reach the air/water interface to initially inflate their SBs is responsible for causing improper inflation. Lastly, this experiment grouped together fish with "partially inflated SBs" and "no SB inflation" due to the difficulty in assessing the differences between both using light microscopy (Figure 13 B-C). Being able to decipher whether SBs are present, but not inflated, compared to the absence of SBs entirely would be very advantageous in determining whether aberrant development or impaired locomotion is responsible for the trend seen in bladder inflation. Therefore, preparing and visualizing sections of zebrafish larvae to assess the presence of the bladder should logically follow to validate the results of this experiment.

4.2.3 Free-Swimming Behaviour of Cannabidiol and Purmorphamine treated fish

Two previous parameters of CBD teratogenicity – hatching and swim bladder inflation – are also mediated by locomotive ability of the larvae, which became an important metric to assess. I hypothesized that CBD treated fish would result in reduced swimming behaviour, in line with previous experiments investigating THC [155]. If reduced activity is caused by downregulation of SHH activity by CBD, then introducing PM should counteract the effects of CBD and result in fish achieving baseline levels of activity, as demonstrated by the vehicle control.

Four parameters were chosen to give a comprehensive overview of free-swimming behaviour: total distance travelled (mm) (Figure 14A), average speed (cm/s) (Figure 14B), Frequency of movements per hour (Figure 14C), and percentage of activity per hour (Figure

14D). As predicted, CBD treatments caused decreased activity in all four parameters tested. However, distance travelled and the frequency of movements were the only two metrics that demonstrated a significant increase in a PM treated sample, with CBD + 10 μM PM treated fish showing significant increases in activity with both metrics (Figure 14B, D). In all four metrics, it appears as though there may be a trend of increased activity for all four concentrations of PM in comparison to CBD alone, but due to large variability within each treatment group, these results were not significant.

From these experiments, I can conclude that CBD treated fish indeed displayed low levels of activity for each parameter observed. Although it seems as though PM was able to increase activity to a certain degree, these results were only significant for embryos treated with 10 μM PM in total distance travelled and the frequency of movements per hour. Low locomotive ability of CBD treated fish likely accounted for their low hatching rates, which require spontaneous movement to be able to break free from their chorions. Additionally, these results may be applied to SB inflation, because fish unable to swim to the surface of the air/water interface would be able to inflate their bladders. Since there was no significance between PM treated fish and CBD treated fish in most metrics and treatment groups, it is possible that fish co-exposed to PM also experienced impaired locomotive ability, which may explain the poor rates of SB inflation. Despite great variation within treatment groups, the ability of PM to increase locomotive ability in distance travelled and frequency of movements indicates that CBD impairs free-swimming behaviour in a mechanism that is at least partially mediated by the SHH pathway.

4.2.4 Cannabidiol and Purmorphamine on *ptch2* Expression

Previous experiments were conducted to determine whether upregulating the SHH pathway in the presence of CBD would rescue the teratogenic effects of CBD. Despite strong evidence suggesting that CBD is indeed downregulating the SHH pathway, which can be rescued by activating the SHH pathway, I lacked evidence of altered SHH signaling at a molecular level. In order to determine changes in SHH signaling at the transcriptional level, I chose to investigate *ptch2*, which codes for one of two PTCH homologues [194]. I hypothesized that CBD exposure would reduce *ptch2* expression to compensate for reduced SMO activity. If CBD indeed downregulated *ptch2* transcription, then I predicted that PM exposures would thus increase SHH levels to baseline, which would result in similar expression patterns to the vehicle control.

The PTCH receptor regulates the SHH pathway by constitutively inhibiting SMO, until bound by the SHH ligand, which stimulates internalization and degradation of the receptor and ultimately relieves the suppression on SMO. *Ptch* expression is highly dynamic and regulates the activity of the pathway – as such, *smo* mutants have shown almost no *ptch* expression to correct for the lack of SHH signaling [195]. At the end of gastrulation, *ptch2* is present in the ventral neural plate and adaxial cells, which are precursors to slow muscle cells [164]. At 1 dpf, expression is located in the posterior notochord, floor plate, adaxial cells, ventral brain [158]. I chose to investigate both timepoints to observe whether 1) *ptch2* expression is altered immediately following a 5.5 hour exposure to CBD and PM, and 2) CBD has long-term effects on *ptch2* transcription levels.

Embryos treated with CBD probed for *ptch2* at the end of gastrulation (10.75 hpf) showed a decrease in expression, which was shared amongst embryos co-exposed with 1 and 5 μM PM (Figure 15A-C). There appeared to be an increase in expression at CBD plus 20 μM PM, which

was consistent between the 20 μM control and vehicle control (Figure 15D-F). However, due to the semi-quantitative nature of in situ hybridizations, firm conclusions regarding expression levels cannot be made. Interestingly, embryos treated with CBD, and co-exposures of 1 and 5 μM PM demonstrated aberrant organization of the adaxial cells. Typically, adaxial cells are present in two parallel tracts on either side of the notochord [196]. Embryos treated with CBD and low doses of PM showed severe divergence of the tracts, suggesting that CBD treatment induces midline abnormalities (Figure 15A-C). Midline abnormalities often manifest in defective gross morphology, most commonly reflected in axial curvature [197], which is a common observation in phytocannabinoid-treated fish [154]. The disorganized midline appears to be resolved with the addition of 20 μM PM, and the level/location of expression appears to be relatively stable between embryos treated with 20 μM PM alone, and the vehicle control (Figure 15D-F).

By 24 hpf, it appears as though there are no longer any differences in spatial expression between treatment groups (Figure 16A-F). However, CBD treated embryos consistently showed decreased *ptch2* expression particularly in the diencephalon compared to all other treatment groups, which appeared to be relatively stable.

Taken together, these results suggest that CBD affects the level of *ptch2* expression directly following exposure during gastrulation, but may also have long-lasting effects that extend over 12 hours after the exposure has been removed. Additionally, CBD induces midline effects that are observable by 10.75 hpf, which may account for defective axial curvature signature of CBD treated embryos. Future studies should assess *ptch2* expression quantitively using qPCR to provide a definitive assessment of relative transcript abundance, due to the difficulty in appraising expression levels via in situ hybridization. To determine if

disorganization of adaxial cells results in improper muscle development, electron microscopy of slow muscle fibres of older fish should be conducted. Aberrant muscle organization would indicate that disrupted adaxial cells manifests in long-term developmental effects.

4.3 Downregulating the SHH Pathway with Cyclopamine

Previously, I have shown that CBD exposure during gastrulation results in developmental abnormalities including reduced body length, increased mortality rates, and decreased hatching, with the hypothesis that these effects are mediated through the SHH pathway. To confirm whether these parameters are characteristic of decreased SHH signaling during gastrulation, the same exposure paradigm was repeated with cyclopamine, a known SMO antagonist, and compared to CBD treated fish. If CBD exerts its effects by downregulating the SHH pathway at SMO, then cyclopamine exposure should also result in similar detrimental developmental outcomes. Concentrations of 25, 50, and 100 μM were chosen in accordance with previous literature [198–200]. A vehicle control of 1% DMSO was chosen to reflect the highest volume of DMSO required, equivalent to the 100 μM treatment.

CBD and cyclopamine treated fish both exhibited axial curvature, which became more severe when cyclopamine was increased in concentration from 25 to 100 μM (Figure 17A-C). CBD treated fish typically exhibit individual variation in the severity of axial curvature, as seen in Figure 17D and E, which are similar to larvae treated with 25 and 50 μM of cyclopamine. Cyclopamine and CBD treated fish also exhibit pericardial edema.

The body lengths of cyclopamine treated fish decreased in a dose-dependent pattern (Figure 17F). All concentrations of cyclopamine caused smaller body lengths than CBD treated

fish in this experiment (3.33 ± 0.06 mm), but previous experiments showed that CBD treated fish have an average length of 2.7 ± 0.087 mm, which are comparable to body lengths of fish treated with 25 μM of cyclopamine (2.89 ± 0.1 mm). This discrepancy in size between CBD-treated fish of different experiments is likely attributed to a less-potent batch of CBD, which was used throughout the duration of this experiment. In conclusion – cyclopamine exposure during gastrulation was capable of reducing the body lengths of fish in a dose-dependent mechanism.

Hatching rate was also severely affected by the addition of cyclopamine, with the 25 μM treatment giving similar trends to CBD treated fish (Figure 18B). 50 μM and 100 μM treatments resulted in 0% hatching rates throughout the duration of the experiment, which was likely due to severe axial curvature preventing movement of the embryos. Cyclopamine exposures confirmed that downregulation of the SHH pathway impairs ability of the larvae to hatch within 5 dpf.

Unexpectedly, cyclopamine exposures did not affect survival rates at any concentration (Figure 18A). Despite predicting that the toxic effects imparted by CBD exposure was the result of SHH downregulation, resulting in increased mortality rates, exposure to cyclopamine did not support this conclusion. It is possible that the concentrations tested were not sufficient at inducing toxic effects, and increasing the concentration beyond 100 μM would potentially result in increased mortality. However, due to the severe morphological defects seen at 100 μM, increasing the concentration beyond that would no longer be comparable to 3 mg/L of CBD, which does not induce similar levels of morphological abnormalities. It is also possible that CBD exerts different effects on SMO compared to cyclopamine. CBD has been described as a potential inverse agonist at SMO, by acting as an allosteric modulator to prevent interaction by other ligands, including cyclopamine [133]. Therefore, CBD inhibition of SMO may induce different effects compared to cyclopamine, which manifest in reduced survival. Since increased

mortality rates following CBD exposure cannot be directly explained by downregulation of SHH, this metric warrants further investigation.

In summary, the teratogenic effects of cyclopamine exposure during gastrulation mirrored effects that are observed by CBD, which supports the hypothesis that downregulation of the SHH pathway is able to induce morphological and behavioural abnormalities.

5. Conclusions and Future Directions

The ECS has become a popular focus within recent research due to the legalization, and increased prevalence of cannabis use in recent history. As cannabis is the most commonly used recreational drug in pregnancy, it is imperative to determine whether the endocannabinoid system plays a role in the developing embryo, and to characterize phytocannabinoid-mediated disruptions that lead to teratogenic effects. This work served to document the progression of endocannabinoid receptors throughout development, and investigated the mechanism of CBD-mediated teratogenicity by implicating the SHH pathway.

Zebrafish are robust model organisms that are especially well suited to study ECS development due to the high level of conservation between humans and zebrafish. However, using this model to study ECS development has been hampered by the lack of data available regarding the expression of ECS components throughout early development. Based on this gap in the literature, I chose to develop a comprehensive timeline of spatial, temporal, and semi-quantitative expression of six key cannabinoid receptors from 6 hpf to 3 dpf. I hypothesized that all receptors would be expressed during early development, and likely enriched within the central and peripheral nervous system. As expected, each receptor was present between 6 hpf and 3 dpf, and all receptors, with the exception of *cb2*, demonstrated expression within the nervous system.

The creation of a timeline mapping expression of key cannabinoid receptors throughout development aims to serve as foundation to investigate the role of each receptor during development. For example, exposure to specific antagonists of each receptor, administered during the timepoints at which expression is occurring, may reveal whether blocking receptor activity causes adverse developmental effects. Additionally, knowing timepoints and tissues that

express ECS receptors is valuable for studying perturbation by phytocannabinoids, which connects with the second half of this research. The developmental timeline showed that *cb2* may be the only receptor with meaningful levels of expression during gastrulation, the timepoint at which CBD was exposed to the developing embryo. Therefore, modulation of CB2 signaling is most likely to be responsible for abnormal development, in addition to disruption of SHH signaling. Performing targeted exposures of CBD or other phytocannabinoids at timepoints enriched with ECS receptor expression, such as timepoints following 1 dpf, may reveal whether perturbation of ECS receptor signaling leads to adverse developmental effects.

Previous studies have suggested that endo- and phytocannabinoids are negative regulators of the SHH pathway by inhibiting SMO, resulting in reduced transcription of SHH target genes. I hypothesized that CBD-mediated downregulation of SMO may be responsible for causing classic teratogenic effects observed by CBD-treated fish, which would be resolved by co-exposure to a potent SMO agonist. Co-incubation of CBD and PM confirmed that PM is able to rescue teratogenic effects of CBD by increasing body length, survival/hatching rate, and free-swimming activity. Moreover, CBD was shown to reduce expression of *ptch2*, a regulatory receptor within the SHH pathway, at both 10.75 and 24 hpf, and cause disorganization of adaxial cells at 10.75 hpf. Finally, CBD exposures disrupted proper SB inflation, which was marginally rescued by low and high concentrations of PM. Taken together, these experiments provide strong evidence that CBD acts on the SHH pathway to cause teratogenic effects, which can be resolved by simultaneous upregulation of SMO.

Additionally, to confirm that inhibition of SMO is able to induce the teratogenic effects seen by CBD, embryos were exposed to cyclopamine, a known SMO antagonist, during gastrulation. Cyclopamine was able to induce similar detrimental effects on morphology, body

length, and hatching, but had no effect on mortality. While this metric warrants further investigation, exposure to cyclopamine generally mirrors the effects of CBD, which provides further evidence that CBD exerts its effects through the SHH pathway.

This research took advantage of pharmacological agents, including PM and cyclopamine, to upregulate or downregulate the SHH pathway, respectively. Although both reagents are commonly used to modify activity of the SHH pathway, this work relies on the assumption that both compounds are indeed able to cross the chorion and act via their predicted mechanisms. To confirm that PM especially is able to increase activity of the SHH pathway, and that CBD is indeed able to decrease SHH activity, protein levels of PTCH, the main regulatory receptor, should be investigated. Using a fluorescent reporter strain to confirm that CBD exposure reduces PTCH accumulation in the membrane, which is then rescued by the addition of PM, would provide strong evidence that CBD does indeed modulate activity of the SHH pathway.

Furthermore, this thesis laid the foundation for investigating phytocannabinoid mediated downregulation of the SHH pathway, but there is much more that should be investigated. One area of expansion within this work is the focus on CBD, which may not be representative of other major components of cannabis such as THC, or cannabis preparations that usually contain hundreds of different compounds [69]. Therefore, further experiments combining the actions of THC and CBD, as well as using prepared extracts that contain the full range of compounds found in cannabis products will serve as a realistic representation of cannabis consumption in pregnancy.

In summary, this research aimed to elucidate the expression of the ECS throughout early development while also investigating a prime candidate for the mechanism of phytocannabinoid mediated teratogenicity. Both components of this thesis provide a strong basis for future

research, which is necessary to fully understand the ECS in development, and how it may be relevant in preventing deleterious effects from prenatal cannabis exposure.

Literature Cited

1. Mercuri AM, Accorsi CA, Bandini Mazzanti M (2002) The long history of Cannabis and its cultivation by the Romans in central Italy, shown by pollen records from Lago Albano and Lago di Nemi. Veg Hist Archaeobot 11:263–276. https://doi.org/10.1007/s003340200039

2. Gaoni Y, Mechoulam R (1964) Isolation, Structure, and Partial Synthesis of an Active Constituent of Hashish. J Am Chem Soc 86:1646–1647. https://doi.org/10.1021/ja01062a046

3. Adams R, Hunt M, Clark JH (1940) Structure of Cannabidiol, a Product Isolated from the Marihuana Extract of Minnesota Wild Hemp. I. J Am Chem Soc 62:196–200. https://doi.org/10.1021/ja01858a058

4. Serpell M, Ratcliffe S, Hovorka J, et al (2014) A double-blind, randomized, placebo-controlled, parallel group study of THC/CBD spray in peripheral neuropathic pain treatment. Eur J Pain (United Kingdom) 18:999–1012. https://doi.org/10.1002/j.1532-2149.2013.00445.x

5. Capano A, Weaver R, Burkman E (2020) Evaluation of the effects of CBD hemp extract on opioid use and quality of life indicators in chronic pain patients: a prospective cohort study. Postgrad Med 132:56–61. https://doi.org/10.1080/00325481.2019.1685298

6. Li X, Vigil JM, Stith SS, et al (2019) The effectiveness of self-directed medical cannabis treatment for pain. Complement Ther Med 46:123–130. https://doi.org/10.1016/j.ctim.2019.07.022

7. Kasper AM, Andy Sparks S, Hooks M, et al (2020) High prevalence ofcannabidiol use within male professional rugby union and league players: A quest for pain relief and enhanced recovery. Int J Sport Nutr Exerc Metab 30:315–322. https://doi.org/10.1123/IJSNEM.2020-0151

8. Prud'Homme M, Cata R, Jutras-Aswad D (2015) Cannabidiol as an intervention for addictive behaviors: A systematic review of the evidence. Subst Abus Res Treat 9:33–38.

https://doi.org/10.4137/SART.S25081

9. Bergamaschi MM, Queiroz RHC, Chagas MHN, et al (2011) Cannabidiol reduces the anxiety induced by simulated public speaking in treatment-nave social phobia patients. Neuropsychopharmacology 36:1219–1226. https://doi.org/10.1038/npp.2011.6

10. Shannon S, Lewis N, Lee H, Hughes S (2019) Cannabidiol in Anxiety and Sleep: A Large Case Series. Perm J 23:18–041. https://doi.org/10.7812/TPP/18-041

11. Shannon S, Opila-Lehman J (2016) Effectiveness of Cannabidiol Oil for Pediatric Anxiety and Insomnia as Part of Posttraumatic Stress Disorder: A Case Report. Perm J 20:108–111. https://doi.org/10.7812/TPP/16-005

12. De Souza Crippa JA, Zuardi AW, Garrido GEJ, et al (2004) Effects of Cannabidiol (CBD) on Regional Cerebral Blood Flow. Neuropsychopharmacology 29:417–426. https://doi.org/10.1038/sj.npp.1300340

13. Lotan I, Treves TA, Roditi Y, Djaldetti R (2014) Cannabis (Medical Marijuana) treatment for motor and non-motor symptoms of parkinson disease: An open-label observational study. Clin Neuropharmacol 37:41–44. https://doi.org/10.1097/WNF.0000000000000016

14. Carroll CB, Bain PO, Teare L, et al (2004) Cannabis for dyskinesia in Parkinson disease: A randomized double-blind crossover study. Neurology 63:1245–1250. https://doi.org/10.1212/01.WNL.0000140288.48796.8E

15. Lim K, See YM, Lee J (2017) A systematic review of the effectiveness of medical cannabis for psychiatric, movement and neurodegenerative disorders. Clin Psychopharmacol Neurosci 15:301–312. https://doi.org/10.9758/cpn.2017.15.4.301

16. Kluger B, Triolo P, Jones W, Jankovic J (2015) The therapeutic potential of cannabinoids for movement disorders. Mov Disord 30:313–327. https://doi.org/10.1002/mds.26142

17. Consroe P, Laguna J, Allender J, et al (1991) Controlled clinical trial of cannabidiol in Huntington's disease. Pharmacol Biochem Behav 40:701–708. https://doi.org/10.1016/0091-3057(91)90386-G

18. Metternich B, Wagner K, Geiger MJ, et al (2020) Cognitive and behavioral effects of cannabidiol in patients with treatment-resistant epilepsy. Epilepsy Behav 107558. https://doi.org/10.1016/j.yebeh.2020.107558

19. Tzadok M, Uliel-Siboni S, Linder I, et al (2016) CBD-enriched medical cannabis for intractable pediatric epilepsy: The current Israeli experience. Seizure 35:41–44. https://doi.org/10.1016/j.seizure.2016.01.004

20. Hausman-Kedem M, Menascu S, Kramer U (2018) Efficacy of CBD-enriched medical cannabis for treatment of refractory epilepsy in children and adolescents – An observational, longitudinal study. Brain Dev 40:544–551. https://doi.org/10.1016/j.braindev.2018.03.013

21. McGregor IS, Cairns EA, Abelev S, et al (2020) Access to cannabidiol without a prescription: A cross-country comparison and analysis. Int J Drug Policy 85:102935. https://doi.org/10.1016/j.drugpo.2020.102935

22. Rotermann M (2020) What has changed since cannabis was legalized? Heal Reports 31:11–20. https://doi.org/10.25318/82-003-x202000200002-eng

23. Hammond D, Goodman S (2020) Knowledge of Tetrahydrocannabinol and Cannabidiol Levels Among Cannabis Consumers in the United States and Canada. Cannabis Cannabinoid Res X:can.2020.0092. https://doi.org/10.1089/can.2020.0092

24. Amroussia N, Watanabe M, Pearson JL (2020) Seeking safety: a focus group study of young adults' cannabis-related attitudes, and behavior in a state with legalized recreational cannabis. Harm Reduct J 17:1–7. https://doi.org/10.1186/s12954-020-00442-8

25. Finer LB, Zolna MR (2016) Declines in unintended pregnancy in the United States, 2008-2011. N Engl J Med 374:843–852. https://doi.org/10.1056/NEJMsa1506575

26. Burler SA, Khanlian SA, Cole LA (2001) Detection of early pregnancy forms of human chorionic gonadotropin by home pregnancy test devices. Clin Chem 47:2131–2136. https://doi.org/10.1093/clinchem/47.12.2131

27. Rogers JM, Brannen KC, Barbee BD, et al (2004) Methanol Exposure during Gastrulation Causes Holoprosencephaly, Facial Dysgenesis, and Cervical Vertebral Malformations in C57BL/6J Mice. Birth Defects Res Part B - Dev Reprod Toxicol 71:80–88. https://doi.org/10.1002/bdrb.20003

28. Kot-Leibovich H, Fainsod A (2009) Ethanol induces embryonic malformations by competing for retinaldehyde dehydrogenase activity during vertebrate gastrulation. DMM Dis Model Mech 2:295–305. https://doi.org/10.1242/dmm.001420

29. Hutchings DE, Martin BR, Gamagaris Z, et al (1989) Plasma concentrations of delta-9-tetrahydrocannabinol in dams and fetuses following acute or multiple prenatal dosing in rats. Life Sci 44:697–701. https://doi.org/10.1016/0024-3205(89)90380-9

30. Asch RH, Smith CG (1986) Effects of Δ9-THC, the principal psychoactive component of marijuana, during pregnancy in the rhesus monkey. J Reprod Med Obstet Gynecol 31:1071–81

31. Brown QL, Sarvet AL, Shmulewitz D, et al (2017) Trends in marijuana use among pregnant and non-pregnant reproductive-aged women, 2002-2014. JAMA - J Am Med Assoc 317:207–209. https://doi.org/10.1001/jama.2016.17383.Trends

32. Brown M (2018) CBD Oil for Pregnancy: How Moms Are Using It. In: Parents

33. National Institute on Drug Abuse (2020) Letter From the Director: Marijuana Research Report

34. Hoyme HE, Kalberg WO, Elliott AJ, et al (2016) Updated clinical guidelines for diagnosing fetal alcohol spectrum disorders. Pediatrics 138:1–18. https://doi.org/10.1542/peds.2015-4256

35. Gunn JKL, Rosales CB, Center KE, et al (2016) Prenatal exposure to cannabis and maternal and child health outcomes: A systematic review and meta-analysis. BMJ Open 6:1–8. https://doi.org/10.1136/bmjopen-2015-009986

36. Reece AS, Hulse GK (2019) Cannabis Teratology Explains Current Patterns of Coloradan

Congenital Defects: The Contribution of Increased Cannabinoid Exposure to Rising Teratological Trends. Clin Pediatr (Phila) 58:1085–1123. https://doi.org/10.1177/0009922819861281

37. Mclemore GL, Richardson KA (2016) Data from three prospective longitudinal human cohorts of prenatal marijuana exposure and offspring outcomes from the fetal period through young adulthood. Data Br 9:753–757. https://doi.org/10.1016/j.dib.2016.10.005

38. Day NL, Leech SL, Goldschmidt L (2011) The effects of prenatal marijuana exposure on delinquent behaviors are mediated by measures of neurocognitive functioning. Neurotoxicol Teratol. https://doi.org/10.1016/j.ntt.2010.07.006

39. Fried PA, Watkinson B, Gray R (2003) Differential effects on cognitive functioning in 13- to 16-year-olds prenatally exposed to cigarettes and marihuana. Neurotoxicol Teratol. https://doi.org/10.1016/S0892-0362(03)00029-1

40. Smith AM, Mioduszewski O, Hatchard T, et al (2016) Prenatal marijuana exposure impacts executive functioning into young adulthood: An fMRI study. Neurotoxicol. Teratol.

41. Gray KA, Day NL, Leech S, Richardson GA (2005) Prenatal marijuana exposure: Effect on child depressive symptoms at ten years of age. In: Neurotoxicology and Teratology

42. Heifets BD, Castillo PE (2009) Endocannabinoid Signaling and Long-Term Synaptic Plasticity. Annu Rev Physiol. https://doi.org/10.1146/annurev.physiol.010908.163149

43. Chevaleyre V, Castillo PE (2004) Endocannabinoid-mediated metaplasticity in the hippocampus. Neuron. https://doi.org/10.1016/j.neuron.2004.08.036

44. Pertwee RG (2006) Cannabinoid pharmacology: the first 66 years. Br J Pharmacol 147:S163–S171. https://doi.org/10.1038/sj.bjp.0706406

45. Maejima T, Hashimoto K, Yoshida T, et al (2001) Presynaptic inhibition caused by retrograde signal from metabotropic glutamate to cannabinoid receptors. Neuron 31:463–475. https://doi.org/10.1016/S0896-6273(01)00375-0

46. Ohno-Shosaku T, Maejima T, Kano M (2001) Endogenous cannabinoids mediate retrograde signals from depolarized postsynaptic neurons to presynaptic terminals. Neuron 29:729–738. https://doi.org/10.1016/S0896-6273(01)00247-1

47. Di Marzo V, Fontana A, Cadas H, et al (1994) Formation and inactivation of endogenous cannabinoid anandamide in central neurons. Nature 372:686–691. https://doi.org/10.1038/372686a0

48. Stella N, Piomelli D (2001) Receptor-dependent formation of endogenous cannabinoids in cortical neurons. Eur J Pharmacol 425:189–196. https://doi.org/10.1016/S0014-2999(01)01182-7

49. Rancz EA, Häusser M (2006) Dendritic calcium spikes are tunable triggers of cannabinoid release and short-term synaptic plasticity in cerebellar purkinje neurons. J Neurosci 26:5428–5437. https://doi.org/10.1523/JNEUROSCI.5284-05.2006

50. Daniel H, Rancillac A, Crepel F (2004) Mechanisms underlying cannabinoid inhibition of presynaptic Ca2+ influx at parallel fibre synapses of the rat cerebellum. J Physiol. https://doi.org/10.1113/jphysiol.2004.063263

51. Mcallister SD, Griffin G, Satin LS, Abood ME (1999) Cannabinoid receptors can activate and inhibit G protein-coupled inwardly rectifying potassium channels in a Xenopus oocyte expression system. J Pharmacol Exp Ther

52. Bidaut-Russell M, Devane WA, Howlett AC (1990) Cannabinoid Receptors and Modulation of Cyclic AMP Accumulation in the Rat Brain. J Neurochem 55:21–26. https://doi.org/10.1111/j.1471-4159.1990.tb08815.x

53. Bayewitch M, Avidor-Reiss T, Levy R, et al (1995) The peripheral cannabinoid receptor: adenylate cyclase inhibition and G protein coupling. FEBS Lett 375:143–147. https://doi.org/10.1016/0014-5793(95)01207-U

54. Felder CC, Joyce KE, Briley EM, et al (1995) Comparison of the pharmacology and signal transduction of the human cannabinoid CB1 and CB2 receptors. Mol Pharmacol

48:443–450

55. Chevaleyre V, Heifets BD, Kaeser PS, et al (2007) Endocannabinoid-Mediated Long-Term Plasticity Requires cAMP/PKA Signaling and RIM1α. Neuron. https://doi.org/10.1016/j.neuron.2007.05.020

56. Stella N, Schweitzer P, Plomelli D (1997) A second endogenous' cannabinoid that modulates long-term potentiation. Nature 388:773–778. https://doi.org/10.1038/42015

57. Sugiura T, Kodaka T, Nakane S, et al (1999) Evidence that the cannabinoid CB1 receptor is a 2-arachidonoylglycerol receptor: Structure-activity relationship of 2-arachidonoylglycerol, ether- linked analogues, and related compounds. J Biol Chem 274:2794–2801. https://doi.org/10.1074/jbc.274.5.2794

58. Savinainen JR, Järvinen T, Laine K, Laitinen JT (2001) Despite sabstantial degradation, 2-arachidonoylglycerol is a potent full efficacy agonist mediating CB1 receptor-dependent g-protein activation in rat cerebellar membranes. Br J Pharmacol 134:664–672. https://doi.org/10.1038/sj.bjp.0704297

59. Sugiura T, Kondo S, Kishimoto S, et al (2000) Evidence that 2-arachidonoylglycerol but not N-palmitoylethanolamine or anandamide is the physiological ligand for the cannabinoid CB2 receptor. Comparison of the agonistic activities of various cannabinoid receptor ligands in HL-60 cells. J Biol Chem 275:605–612. https://doi.org/10.1074/jbc.275.1.605

60. Gonsiorek W, Lunn C, Fan X, et al (2000) Endocannabinoid 2-arachidonyl glycerol is a full agonist through human type 2 cannabinoid receptor: Antagonism by anandamide. Mol Pharmacol 57:1045–1050

61. Zygmunt PM, Ermund A, Movahed P, et al (2013) Monoacylglycerols activate TRPV1 - A link between phospholipase C and TRPV1. PLoS One 8:. https://doi.org/10.1371/journal.pone.0081618

62. Mackie K, Devane WA, Hille B (1993) Anandamide, an endogenous cannabinoid, inhibits

calcium currents as a partial agonist in N18 neuroblastoma cells. Mol Pharmacol

63. Liu J, Wang L, Harvey-White J, et al (2006) A biosynthetic pathway for anandamide. Proc Natl Acad Sci U S A 103:13345–13350. https://doi.org/10.1073/pnas.0601832103

64. Ueda N, Tsuboi K, Uyama T, Ohnishi T (2011) Biosynthesis and degradation of the endocannabinoid 2-arachidonoylglycerol. BioFactors 37:1–7. https://doi.org/10.1002/biof.131

65. Smart D, Gunthorpe MJ, Jerman JC, et al (2000) The endogenous lipid anandamide is a full agonist at the human vanilloid receptor (hVR1). Br J Pharmacol 129:227–230. https://doi.org/10.1038/sj.bjp.0703050

66. Fenwick AJ, Fowler DK, Wu SW, et al (2017) Direct anandamide activation of TRPV1 produces divergent calcium and current responses. Front Mol Neurosci 10:1–11. https://doi.org/10.3389/fnmol.2017.00200

67. Chávez AE, Chiu CQ, Castillo PE (2011) TRPV1 activation by endogenous anandamide tirggers postsynaptic LTD in dentate gyrus. Nat Neurosci 13:1511–1518. https://doi.org/10.1038/nn.2684.TRPV1

68. Grueter BA, Brasnjo G, Malenka RC (2010) Postsynaptic TRPV1 triggers cell type–specific long-term depression in the nucleus accumbens. Nat Neurosci 13:1519–1525. https://doi.org/10.1038/nn.2685

69. Turner CE, Elsohly MA, Boeren EG (1980) Constituents of Cannabis sativa L. XVII. A Review of the Natural Constituents. J Nat Prod 43:169–234. https://doi.org/10.1021/np50008a001

70. Hanuš LO, Meyer SM, Muñoz E, et al (2016) Phytocannabinoids: A unified critical inventory

71. Marsicano G, Lutz B (1999) Expression of the cannabinoid receptor CB1 in distinct neuronal subpopulations in the adult mouse forebrain. Eur J Neurosci. https://doi.org/10.1046/j.1460-9568.1999.00847.x

72. Kawamura Y, Fukaya M, Maejima T, et al (2006) The CB1 cannabinoid receptor is the major cannabinoid receptor at excitatory presynaptic sites in the hippocampus and cerebellum. J Neurosci 26:2991–3001. https://doi.org/10.1523/JNEUROSCI.4872-05.2006

73. Van Waes V, Beverley JA, Siman H, et al (2012) CB1 cannabinoid receptor expression in the striatum: Association with corticostriatal circuits and developmental regulation. Front Pharmacol 3 MAR:1–8. https://doi.org/10.3389/fphar.2012.00021

74. Domenici MR, Azad SC, Marsicano G, et al (2006) Cannabinoid receptor type 1 located on presynaptic terminals of principal neurons in the forebrain controls glutamatergic synaptic transmission. J Neurosci 26:5794–5799. https://doi.org/10.1523/JNEUROSCI.0372-06.2006

75. Li H, Yang J, Tian C, et al (2020) Organized cannabinoid receptor distribution in neurons revealed by super-resolution fluorescence imaging. Nat Commun 11:. https://doi.org/10.1038/s41467-020-19510-5

76. Graham ES, Angel CE, Schwarcz LE, et al (2010) Detailed characterisation of CB2 receptor protein expression in peripheral blood immune cells from healthy human volunteers using flow cytometry. Int J Immunopathol Pharmacol 23:25–34. https://doi.org/10.1177/039463201002300103

77. Turcotte C, Blanchet MR, Laviolette M, Flamand N (2016) The CB2 receptor and its role as a regulator of inflammation. Cell Mol Life Sci 73:4449–4470. https://doi.org/10.1007/s00018-016-2300-4

78. Eisenstein TK, Meissler JJ, Wilson Q, et al (2007) Anandamide and Δ9-tetrahydrocannabinol directly inhibit cells of the immune system via CB2 receptors. J Neuroimmunol 189:17–22. https://doi.org/10.1016/j.jneuroim.2007.06.001

79. Núñez E, Benito C, Pazos MR, et al (2004) Cannabinoid CB2 receptors are expressed by perivascular microglial cells in the human brain: An Immunohistochemical Study. Synapse 53:208–213. https://doi.org/10.1002/syn.20050

80. Sviženská I, Dubový P, Šulcová A (2008) Cannabinoid receptors 1 and 2 (CB1 and CB2), their distribution, ligands and functional involvement in nervous system structures - A short review. Pharmacol. Biochem. Behav.

81. Atwood BK, MacKie K (2010) CB 2: A cannabinoid receptor with an identity crisis. Br J Pharmacol 160:467–479. https://doi.org/10.1111/j.1476-5381.2010.00729.x

82. Lanciego JL, Barroso-Chinea P, Rico AJ, et al (2011) Expression of the mRNA coding the cannabinoid receptor 2 in the pallidal complex of Macaca fascicularis. J Psychopharmacol 25:97–104. https://doi.org/10.1177/0269881110367732

83. García-Gutiérrez MS, García-Bueno B, Zoppi S, et al (2012) Chronic blockade of cannabinoid CB 2 receptors induces anxiolytic-like actions associated with alterations in GABA A receptors. Br J Pharmacol 165:951–964. https://doi.org/10.1111/j.1476-5381.2011.01625.x

84. Stempel AV, Stumpf A, Zhang HY, et al (2016) Cannabinoid Type 2 Receptors Mediate a Cell Type-Specific Plasticity in the Hippocampus. Neuron 90:795–809. https://doi.org/10.1016/j.neuron.2016.03.034

85. Li Y, Kim J (2015) Neuronal expression of CB2 cannabinoid receptor mRNAs in the mouse hippocampus. Neuroscience 311:253–267. https://doi.org/10.1016/j.neuroscience.2015.10.041

86. Stempel AV, Stumpf A, Zhang H-Y, et al (2016) Cannabinoid Type 2 Receptors Mediate a Cell Type-Specific Plasticity in the Hippocampus. Neuron 90:795–809. https://doi.org/10.1016/j.neuron.2016.03.034

87. Van Sickle MD, Duncan M, Kingsley PJ, et al (2005) Neuroscience: Identification and functional characterization of brainstem cannabinoid CB2 receptors. Science (80-) 310:329–332. https://doi.org/10.1126/science.1115740

88. Laaris N, Good CH, Lupica CR (2010) Δ9-tetrahydrocannabinol is a full agonist at CB1 receptors on GABA neuron axon terminals in the hippocampus. Neuropharmacology

59:121–127. https://doi.org/10.1016/j.neuropharm.2010.04.013

89. Paronis CA, Nikas SP, Shukla VG, Makriyannis A (2012) Δ9-Tetrahydrocannabinol acts as a partial agonist/antagonist in mice. Behav Pharmacol 23:802–805. https://doi.org/10.1097/FBP.0b013e32835a7c4d

90. Pertwee RG (2008) The diverse CB 1 and CB 2 receptor pharmacology of three plant cannabinoids: Δ 9-tetrahydrocannabinol, cannabidiol and Δ 9-tetrahydrocannabivarin. Br J Pharmacol 153:199–215. https://doi.org/10.1038/sj.bjp.0707442

91. Almeida DL De, Devi LA (2020) Diversity of molecular targets and signaling pathways for CBD. Pharmacol Res Perspect e00682:1–10. https://doi.org/10.1002/prp2.682

92. Thomas A, Baillie GL, Phillips AM, et al (2007) Cannabidiol displays unexpectedly high potency as an antagonist of CB1and CB2receptor agonists in vitro. Br J Pharmacol 150:613–623. https://doi.org/10.1038/sj.bjp.0707133

93. Hashimotodani Y, Ohno-Shosaku T, Kano M (2007) Presynaptic monoacylglycerol lipase activity determines basal endocannabinoid tone and terminates retrograde endocannabinoid signaling in the hippocampus. J Neurosci 27:1211–1219. https://doi.org/10.1523/JNEUROSCI.4159-06.2007

94. Storozhuk M V., Zholos A V. (2017) TRP Channels as Novel Targets for Endogenous Ligands: Focus on Endocannabinoids and Nociceptive Signalling. Curr Neuropharmacol 16:137–150. https://doi.org/10.2174/1570159x15666170424120802

95. Muller C, Morales P, Reggio PH (2019) Cannabinoid ligands targeting TRP channels. Front Mol Neurosci 11:1–15. https://doi.org/10.3389/fnmol.2018.00487

96. Kowalski CW, Ragozzino FJ, Lindberg JEM, et al (2020) Cannabidiol activation of vagal afferent neurons requires TRPA1. J Neurophysiol 1388–1398. https://doi.org/10.1152/jn.00128.2020

97. Starkus J, Jansen C, Shimoda LMN, et al (2019) Diverse TRPV1 responses to cannabinoids. Channels 13:172–191. https://doi.org/10.1080/19336950.2019.1619436

98. Oakes M, Law WJ, Komuniecki R (2019) Cannabinoids stimulate the TRP channel-dependent release of both serotonin and dopamine to modulate behavior in C. elegans. J Neurosci 39:4142–4152. https://doi.org/10.1523/JNEUROSCI.2371-18.2019

99. Kano M (2014) Control of synaptic function by endocannabinoid-mediated retrograde signaling. Proc. Japan Acad. Ser. B Phys. Biol. Sci.

100. Wang H, Siemens J (2015) TRP ion channels in thermosensation, thermoregulation and metabolism. Temperature 2:178–187. https://doi.org/10.1080/23328940.2015.1040604

101. Mickle AD, Shepherd AJ, Mohapatra DP (2016) Nociceptive TRP channels: Sensory detectors and transducers in multiple pain pathologies. Pharmaceuticals 9:1–26. https://doi.org/10.3390/ph9040072

102. Gau P, Curtright A, Condon L, et al (2017) An ancient neurotrophin receptor code; a single Runx/Cbfβ complex determines somatosensory neuron fate specification in zebrafish. PLoS Genet 13:1–30. https://doi.org/10.1371/journal.pgen.1006884

103. Mickle AD, Shepherd AJ, Mohapatra DP (2015) Sensory TRP Channels. In: Physiology & behavior. pp 73–118

104. Dux M, Rosta J, Messlinger K (2020) TRP channels in the focus of trigeminal nociceptor sensitization contributing to primary headaches. Int J Mol Sci 21:. https://doi.org/10.3390/ijms21010342

105. Bisogno T, Hanuš L, De Petrocellis L, et al (2001) Molecular targets for cannabidiol and its synthetic analogues: Effect on vanilloid VR1 receptors and on the cellular uptake and enzymatic hydrolysis of anandamide. Br J Pharmacol 134:845–852. https://doi.org/10.1038/sj.bjp.0704327

106. Iannotti FA, Hill CL, Leo A, et al (2014) Nonpsychotropic plant cannabinoids, Cannabidivarin (CBDV) and Cannabidiol (CBD), activate and desensitize Transient Receptor Potential Vanilloid 1 (TRPV1) channels in vitro: Potential for the treatment of neuronal hyperexcitability. ACS Chem Neurosci 5:1131–1141.

https://doi.org/10.1021/cn5000524

107. Costa B, Giagnoni G, Franke C, et al (2004) Vanilloid TRPV1 receptor mediates the antihyperalgesic effect of the nonpsychoactive cannabinoid, cannabidiol, in a rat model of acute inflammation. Br J Pharmacol 143:247–250. https://doi.org/10.1038/sj.bjp.0705920

108. Oda M, Kurogi M, Kubo Y, Saitoh O (2016) Sensitivities of two zebrafish TRPA1 paralogs to chemical and thermal stimuli analyzed in heterologous expression systems. Chem Senses 41:261–272. https://doi.org/10.1093/chemse/bjv091

109. Prober DA, Zimmerman S, Myers BR, et al (2008) Zebrafish TRPA1 channels are required for chemosensation but not for thermosensation or mechanosensory hair cell function. J Neurosci 28:10102–10110. https://doi.org/10.1523/JNEUROSCI.2740-08.2008

110. Sawzdargo M, Nguyen T, Lee DK, et al (1999) Identification and cloning of three novel human G protein-coupled receptor genes GPR52, ΨGPR53 and GPR55: GPR55 is extensively expressed in human brain. Mol Brain Res 64:193–198. https://doi.org/10.1016/S0169-328X(98)00277-0

111. Baker D, Pryce G, Davies WL, Hiley CR (2006) In silico patent searching reveals a new cannabinoid receptor. Trends Pharmacol Sci 27:1–4. https://doi.org/10.1016/j.tips.2005.11.003

112. Lauckner JE, Jensen JB, Chen HY, et al (2008) GPR55 is a cannabinoid receptor that increases intracellular calcium and inhibits M current. Proc Natl Acad Sci U S A 105:2699–2704. https://doi.org/10.1073/pnas.0711278105

113. Ryberg E, Larsson N, Sjögren S, et al (2007) The orphan receptor GPR55 is a novel cannabinoid receptor. Br J Pharmacol 152:1092–1101. https://doi.org/10.1038/sj.bjp.0707460

114. A. Marichal-Cancino B, Fajardo-Valdez A, E. Ruiz-Contreras A, et al (2016) Advances in the Physiology of GPR55 in the Central Nervous System. Curr Neuropharmacol 15:771–778. https://doi.org/10.2174/1570159x14666160729155441

115. Johnson RL, Laufer E, Riddle RD, Tabin C (1994) Ectopic expression of Sonic hedgehog alters dorsal-ventral patterning of somites. Cell 79:1165–1173. https://doi.org/10.1016/0092-8674(94)90008-6

116. Concordet JP, Lewis KE, Moore JW, et al (1996) Spatial regulation of a zebrafish patched homologue reflects the roles of sonic hedgehog and protein kinase A in neural tube and somite patterning. Development 122:2835–2846

117. Varga ZM, Amores A, Lewis KE, et al (2001) Zebrafish smoothened functions in ventral neural tube specification and axon tract formation. Development 128:3497–3509

118. Iwamoto M, Enomoto-Iwamoto M, Kurisu K (1999) Actions of hedgehog proteins on skeletal cells. Crit Rev Oral Biol Med 10:477–486. https://doi.org/10.1177/10454411990100040401

119. Yang J, Andre P, Ye L, Yang YZ (2015) The Hedgehog signalling pathway in bone formation. Int J Oral Sci 7:73–79. https://doi.org/10.1038/ijos.2015.14

120. Elia D, Madhala D, Ardon E, et al (2007) Sonic hedgehog promotes proliferation and differentiation of adult muscle cells: Involvement of MAPK/ERK and PI3K/Akt pathways. Biochim Biophys Acta - Mol Cell Res 1773:1438–1446. https://doi.org/10.1016/j.bbamcr.2007.06.006

121. Komada M (2012) Sonic hedgehog signaling coordinates the proliferation and differentiation of neural stem/progenitor cells by regulating cell cycle kinetics during development of the neocortex. Congenit Anom (Kyoto) 52:72–77. https://doi.org/10.1111/j.1741-4520.2012.00368.x

122. Cayuso J, Ulloa F, Cox B, et al (2006) The Sonic hedgehog pathway independently controls the patterning, proliferation and survival of neuroepithelial cells by regulating Gli activity. Development 133:517–528. https://doi.org/10.1242/dev.02228

123. Charrier JB, Lapointe F, Le Douarin NM, Teillet MA (2001) Anti-apoptotic role of Sonic hedgehog protein at the early stages of nervous system organogenesis. Development

128:4011–4020

124. Jeng KS, Chang CF, Lin SS (2020) Sonic hedgehog signaling in organogenesis, tumors, and tumor microenvironments. Int J Mol Sci 21:. https://doi.org/10.3390/ijms21030758

125. Carty DR, Thornton C, Gledhill JH, Willett KL (2018) Developmental Effects of Cannabidiol and Δ9-Tetrahydrocannabinol in Zebrafish. Toxicol Sci 162:137–145. https://doi.org/10.1093/toxsci/kfx232

126. Carballo GB, Honorato JR, De Lopes GPF, Spohr TCLDSE (2018) A highlight on Sonic hedgehog pathway. Cell Commun Signal. https://doi.org/10.1186/s12964-018-0220-7

127. Wang Y, Zhou Z, Walsh CT, McMahon AP (2009) Selective translocation of intracellular Smoothened to the primary cilium in response to Hedgehog pathway modulation. Proc Natl Acad Sci U S A 106:2623–2628. https://doi.org/10.1073/pnas.0812110106

128. Pietrobono S, Gagliardi S, Stecca B (2019) Non-canonical hedgehog signaling pathway in cancer: Activation of GLI transcription factors beyond smoothened. Front Genet 10:1–20. https://doi.org/10.3389/fgene.2019.00556

129. Neve A, Migliavacca J, Capdeville C, et al (2019) Crosstalk between SHH and FGFR signaling pathways controls tissue invasion in medulloblastoma. Cancers (Basel) 11:1–17. https://doi.org/10.3390/cancers11121985

130. Fogarty MP, Emmenegger BA, Grasfeder LL, et al (2007) Fibroblast growth factor blocks Sonic hedgehog signaling in neuronal precursors and tumor cells. Proc Natl Acad Sci U S A. https://doi.org/10.1073/pnas.0605770104

131. Noubissi FK, Yedjou CG, Spiegelman VS, Tchounwou PB (2018) Cross-talk between Wnt and Hh signaling pathways in the pathology of basal cell carcinoma. Int J Environ Res Public Health 15:. https://doi.org/10.3390/ijerph15071442

132. Ma X, Drannik A, Jiang F, et al (2017) Crosstalk between Notch and Sonic hedgehog signaling in a mouse model of amyotrophic lateral sclerosis. Neuroreport 28:141–148. https://doi.org/10.1097/WNR.0000000000000725

133. Khaliullina H, Bilgin M, Sampaio JL, et al (2015) Endocannabinoids are conserved inhibitors of the hedgehog pathway. Proc Natl Acad Sci U S A 112:3415–3420. https://doi.org/10.1073/pnas.1416463112

134. Fish EW, Murdaugh LB, Zhang C, et al (2019) Cannabinoids Exacerbate Alcohol Teratogenesis by a CB1-Hedgehog Interaction. Sci Rep 9:1–16. https://doi.org/10.1038/s41598-019-52336-w

135. Lam CS, Rastegar S, Strähle U (2006) Distribution of cannabinoid receptor 1 in the CNS of zebrafish. Neuroscience 138:83–95. https://doi.org/10.1016/j.neuroscience.2005.10.069

136. Kimmel CB, Ballard WW, Kimmel SR, et al (1995) Stages of embryonic development of the zebrafish. Dev Dyn. https://doi.org/10.1002/aja.1002030302

137. Lawrence C, Adatto I, Best J, et al (2012) Generation time of zebrafish (Danio rerio) and medakas (Oryzias latipes) housed in the same aquaculture facility. Lab Anim (NY) 41:158–165. https://doi.org/10.1038/laban0612-158

138. Schneider M (2009) Cannabis use in pregnancy and early life and its consequences: Animal models. Eur Arch Psychiatry Clin Neurosci 259:383–393. https://doi.org/10.1007/s00406-009-0026-0

139. Rohde LA, Heisenberg CP (2007) Zebrafish Gastrulation: Cell Movements, Signals, and Mechanisms. Int Rev Cytol 261:159–192. https://doi.org/10.1016/S0074-7696(07)61004-3

140. Du Y, Guo Q, Shan M, et al (2016) Spatial and temporal distribution of dopaminergic neurons during development in zebrafish. Front Neuroanat 10:1–7. https://doi.org/10.3389/fnana.2016.00115

141. Panula P, Chen YC, Priyadarshini M, et al (2010) The comparative neuroanatomy and neurochemistry of zebrafish CNS systems of relevance to human neuropsychiatric diseases. Neurobiol Dis 40:46–57. https://doi.org/10.1016/j.nbd.2010.05.010

142. Rodriguez-Martin I, Herrero-Turrion MJ, Marron Fdez de Velasco E, et al (2007)

Characterization of two duplicate zebrafish Cb2-like cannabinoid receptors. Gene 389:36–44. https://doi.org/10.1016/j.gene.2006.09.016

143. Watson S, Chambers D, Hobbs C, et al (2008) The endocannabinoid receptor, CB1, is required for normal axonal growth and fasciculation. Mol Cell Neurosci 38:89–97. https://doi.org/10.1016/j.mcn.2008.02.001

144. Williams EJ, Walsh FS, Doherty P (2003) The FGF receptor uses the endocannabinoid signaling system to couple to an axonal growth response. J Cell Biol 160:481–486. https://doi.org/10.1083/jcb.200210164

145. Acevedo-Canabal A, Colón-Cruz L, Rodriguez-Morales R, et al (2019) Altered Swimming Behaviors in Zebrafish Larvae Lacking Cannabinoid Receptor 2. Cannabis Cannabinoid Res 4:88–101. https://doi.org/10.1089/can.2018.0025

146. Avraham HK, Jiang S, Fu Y, et al (2014) The cannabinoid CB2 receptor agonist AM1241 enhances neurogenesis in GFAP/Gp120 transgenic mice displaying deficits in neurogenesis. Br J Pharmacol 171:468–479. https://doi.org/10.1111/bph.12478

147. Mensching L, Djogo N, Keller C, et al (2019) Stable adult hippocampal neurogenesis in cannabinoid receptor CB2 deficient mice. Int J Mol Sci 20:10–12. https://doi.org/10.3390/ijms20153759

148. Chahardehi AM, Arsad H, Lim V (2020) Zebrafish as a successful animal model for screening toxicity of medicinal plants. Plants 9:1–35. https://doi.org/10.3390/plants9101345

149. Carty DR, Thornton C, Gledhill JH, Willett KL (2018) Developmental Effects of Cannabidiol and Δ9-Tetrahydrocannabinol in Zebrafish. Toxicol Sci 162:137–145. https://doi.org/10.1093/toxsci/kfx232

150. Pandelides Z, Thornton C, Lovitt KG, et al (2020) Developmental exposure to Δ9-tetrahydrocannabinol (THC) causes biphasic effects on longevity, inflammation, and reproduction in aged zebrafish (Danio rerio). GeroScience 42:923–936.

https://doi.org/10.1007/s11357-020-00175-3

151. Pandelides Z, Thornton C, Faruque AS, et al (2020) Developmental exposure to cannabidiol (CBD) alters longevity and health span of zebrafish (Danio rerio). GeroScience 42:785–800. https://doi.org/10.1007/s11357-020-00182-4

152. Taylor DA, Fennessy MR (1977) Biphasic nature of the effects of Δ9-tetrahydrocannabinol on body temperature and brain amines of the rat. Eur J Pharmacol 46:93–99. https://doi.org/10.1016/0014-2999(77)90244-8

153. Grisham MG, Ferraro DP (1972) Biphasic effects of δ9-tetrahydrocannabinol on variable interval schedule performance in rats. Psychopharmacologia 27:163–169. https://doi.org/10.1007/BF00439375

154. Ahmed KT, Amin MR, Shah P, Ali DW (2018) Motor neuron development in zebrafish is altered by brief (5-hr) exposures to THC (Δ9-tetrahydrocannabinol) or CBD (cannabidiol) during gastrulation. Sci Rep 8:1–14. https://doi.org/10.1038/s41598-018-28689-z

155. Amin MR, Ahmed KT, Ali DW (2020) Early exposure to THC alters M-Cell development in zebrafish embryos. Biomedicines 8:1–15. https://doi.org/10.3390/biomedicines8010005

156. Thisse C, Thisse B (2008) High-resolution in situ hybridization to whole-mount zebrafish embryos. Nat Protoc 3:59–69. https://doi.org/10.1038/nprot.2007.514

157. Tang R, Dodd A, Lai D, et al (2007) Validation of zebrafish (Danio rerio) reference genes for quantitative real-time RT-PCR normalization. Acta Biochim Biophys Sin (Shanghai) 39:384–390. https://doi.org/10.1111/j.1745-7270.2007.00283.x

158. Thisse B, Thisse C (2005) High Throughput Expression Analysis of ZF-Models Consortium Clones. In: ZFIN Direct Data Submiss.

159. Colon-Cruz L, Rodriguez-Morales R, Santana-Cruz A, et al (2020) Cnr2 is important for ribbon synapse maturation and function in hair cells and photoreceptors. bioRxiv 1–42. https://doi.org/10.1101/2020.08.18.253120

160. Leighton PLA, Kanyo R, Neil GJ, et al (2018) Prion gene paralogs are dispensable for early zebrafish development and have nonadditive roles in seizure susceptibility. J Biol Chem 293:12576–12592. https://doi.org/10.1074/jbc.RA117.001171

161. Lo H, Hong M, Szutorisz H, Hurd YL (2021) Δ9-tetrahydrocannabinol inhibits Hedgehog-dependent patterning during development. bioRxiv 677:212–241

162. Liu LY, Alexa K, Cortes M, et al (2016) Cannabinoid receptor signaling regulates liver development and metabolism. Dev 143:609–622. https://doi.org/10.1242/dev.121731

163. Gau P, Poon J, Ufret-Vincenty C, et al (2013) The zebrafish ortholog of TRPV1 is required for heat-induced locomotion. Ann Intern Med 158:5249–5260. https://doi.org/10.1523/JNEUROSCI.5403-12.2013

164. Lewis KE, Currie PD, Roy S, et al (1999) Control of muscle cell-type specification in the zebrafish embryo by Hedgehog signalling. Dev Biol 216:469–480. https://doi.org/10.1006/dbio.1999.9519

165. Sufian MS, Amin MR, Kanyo R, et al (2019) CB1 and CB2 receptors play differential roles in early zebrafish locomotor development. J Exp Biol 222:1–12. https://doi.org/10.1242/jeb.206680

166. Migliarini B, Carnevali O (2009) A novel role for the endocannabinoid system during zebrafish development. Mol Cell Endocrinol 299:172–177. https://doi.org/10.1016/j.mce.2008.11.014

167. Esain V, Kwan W, Carroll KJ, et al (2015) Cannabinoid Receptor-2 Regulates Embryonic Hematopoietic Stem Cell Development via Prostaglandin E2 and P-Selectin Activity. Stem Cells 33:2596–2612. https://doi.org/10.1002/stem.2044

168. Buckley NE, Hansson S, Harta G, Mezey É (1997) Expression of the CB1 and CB2 receptor messenger RNAs during embryonic development in the rat. Neuroscience 82:1131–1149. https://doi.org/10.1016/S0306-4522(97)00348-5

169. El-Brolosy MA, Kontarakis Z, Rossi A, et al (2019) Genetic compensation triggered by

mutant mRNA degradation. Nature 568:193–197. https://doi.org/10.1038/s41586-019-1064-z

170. Etzion T, Zmora N, Zohar Y, et al (2020) Ectopic over expression of kiss1 may compensate for the loss of kiss2. Gen Comp Endocrinol 295:113523. https://doi.org/10.1016/j.ygcen.2020.113523

171. Chou SW, Chen Z, Zhu S, et al (2017) A molecular basis for water motion detection by the mechanosensory lateral line of zebrafish. Nat Commun 8:. https://doi.org/10.1038/s41467-017-01604-2

172. Pan YA, Choy M, Prober DA, Schier AF (2012) Robo2 determines subtype-specific axonal projections of trigeminal sensory neurons. Development 139:591–600. https://doi.org/10.1242/dev.076588

173. Reyes R, Haendel M, Grant D, et al (2004) Slow Degeneration of Zebrafish Rohon-Beard Neurons during Programmed Cell Death. Dev Dyn 229:30–41. https://doi.org/10.1002/dvdy.10488

174. Funakoshi K, Nakano M, Atobe Y, et al (2006) Differential development of TRPV1-expressing sensory nerves in peripheral organs. Cell Tissue Res 323:27–41. https://doi.org/10.1007/s00441-005-0013-3

175. Garami A, Pakai E, Oliveira DL, et al (2011) Thermoregulatory phenotype of the Trpv1 knockout mouse: Thermoeffector dysbalance with hyperkinesis. J Neurosci 31:1721–1733. https://doi.org/10.1523/JNEUROSCI.4671-10.2011

176. Corey DP, Garcia-Añoveros J, Holt JR, et al (2004) TRPA1 is a candidate for the mechanosensitive transduction channel of vertebrate hair cells. Nature 432:723–730. https://doi.org/10.1038/nature03066

177. Johnstone AD, De Léon A, Unsain N, et al (2019) Developmental axon degeneration requires trpv1-dependent Ca 2+ influx. eNeuro 6:. https://doi.org/10.1523/ENEURO.0019-19.2019

178. Chechik G, Meilijson I, Ruppin E (1999) Neuronal regulation: A mechanism for synaptic pruning during brain maturation. Neural Comput 11:2061–2080. https://doi.org/10.1162/089976699300016089

179. Crucke J, Van de Kelft A, Huysseune A (2015) The innervation of the zebrafish pharyngeal jaws and teeth. J Anat 227:62–71. https://doi.org/10.1111/joa.12321

180. Vilceanu D, Stucky CL (2010) TRPA1 Mediates Mechanical currents in the plasma membrane of Mouse Sensory Neurons. PLoS One 5:1–10. https://doi.org/10.1371/journal.pone.0012177

181. Cherif H, Argaw A, Cécyre B, et al (2015) Role of GPR55 during axon growth and target innervation. eNeuro 2:. https://doi.org/10.1523/ENEURO.0011-15.2015

182. Guy AT, Nagatsuka Y, Ooashi N, et al (2015) Glycerophospholipid regulation of modality-specific sensory axon guidance in the spinal cord. Science (80-) 349:974–977. https://doi.org/10.1126/science.aab3516

183. Winata CL, Korzh S, Kondrychyn I, et al (2009) Development of zebrafish swimbladder: The requirement of Hedgehog signaling in specification and organization of the three tissue layers. Dev Biol 331:222–236. https://doi.org/10.1016/j.ydbio.2009.04.035

184. Pillai-Kastoori L, Wen W, Wilson SG, et al (2014) Sox11 Is Required to Maintain Proper Levels of Hedgehog Signaling during Vertebrate Ocular Morphogenesis. PLoS Genet 10:. https://doi.org/10.1371/journal.pgen.1004491

185. Aanstad P, Santos N, Corbit KC, et al (2010) The extracellular domain of Smoothened regulates ciliary localisation and is required for maximal Hh pathway activation in zebrafish. Curr Biol 19:1034–1039. https://doi.org/10.1016/j.cub.2009.04.053.The

186. Ohlsson A, Lindgren J - E, Andersson S, et al (1986) Single- dose kinetics of deuterium-labelled cannabidiol in man after smoking and intravenous administration. Biol Mass Spectrom 13:77–83. https://doi.org/10.1002/bms.1200130206

187. Schmitz SM, Lopez HL, Marinotti O (2020) Post Marketing Safety of Plus CBD™

Products, a Full Spectrum Hemp Extract: A 2-Year Experience. J Diet Suppl 17:587–598. https://doi.org/10.1080/19390211.2020.1767255

188. Brox S, Ritter AP, Küster E, Reemtsma T (2014) A quantitative HPLC-MS/MS method for studying internal concentrations and toxicokinetics of 34 polar analytes in zebrafish (Danio rerio) embryos. Anal Bioanal Chem 406:4831–4840. https://doi.org/10.1007/s00216-014-7929-y

189. Serrano M, Han M, Brinez P, Linask KK (2010) Fetal alcohol syndrome: cardiac birth defects in mice and prevention with folate. Am J Obstet Gynecol 203:75.e7-75.e15. https://doi.org/10.1016/j.ajog.2010.03.017

190. De La Paz JF, Beiza N, Paredes-Zúñiga S, et al (2017) Triazole fungicides inhibit zebrafish hatching by blocking the secretory function of hatching gland cells. Int J Mol Sci 18:. https://doi.org/10.3390/ijms18040710

191. Carballo C, Chronopoulou EG, Letsiou S, et al (2019) Genomic and phylogenetic analysis of choriolysins, and biological activity of hatching liquid in the flatfish Senegalese sole. PLoS One 14:1–18. https://doi.org/10.1371/journal.pone.0225666

192. Zheng W, Wang Z, Collins JE, et al (2011) Comparative transcriptome analyses indicate molecular homology of zebrafish swimbladder and mammalian lung. PLoS One 6:. https://doi.org/10.1371/journal.pone.0024019

193. Lindsey BW, Smith FM, Croll RP (2010) From inflation to flotation: Contribution of the swimbladder to whole-body density and swimming depth during development of the zebrafish (Danio rerio). Zebrafish 7:85–96. https://doi.org/10.1089/zeb.2009.0616

194. Koudijs MJ, Den Broeder MJ, Groot E, Van Eeden FJM (2008) Genetic analysis of the two zebrafish patched homologues identifies novel roles for the hedgehog signaling pathway. BMC Dev Biol 8:1–17. https://doi.org/10.1186/1471-213X-8-15

195. Chen W, Burgess S, Hopkins N (2001) Analysis of the zebrafish smoothened mutant reveals conserved and divergent functions of hedgehog activity. Development 128:2385–

2396

196. Yin C, Solnica-Krezel L (2007) Convergence and extension movements mediate the specification and fate maintenance of zebrafish slow muscle precursors. Dev Biol 304:141–155. https://doi.org/10.1016/j.ydbio.2006.12.030

197. Brand M, Heisenberg CP, Warga RM, et al (1996) Mutations affecting development of the midline and general body shape during zebrafish embryogenesis. Development 123:129–142

198. Mich JK, Blaser H, Thomas NA, et al (2009) Germ cell migration in zebrafish is cyclopamine-sensitive but Smoothened-independent. Dev Biol 328:342–354. https://doi.org/10.1016/j.ydbio.2009.01.036

199. Büttner A, Busch W, Klüver N, et al (2012) Transcriptional responses of zebrafish embryos exposed to potential sonic hedgehog pathway interfering compounds deviate from expression profiles of cyclopamine. Reprod Toxicol 33:254–263. https://doi.org/10.1016/j.reprotox.2011.12.010

200. Jackman WR, Yoo JJ, Stock DW (2010) Hedgehog signaling is required at multiple stages of zebrafish tooth development. BMC Dev Biol 10:. https://doi.org/10.1186/1471-213X-10-119